# COMPARISON OF CONCURRENT LEARNING AND DERIVATIVE-FREE MODEL REFERENCE ADAPTIVE CONTROL AGAINST PARAMETER VARIATION

A THESIS SUBMITTED TO
THE GRADUATE SCHOOL OF NATURAL AND APPLIED SCIENCES
OF
MIDDLE EAST TECHNICAL UNIVERSITY

BY

SELAHATTİN BURAK SARSILMAZ

IN PARTIAL FULFILLMENT OF THE REQUIREMENTS
FOR
THE DEGREE OF MASTER OF SCIENCE
IN
AEROSPACE ENGINEERING

JULY 2016

Approval of the thesis:

**COMPARISON OF CONCURRENT LEARNING AND DERIVATIVE-FREE MODEL REFERENCE ADAPTIVE CONTROL AGAINST PARAMETER VARIATION**

submitted by **SELAHATTİN BURAK SARSILMAZ** in partial fulfillment of the requirements for the degree of **Master of Science in Aerospace Engineering Department, Middle East Technical University** by,

Prof. Dr. Gülbin Dural Ünver _____
Dean, Graduate School of **Natural and Applied Sciences**

Prof. Dr. Ozan Tekinalp _____
Head of Department, **Aerospace Engineering**

Assist. Prof. Dr. Ali Türker Kutay _____
Supervisor, **Aerospace Engineering Dept., METU**

**Examining Committee Members:**

Prof. Dr. Metin Uymaz Salamcı _____
Mechanical Engineering Dept., Gazi University

Assist. Prof. Dr. Ali Türker Kutay _____
Aerospace Engineering Dept., METU

Assoc. Prof. Dr. Umut Orguner _____
Electrical and Electronics Engineering Dept., METU

Assoc. Prof. Dr. İlkay Yavrucuk _____
Aerospace Engineering Dept., METU

Assist. Prof. Dr. Ercan Gürses _____
Aerospace Engineering Dept., METU

**Date:** July 21, 2016

**I hereby declare that all information in this document has been obtained and presented in accordance with academic rules and ethical conduct. I also declare that, as required by these rules and conduct, I have fully cited and referenced all material and results that are not original to this work.**

Name, Last Name: SELAHATTİN BURAK SARSILMAZ

Signature:

# ABSTRACT

COMPARISON OF CONCURRENT LEARNING AND DERIVATIVE-FREE MODEL REFERENCE ADAPTIVE CONTROL AGAINST PARAMETER VARIATION

Sarsılmaz, Selahattin Burak

M.S., Department of Aerospace Engineering

Supervisor: Assist. Prof. Dr. Ali Türker Kutay

July 2016, 98 pages

For adaptive laws using only instantaneous data, it is well known that parameter convergence is impossible without persistency of excitation. Concurrent Learning Model Reference Adaptive Control (CL-MRAC) is a novel adaptive controller that solves the parameter convergence problem, about forty year old adaptive control problem, without requiring persistency of excitation. This solution relies on the concurrent usage of recorded and current data. Derivative-Free Model Reference Adaptive Control (DF-MRAC) is another novel adaptive controller that challenges the derivative-based adaptive laws and the integral action of them. Instead of constant ideal parameters assumption, DF-MRAC uses less strict assumption which allows time-varying ideal parameters. Due to these contributions, both CL-MRAC and DF-MRAC deserve attention. This research mainly addresses their robustness to parameter variation.

In this thesis, standard exponential stability theorem of CL-MRAC and uniform ultimate boundedness theorem of DF-MRAC with minor changes in their statements are proved. Some missing parts in these theorems are either filled or emphasized. To make a fair comparison between CL-MRAC and DF-MRAC, constant ideal parameters assumption imposed in CL-MRAC is replaced with time-varying ideal parameters assumption which is similar to the one in DF-MRAC but still stricter than it. Under this relaxed assumption, uniform ultimate boundedness of the solution of the closed-loop system is proved. According to this theorem, existing data recording algorithms are modified and the performances of CL-MRAC with modified algorithms are inspected under time-varying ideal parameters in a sample regulation and tracking problem. The simulation results show that the performance of CL-MRAC is dependent on problems and data recording algorithms.

Wing rock problem with time-varying angle of attack is considered a useful benchmark for numerical illustration. Under high level uncertainty and random disturbance, controllers are tested and DF-MRAC performs better than CL-MRAC. Since DF-MRAC suppresses the uncertainty effectively and makes no attempt to learn it in the simulations, its performances with different basis functions are also tested. The simulation results present the excellent performance of DF-MRAC. Although it is shown that both CL-MRAC and DF-MRAC have bounded solutions under parameter variations, their adaptation strategies are completely different and the effect of this difference in the performance is obviously seen in the simulations.

Keywords: Model Reference Adaptive Control, Time-Varying Parameters, Uniform Ultimate Boundedness, Wing Rock Motion

# ÖZ

EŞ ZAMANLI ÖĞRENEN VE TÜREVSİZ MODEL REFERANS ADAPTİF KONTROLÜN PARAMETRE DEĞİŞİMİNE KARŞI KIYASLAMASI

Sarsılmaz, Selahattin Burak

Yüksek Lisans, Havacılık ve Uzay Mühendisliği Bölümü

Tez Yöneticisi: Yrd. Doç. Dr. Ali Türker Kutay

Temmuz 2016, 98 sayfa

Sadece anlık veri kullanan adaptif yasaları için, sürekli uyarım olmadan parametre yakınsamasının mümkün olmadığı bilinmektedir. Yaklaşık kırk yıldır adaptif kontrolde süregelen parametre yakınsama sorununu, özgün Eş Zamanlı Öğrenen Model Referans Adaptif Kontrol (CL-MRAC) yöntemi sürekli uyarıma ithiyaç duymadan çözmektedir. Bu çözüm, kaydedilen ve anlık verinin eş zamanlı kullanımına dayanmaktadır. Bir diğer özgün adaptif kontrol yöntemi olan Türevsiz Model Referans Adaptif Kontrol (DF-MRAC) yöntemi, türev bazlı adaptif yasalarına ve onların integral etkisine karşı çıkmaktadır. Sabit ideal parametre varsayımı yerine, DF-MRAC zamanla değişen ideal parametrelere izin veren daha esnek bir varsayım kullanmaktadır. Bahsedilen bu katkılar nedeniyle, hem CL-MRAC hem de DF-MRAC dikkate değer bulunmaktadır. Bu araştırma, ana hatlarıyla bu kontrol yöntemlerinin parametre değişimine karşı gürbüzlüklerini konu almaktadır.

Bu tezde, CL-MRAC yönteminin standart üstel kararlılık teoremi ve DF-MRAC yönteminin düzgün nihai sınırlılık teoremi, her iki teoremin de ifadelerinde ufak değişiklikler yapılarak ispatlanmıştır. Teoremlerdeki bazı eksik bölümler tamamlanmış veya eksiklikleri vurgulanmıştır. Bu iki kontrol yöntemini adil bir şekilde kıyaslayabilmek için CL-MRAC yönteminde kullanılan sabit ideal parametre varsayımı DF-MRAC yönteminde kullanılan varsayıma benzer; ama daha katı olan zamanla değişen ideal parameterler varsayımıyla değiştirilmiştir. Bu esnetilmiş varsayım altında, kapalı döngü sistem çözümünün düzgün nihai sınırlılığı ispatlanmıştır. Bu teoreme göre mevcut veri kayıt algoritmaları modifiye edilmiş ve zamanla değişen ideal parametreler içeren örnek düzenleme ve takip problemlerinde, CL-MRAC yönteminin modifiye edilen algoritmalarla birlikte performansı incelenmiştir. Benzetim sonuçları, CL-MRAC performansının uygulandığı problemlere ve veri kayıt algoritmalarına bağlı olduğunu göstermektedir.

Zamanla değişen hücum açısı barındıran kanat sallanma problemi sayısal gösterim için kullanışlı bir kıstas olarak düşünülmektedir. Yüksek seviyede belirsizlik ve rassal bozucu altında, iki kontrol yöntemi sınanmış ve DF-MRAC yöntemi CL-MRAC yöntemine kıyasla daha yüsek performans göstermiştir. Benzetimlerde, DF-MRAC yöntemi belirsizliği etkin bir şekilde baskıladığı ve bu belirsizliği öğrenme girişiminde bulunmadığı için performansı, farklı taban foksiyonları kullanılarak da sınanmıştır. Benzetim sonuçları, DF-MRAC yönteminin mükemmel performansını ortaya koymuştur. Her iki kontrol yönteminin parametre değişimlerine karşı sınırlı çözümlere sahip olduğu gösterilmiş olmasına rağmen, uyarlama stratejileri tamamen faklıdır ve bu farkın performanslara etkisi benzetimlerde açıkça görülmektedir.

Anahtar Kelimeler: Model Referans Adaptif Kontrol, Zamanla Değişen Parametreler, Düzgün Nihai Sınırlılık, Kanat Sallanma Hareketi

*To the memory of*

*Aysun Aktaş*

# ACKNOWLEDGMENTS

Until taking “System Dynamics” course from Dr. Ali Türker Kutay in 3rd year of my BS, little did I think that something in my life would be as attractive as music. After taking “Modern Control” course in 4th year of my BS again from Dr. Ali Türker Kutay, I was sure that “Control” must be in the center of my life. Therefore, it was a great honor to work with him for the last three years. I am also grateful to him for giving me the utmost freedom for the completion of this work.

In MS, I have been fortunate to take courses from Dr. Umut Orguner and Dr. Sezai Emre Tuna. I am thankful to them for their well organized and clearly presented courses. These courses have encouraged me to learn being rigorous. I shall thank them for their reference letters and valuable talks during my PhD applications. I would also like to thank Dr. Hassan K. Khalil from Michigan State University for his excellent teaching. Taking courses from him was an invaluable experience for me. I have been very impressed by his wisdom and he has broadened my view of control. I shall also thank him for his references.

I would like to thank Dr. Metin Uymaz Salamcı from Gazi University for his considerable support during my PhD applications. I am also thankful to Dr. Tansel Yücelen from University of South Florida for providing me an opportunity to study with him in PhD. Our discussions with him about “derivative-free adaptive law” helped me to organize this work.

I would like to thank Dr. Metin Uymaz Salamcı, Dr. Ali Türker Kutay, Dr. Umut Orguner, Dr. İlkay Yavrucuk, and Dr. Ercan Gürses for being in my committee.

My time at Turkish Aerospace Industry (TAI) has been made gratifying by my managers, Dr. Volkan Nalbantoğlu and Dr. Uğur Zengin. Their support for academic

study is helpful during MS. My best wishes are also for my co-workers, especially Umut Türe, Can Onur, İsmail Hakkı Şahin, and Sinan Özcan. Our discussions about control engineering have been enjoyable.

My deepest thanks are also for Emre Yılmaz who was the best assistant in our department. His advice about course selection helped me determine and be aware of the research directions that I like. Besides, I appreciate the cooperation and friendship of Metehan Yayla. If I had not been prevented from working as an assistant, we would have done research and published elegant outputs together. I am also grateful to Murat Şenipek for his never-ending support, brotherhood, and moments we shared for invaluable twelve years.

I want to specially thank my close friends Bilge Miraç Atıcı, Bengi İçli, Berk Can Duva, Damla Sönmez, Ali Can Sungur, İrem Bozkurt, Mertcan Örmeci, Gözde Keskin, and İsmail Tugay Güzel for encouraging me in confusing times. Moreover, I am so lucky to be a member of "Motif". This band is the best thing that ever happened to me. I am indebted to Ayşe Yazgın, Serhat Bilyaz, Tutku Gizem Yazıcı, Volkan Özdemir, and Semih Ali Aksoy. The moments and stories we shared are unforgettable.

Finally, I would like to express my deepest gratitude to my mother Zerrin, my father Gürbüz, and my sister Bengi. Without their support and understanding, this work would have been impossible.

# TABLE OF CONTENTS

# LIST OF TABLES

TABLES

# LIST OF FIGURES

FIGURES

# LIST OF ABBREVIATIONS

| | |
|---|---|
| MRAC | Model Reference Adaptive Control |
| CL-MRAC | Concurrent Learning Model Reference Adaptive Control |
| DF-MRAC | Derivative-Free Model Reference Adaptive Control |
| PE | Persistently Exciting |
| BIBO | Bounded-Input, Bounded-Output |
| UUB | Uniformly Ultimately Bounded |
| CBS | Cauchy-Bunyakovskii-Schwarz Inequality |

# NOTATION

| | |
|---|---|
| $N$ | natural numbers |
| $R$ | real numbers |
| $\|\cdot\|$ | absolute value of a number |
| $\|\|\cdot\|\|$ | Euclidean vector norm |
| $\|\|\cdot\|\|_2$ | matrix norm induced by Euclidean vector norm |
| $\|\|\cdot\|\|_F$ | Frobenius matrix norm |
| $:=$ | equal by definition |
| $vec$ | column stacking operator |
| $tr$ | trace |
| $I$ | identity matrix with appropriate order |
| $\lambda_{min}(\lambda_{max})$ | smallest (largest) eigenvalue |
| $\sigma_{min}(\sigma_{max})$ | smallest (largest) singular value |
| $<\cdot,\cdot>$ | standard inner products for vectors and matrices |
| $null$ | null space |
| $dim$ | dimension of a vector space |
| $\oplus$ | direct sum |
| $\otimes$ | Kronecker product |

# CHAPTER 1

# INTRODUCTION

Control technologies have become indispensable part of modern systems such as aircrafts and space vehicles. Historically, well-established control approaches have dominated modern systems and these approaches rely on mathematical models of systems. However, mathematical models do not represent physical systems exactly. On the contrary, there is a wide range of model uncertainty due to assumptions in modeling, linearization, model order reduction, and disturbances. With the increase in performance and safety demand of modern systems, researchers have extensively studied robust and adaptive controllers to deal with model uncertainty. In robust control, model uncertainty is regarded as perturbation of a nominal system and controller is designed to meet the stability and performance objectives for any model within the given bounds on the model uncertainty. Conservatism is inherent in robust control and degradation in performance may be experienced, depending on level of uncertainty. On the other hand, adaptive controller is designed to cancel the uncertainty online and thus the upper bounds on the uncertainty are not necessarily required to be known. Besides, adaptive controllers encounter less performance degradation than robust controllers under high level of uncertainty. These features of adaptive controllers make it attractive to researchers and engineers.

Adaptive controllers can be put into two groups, namely “direct adaptive controllers” and “indirect adaptive controllers”. Direct adaptive controllers adapt controller parameters directly and they are known for fast control response but short-term learning. On the other hand, indirect adaptive controllers employ parameter estimation algorithm

to estimate the unknown parameters and use them to calculate the controller parameters. Their performances depend on the accuracy of the estimation. If the initial estimates are poor, then the transient response and stability cannot be guaranteed.

Model Reference Adaptive Control (MRAC) is a popular and significant direct adaptive controller [1], [2], [3]. Concurrent Learning MRAC (CL-MRAC) is a novel adaptive controller which combines the advantages of direct and indirect adaptive controllers [4]. Derivative-Free MRAC (DF-MRAC) is another novel adaptive controller which is very responsive to sudden changes in system dynamics [5]. This study presents the comparison of CL-MRAC and DF-MRAC against parameter variations.

## 1.1 Model Reference Adaptive Control

The main objective of MRAC is to make an uncertain system track the desired response which is defined by a reference model. To achieve this goal, MRAC uses three main elements. These are reference model, uncertainty parameterization, and weight update law. Reference model characterizes the desired performance of the closed-loop system. Uncertainty parameterization component, which corresponds to adaptive control signal, is used to cancel the actual uncertainty. Based on the comparison between the state (output) of the uncertain system and reference model, weight update law tries to estimate the parameters required by adaptive control.

In MRAC architecture, nominal controller is augmented by adaptive control signal to cancel the uncertainty. If the structure of the uncertainty is known, that is, uncertainty is a weighted combination of known basis functions, and then uniform cancellation of the uncertainty is possible. This type of uncertainty parameterization is extensively used in adaptive control, for example in [5], [6], [7], [8]. In this study, we also formulate problems assuming that basis functions are known.

From Lyapunov stability theory, it was proved that conventional adaptive law in MRAC architecture guarantees the boundedness of the tracking and parameter (weight) error for

constant ideal parameters. With an application of Barbalat's lemma, it can be shown that the tracking error goes to zero as time goes to infinity. However, same discussion is not valid for the weight error. These issues degrade the transient performance and robustness of the closed-loop system. Furthermore, weight error can be unbounded under bounded disturbances [1], [2], [3]. When the systems states are persistently exciting (PE), parameter convergence is achieved and thus tacking error vanishes exponentially. Therefore, performance and robustness of the closed-loop system improve. It should be noted that for adaptive laws using only instantaneous data, PE is necessary for parameter convergence and depends on reference inputs [10]. It means that reference inputs should be monitored such that PE is satisfied. However, this is not practical in online applications because reference inputs are in general event based and not known before the operation. Moreover, PE reference inputs may be unsuitable for desired missions [4].

In order to increase the robustness and efficiency of uncertainty suppression without PE reference inputs, many modifications to weight update law have been introduced in the literature. Fixed damping has been added to the weight update law by $\sigma$ modification [11]. It limits adaptation to the uncertainty. On the other hand, $e$ modification adds variable damping such that damping increases with the tracking error and thus it allows adaptation process when the tracking error is small [12]. Both $\sigma$ and $e$ modifications provide bounded weight error. Parameter projection is another modification which ensures that estimated weight stays in a predefined compact set [13]. In addition to these well-known modifications, some of the recently developed important modifications can be found in [14], [15], [16]. The main focus in these modifications is efficient uncertainty suppression instead of parameter convergence.

## 1.2 Concurrent Learning Model Reference Adaptive Control

As it is mentioned in the previous section, parameter convergence is impossible without persistency of excitation for adaptive laws using only instantaneous data. However,

persistency of excitation may not be necessary for parameter convergence if adaptive laws use memory. CL-MRAC has been motivated by the foregoing idea and introduced in [4]. CL-MRAC utilizes concurrent usage of recorded and current data to guarantee exponential convergence of tracking error and parameter. In the formulation of CL-MRAC, PE reference inputs have been replaced with exciting reference inputs over finite interval. When sufficiently rich data is recorded during this finite interval, parameter convergence dependency of adaptive laws on future reference inputs are ruled out. The sufficiency of rich data can be easily determined by online verifiable rank condition on recorded data. It should also be noted that CL-MRAC requires first derivative of the state for a recorded data point. This additional information is the price we pay for non PE reference inputs. If this derivative is measured, it can be directly used. Otherwise, it should be estimated in finite time after the record. That is, it does not have to be estimated at the current time instant [4], [7].

Standard exponential stability theorem of concurrent learning for a different class of plants and its applications can be found in [4], [17], [7], [18], [19]. The estimate of convergence rate has revealed that the convergence rate depends on the spectral properties of recorded data. In [20], it was demonstrated that data recording algorithm which relies on the estimate of convergence rate provides the fastest parameter convergence among three data recording algorithms.

Similar to other derivative-based adaptive laws, all studies about CL-MRAC have the underlying assumption that there exist constant unknown ideal weights. Under this assumption, CL-MRAC provides long-term learning with the aid of parameter convergence capability and improves performance when the system tracks repeated commands. In [4], the author claims that CL-MRAC would recover the performance and robustness of the reference model and could pave the way for flight certification of adaptive controllers. However, its robustness to disturbances and/or time-varying ideal parameters has not been analyzed yet. In this study, we analyze the robustness of CL-MRAC and check the performances in sample problems to see whether the claim in [4] deserves credit for the certification issue.

## 1.3 Derivative-Free Model Reference Adaptive Control

DF-MRAC has been developed for uncertain systems which experience sudden or fast time-varying changes in dynamics [5]. For instance, these changes in dynamics can be due to structural damage, disturbance, and deployment of a payload. In these situations, MRAC may require so high learning rate that they may excite unmodeled dynamics and cause high frequency oscillations in control. It may also fail to achieve the defined task [5]. The constant unknown ideal weights assumption used in derivative-based adaptive laws extensively has been replaced with the existence of time-varying ideal weights during the construction of DF-MRAC. For this generalized assumption, parameter convergence is not possible anymore. Instead, we can only achieve bounded weight error. In [5], [21], using a Lyapunov-Krasovskii function, it has been proved that the solution of the closed-loop system is uniformly ultimately bounded (UUB). It should be noted that derivative-free weight update law does not require any modification term to provide bounded weight error.

Derivative-free adaptive law uses both delayed weight estimates and current system states and errors to suppress the effects of time-varying matched uncertainty. This update law challenges the derivative-based adaptive laws and the integral action of them. In other words, it queries the adaptive control usage for matched constant disturbance. In fact, the authors in [5] support the usage of nonadaptive controllers with integral action in bias correction.

## 1.4 Contributions of This Thesis

The purpose of this thesis is to make a fair comparison of CL-MRAC and DF-MRAC against parameter variation. In order to make a fair comparison, we should make sure that both CL-MRAC and DF-MRAC have similar theoretical results under similar assumptions. Then, comparison of their performances is meaningful.

We planned to start with the robustness analysis of CL-MRAC to time-varying ideal parameters. Since we have observed one misuse, one unnecessary use of stability theorems and one claim without reasoning in the standard exponential stability theorem of CL-MRAC developed in [4], [7], we start with the proof of this theorem. These observations are given respectively:

- In the proof of Theorem 3.2 in [4], the author uses Theorem 3.1 in [22] which is applicable to autonomous systems. However, the closed-loop system in CL-MRAC architecture is nonautonomous. The author should consider Theorem 4.10 in [9] or Theorem 4.6 in [22]. In the proof, we apply the correct theorem.
- When the dynamic history-stack, that is, the online removal or inclusion of data points is allowed, Remark 3.6 in [4] claims that exponential stability is still guaranteed as long as the introduced rank condition for recorded data points is satisfied. The author made reference to Theorem 1 in [23] and thus Theorem 2.1 in [24]. First, mentioned theorem in [24] applies to autonomous switched systems. It should be clarified whether this theorem is applicable or not. Second, even if this theorem is applicable to nonautonomous switched systems, we do not have to use this theorem because Theorem 4.10 in [9] is still valid. It is applicable to systems which have piecewise continuous right hand side in time. Third, the introduced rank condition is not sufficient to guarantee the exponential stability when we use dynamic history-stack because the derivative of the Lyapunov function along the trajectories of the closed-loop system cannot be upper bounded by one negative definite function. In order to solve this problem, we introduce an additional condition in Remark 3. It actually emphasizes the difference between being positive and being positive & separated from zero.
- In the proof of Theorem 4.1 in [7], the author claims that minimum singular value of the history-stack is monotonically increasing. When the number of stored data points is equal to the maximum allowable number of recorded data points, the claim is correct without any doubt due to the singular value maximization algorithm. However, when the number of stored data points is less than the maximum allowable number of recorded data points, the claimed

monotonicity is not obvious. In Remark 6, we show that the claim is correct by using one of the monotonicity theorems in [25]. Moreover, the condition mentioned in the previous observation holds by means of this fact.

After the observations about the exponential stability theorem of CL-MRAC, its robustness to time-varying ideal parameters is addressed. To analyze the robustness, the constant ideal parameters assumption is replaced with uniformly bounded continuously differentiable ideal parameters with uniformly bounded derivatives. Under this relaxed assumption, we prove that the solution of the closed-loop system is UUB. This proof also means that parameter drift instability in MRAC is ruled out by CL-MRAC without adding a modification term. Moreover, estimates of the ultimate bound and exponential convergence rate to that ultimate bound are provided. According to these estimates, constraints due to the theorem, and intuitive explanations, existing data recording algorithms are modified. We test CL-MRAC with modified algorithms in simulation by using sample regulation and tracking problem which include time-varying ideal parameters and disturbance. The simulation results show that the performance of CL-MRAC is highly dependent on problems and data recording algorithms. Thus, this study formally discusses the author's expectation, in [4], that CL-MRAC would recover the performance and robustness of the reference model and could pave the way for flight certification of adaptive controllers. Furthermore, the simulation results show that CL-MRAC is not as promising as it is expected in [4].

With the uniform ultimate boundedness theorem of CL-MRAC, the prerequisite for the fair performance comparison is completed. However, we have observed one missing part and one incorrect expression in the uniform ultimate boundedness theorem of DF-MRAC developed in [5], [21]. Therefore, this theorem with minor variations in its statements is also proved. These observations are given respectively:

- In the proof of Corollary 2 in [5], the authors upper bound the derivative of the Lyapunov-Krasovskii function by an expression which is a function of the error vector defined in Lyapunov-Krasovskii function. However, the intermediate

steps are not given in [5]. Therefore, we emphasize this missing part. The authors should explain the rationale behind this inequality.

- In the proof of Corollary 2 in [5], the authors end up with an incorrect expression for the exponential convergence rate to the ultimate bound. We correct this expression.

Wing rock problem with time-varying angle of attack is considered a useful benchmark for numerical illustration. Under high level uncertainty and random disturbance, controllers are tested and DF-MRAC performs better than CL-MRAC. Although it is shown that both CL-MRAC and DF-MRAC have bounded solutions under parameter variations, their adaptation strategies are completely different and the effect of this difference in the performance is obviously seen in the simulations.

## 1.5 Outline of this Thesis

In the first chapter, we make a brief introduction about the adaptive control. Then, a literature survey about MRAC and two novel adaptive controllers, namely CL-MRAC and DF-MRAC is presented. Finally, the contribution of this thesis is given.

In the second chapter, we start with the formulation of MRAC. Then, standard exponential stability theorem of CL-MRAC with minor changes in its statement is proved. With the aid of some remarks, missing parts of the theory are filled. For switching ideal parameters, the performances of CL-MRAC with existing two different data recording algorithms are evaluated in a sample problem. To analyze the robustness of CL-MRAC to time-varying ideal parameters, constant ideal parameters assumption is replaced with uniformly bounded continuously differentiable ideal parameters with uniformly bounded derivatives. Under this relaxed assumption, we prove that the solution of the closed-loop system is UUB. Moreover, estimates of the ultimate bound and exponential convergence rate to that ultimate bound are provided. According to these estimates, constraints due to the theorem, and intuitive explanations, existing data

recording algorithms are modified. We test CL-MRAC with modified algorithms in simulation by using sample regulation and tracking problem which include time-varying ideal parameters and disturbance. Under further relaxed assumption, uniformly bounded piecewise continuous ideal parameters, the uniform ultimate boundedness proof of DF-MRAC is examined. A missing part in the proof is emphasized and incorrect expression for the exponential convergence rate to the ultimate bound is corrected.

In the third chapter, wing rock problem with time-varying angle of attack is studied for numerical illustration. Under high level uncertainty and random disturbance, controllers are tested and it is shown that DF-MRAC performs better than CL-MRAC. Due to the excellent performance of DF-MRAC and its efficient adaptation strategy, its performances with different basis functions are also tested.

In the fourth chapter, the thesis is concluded with recommended future research directions.

# CHAPTER 2

# CONCURRENT LEARNING & DERIVATIVE-FREE MODEL REFERENCE ADAPTIVE CONTROL

## 2.1 Introduction

Concurrent Learning Model Reference Adaptive Control (CL-MRAC) is a recently introduced controller which utilizes concurrent usage of recorded and current data to guarantee exponential convergence of tracking error and parameter. Its theorem for different class of plants can be found in [4], [17], [7], [18], [19]. This theorem depends on the existence of constant unknown ideal parameters. Derivative-Free Model Reference Adaptive Control (DF-MRAC) is another recently introduced controller which allows time-varying ideal parameters and provides uniformly ultimately bounded (UUB) closed-loop solution [5], [21].

In this chapter, the constant ideal parameters assumption of CL-MRAC is replaced with time-varying ideal parameters assumption which is similar to the one in DF-MRAC but still stricter than it. Then, we prove that the solution of the closed-loop system is UUB. Moreover, estimates of the ultimate bound and exponential convergence rate to that ultimate bound are provided. According to these estimates, constraints due to the theorem, and intuitive explanations, existing data recording algorithms are modified. We test CL-MRAC with modified algorithms in simulation by using sample regulation and tracking problem. Besides this new analysis, the proofs of the existing CL-MRAC and DF-MRAC theorems are examined to fill or emphasize the observed missing parts.

## 2.2 Model Reference Adaptive Control (MRAC)

In this section, we start with a formulation of MRAC problem. Consider the following uncertain system

$$\dot{x}(t) = Ax(t) + B\big[u(t) + \Delta\big(x(t)\big)\big], \tag{1}$$

where $x(t) \in R^n$ is the state vector, $u(t) \in R^m$ is the control input vector, $A \in R^{n \times n}$ and $B \in R^{n \times m}$ are known matrices such that the pair $(A, B)$ is controllable, and $\Delta\big(x(t)\big) : R^n \to R^m$ is a matched uncertainty. It is also assumed that full state is available for feedback and control input is restricted to the class of admissible controls consisting of measurable functions.

A reference model that characterizes the desired closed-loop response of the system in (1) is given by

$$\dot{x}_m(t) = A_m x_m(t) + B_m r(t), \tag{2}$$

where $x_m(t) \in R^n$ is the reference state vector, $r(t) \in R^r$ is bounded piecewise continuous reference input, $A_m \in R^{n \times n}$ is Hurwitz, and $B_m \in R^{n \times r}$ with $r \leq m$. Since $A_m$ is Hurwitz and $r(t)$ is bounded, $x_m(t)$ is uniformly bounded for all $x_m(0)$.

**Assumption 1** The matched uncertainty in (1) can be linearly parameterized as

$$\Delta(x) = W^T \beta(x), \qquad x \in \Omega_x, \tag{3}$$

where $W \in R^{s \times m}$ is the unknown constant weight matrix, $\beta\big(x(t)\big) : R^n \to R^s$ is a vector of known basis functions $\beta(x) = [\beta_1(x),\ \beta_2(x),\ \dots,\ \beta_s(x)]^T \in R^s$ and $\Omega_x$ is a sufficiently large compact subset of $R^n$. Note that (1) is either linear or nonlinear uncertain system, depending on $\beta(x)$.

*An example of (3)*:

$$\Delta(x) = w_1 \sin(x) + w_2 \cos(x) + w_3 x^2, \qquad x \in R,$$

where $W = [w_1,\ w_2,\ w_3]^T$, $\beta(x) = [\sin(x),\ \cos(x),\ x^2]^T$.

The tracking control law is specified by

$$u(t) = u_n(t) - u_{ad}(t), \tag{4}$$

where $u_n(t)$ is a nominal controller given by

$$u_n(t) = -K_1 x(t) + K_2 r(t), \tag{5}$$

where $K_1 \epsilon R^{m \times n}$ and $K_2 \epsilon R^{m \times r}$ are nominal controller gains, and adaptive feedback control component given by

$$u_{ad}(t) = \widehat{W}^T(t)\beta\big(x(t)\big), \tag{6}$$

where $\widehat{W}(t) \epsilon R^{s \times m}$ denotes the estimate of $W$.

**Assumption 2** (*Matching Condition*) There exist $K_1 \epsilon R^{m \times n}$ and $K_2 \epsilon R^{m \times r}$ such that $A_m = A - BK_1$ and $B_m = BK_2$.

Define the state tracking error as

$$e(t) \coloneqq x(t) - x_m(t). \tag{7}$$

Differentiating (7)

$$\dot{e}(t) = Ax(t) + Bu(t) + B\Delta\big(x(t)\big) - A_m x_m(t) - B_m r(t), \tag{8}$$

using the control law in (4)

$$\begin{aligned} \dot{e}(t) = (A - BK_1)x(t) + BK_2 r(t) - A_m x_m(t) - B_m r(t) \\ +B\big[\Delta\big(x(t)\big) - u_{ad}(t)\big], \end{aligned} \tag{9}$$

(9) subject to Assumption 2

$$\dot{e}(t) = A_m e(t) + B\big[\Delta\big(x(t)\big) - u_{ad}(t)\big], \tag{10}$$

(10) represents the state tracking error dynamics.

Since $A_m$ is Hurwitz, for every symmetric positive-definite matrix $Q \in R^{n \times n}$, there exists a unique symmetric positive-definite solution $P \in R^{n \times n}$ to the Lyapunov equation

$$A_m^T P + P A_m = -Q. \tag{11}$$

For the uncertainty given in Assumption 1, it is well known from [1], [2] that the baseline adaptive law

$$\dot{\widehat{W}}(t) = \Gamma \beta\big(x(t)\big) e^T(t) P B, \tag{12}$$

where $\Gamma$ is a positive learning rate, guarantees that $\widehat{W}(t)$ remains bounded and $e(t) \to 0$ as $t \to \infty$. However, (12) does not guarantee the convergence of $\widehat{W}(t)$ and rate of convergence of $e(t)$. It is also known that $e(t) \to 0$ and $\widehat{W}(t) \to W$ as $t \to \infty$ if and only if $\beta(x(t))$ is persistently exciting (PE) [1], [10].

## 2.3 Concurrent Learning Model Reference Adaptive Control (CL-MRAC)

Concurrent learning adaptive control uses recorded and current data concurrently to guarantee exponential tracking and parameter error convergence without requiring persistence excitation of the states [4].

Concurrent learning adaptive law has the following form

$$\dot{\widehat{W}}(t) = \Gamma \left( \beta\big(x(t)\big) e^T(t) P B + \sum_{j=1}^{p} \beta\big(x_j\big) \varepsilon_j^T(t) \right), \tag{13}$$

where $j$ denotes the recorded data point at time $t_j$, and

$$\varepsilon_j(t) = \Delta\big(x_j\big) - \widehat{W}^T(t) \beta\big(x_j\big). \tag{14}$$

To evaluate (13), $\beta\big(x_j\big)$ and $\Delta\big(x_j\big)$ are required for the $j^{th}$ data point. The basis vector $\beta\big(x_j\big) \in R^s$ is stored in a history-stack such that the Condition 1 is satisfied.

**Condition 1** If $Z = [\beta(x_1),\ \beta(x_2),\ \dots,\ \beta(x_p)] \epsilon\ R^{s \times p}$ represents the history-stack, then $rank(Z) = s$. That is, the history stack contains as many linearly independent columns as the dimension of the basis vector.

Note that Condition 1 directly implies that the number of basis vectors $p$ stored in $Z$ must be at least the dimension of the basis vector $s$, i.e. $p \geq s$. In addition to the basis vector $\beta(x_j)$, (13) requires the associated model error $\Delta(x_j)$.

**Remark 1** If $B$ has full column rank, $\Delta(x_j)$ can be observed from (1) by using left pseudo inverse of $B$

$$\Delta(x_j) = (B^T B)^{-1} B^T [\dot{x}_j - A x_j - B u_j]. \tag{15}$$

In order to estimate the system uncertainty, we require only the estimation of $\dot{x}$ because $A, B, x_j$, and $u_j$ are known. If the explicit measurement of $\dot{x}$ is available, (15) can be directly used to calculate the system uncertainty. Otherwise, $\dot{x}_j$ can be estimated using an implementation of a fixed point smoother as it is done in [17], [7]. In the thesis, it is assumed that the explicit measurement of $\dot{x}$ is available or $\dot{x}_j$ is estimated without any error.

Define the weight error as

$$\widetilde{W}(t) \coloneqq W - \widehat{W}(t). \tag{16}$$

Then, the state tracking error dynamics in (10) with Assumption 1 is given by

$$\dot{e}(t) = A_m e(t) + B \widetilde{W}^T(t) \beta(x(t)). \tag{17}$$

(14) can be written as

$$\varepsilon_j(t) = \widetilde{W}^T(t) \beta(x_j). \tag{18}$$

Using (18) and noting that $W$ is constant, the weight error dynamics can be obtained from (13):

$$\dot{\widetilde{W}}(t) = -\Gamma\left(\beta\big(x(t)\big)e^T(t)PB + \sum_{j=1}^{p}\beta\big(x_j\big)\beta^T\big(x_j\big)\widetilde{W}(t)\right). \tag{19}$$

The following theorem and its proof for different class of plants can be found in [4], [17], [7], [18], [19]. For the sake of completeness, the theorem with minor variations in its statement is proved. Remarks about its usage and missing parts are made in this section.

**Theorem 1** Consider the system in (1) subject to Assumption 1, the reference model in (2), and the tracking control law in (4), with the nominal control component given by (5) subject to Assumption 2 and the adaptive feedback control component given by (6) which has the concurrent learning weight update law in (13). It is also assumed that the recorded data points satisfy Condition 1 at $t = t_0$ and the history-stack is static, i.e. it is not overwritten, then the origin, i.e. $\left(e(t),\ \widetilde{W}(t)\right) \equiv 0$ of the system given by (17) and (19) is exponentially stable.

**Proof:** To keep the formulas short, drop the argument $t$ in the proof.

Define $\xi \coloneqq \left[e^T,\ vec\big(\widetilde{W}\big)^T\right]^T$ and try the following continuously differentiable function as a Lyapunov function candidate

$$V\big(e,\widetilde{W}\big) = \frac{1}{2}e^TPe + \frac{1}{2\Gamma}tr\big(\widetilde{W}^T\widetilde{W}\big). \tag{20}$$

By using $tr\big(\widetilde{W}^T\widetilde{W}\big) = vec\big(\widetilde{W}\big)^T vec(\widetilde{W})$, we have

$$V(\xi) = \frac{1}{2}\xi^T\tilde{P}\xi, \tag{21}$$

where $\tilde{P} = diag[P,\ \Gamma^{-1}I]$. Then, (21) can be bounded from below and above by

$$\frac{1}{2}\min\{\lambda_{min}(P),\Gamma^{-1}\}\,\|\xi\|^2 \le V(\xi) \le \frac{1}{2}\max\{\lambda_{max}(P),\Gamma^{-1}\}\,\|\xi\|^2. \tag{22}$$

Note that $V(0) = 0$ and $V(\xi) > 0,\ \ \forall\,\xi \neq 0$.

From (22), define the following positive constants,

$$\alpha \coloneqq 2, \tag{23}$$

$$k_1 \coloneqq \frac{1}{2}\min\{\lambda_{min}(P), \Gamma^{-1}\}, \tag{24}$$

$$k_2 \coloneqq \frac{1}{2}\max\{\lambda_{max}(P), \Gamma^{-1}\}. \tag{25}$$

The time derivative of (20) along trajectories of (17) and (19) can be expressed as

$$\begin{aligned}\dot{V}\left(t, e, \widetilde{W}\right) &= \frac{1}{2}e^T[A_m^T P + PA_m]e + e^T PB\widetilde{W}^T\beta(x) + \Gamma^{-1}tr(\widetilde{W}^T\dot{\widetilde{W}}) \\ &= \frac{1}{2}e^T[A_m^T P + PA_m]e + e^T PB\widetilde{W}^T\beta(x) \\ &\quad -tr\left(\widetilde{W}^T\beta(x)e^T PB + \widetilde{W}^T\sum_{j=1}^{p}\beta(x_j)\beta^T(x_j)\widetilde{W}\right).\end{aligned} \tag{26}$$

For any arbitrary matrices $S,\ T \epsilon R^{m\times m}$, $tr(S+T) = tr(S) + tr(T)$. Using the given property of trace and the Lyapunov equation in (11), we have

$$\begin{aligned}\dot{V}\left(t, e, \widetilde{W}\right) &= -\frac{1}{2}e^T Qe + e^T PB\widetilde{W}^T\beta(x) - tr\left(\widetilde{W}^T\beta(x)e^T PB\right) \\ &\quad -tr\left(\widetilde{W}^T\sum_{j=1}^{p}\beta(x_j)\beta^T(x_j)\widetilde{W}\right).\end{aligned} \tag{27}$$

For any arbitrary row vectors $a,\ b\ \epsilon R^{1\times m}$, $tr(a^T b) = ba^T = \sum_{i=1}^{m} a_i b_i$. Therefore, $e^T PB\widetilde{W}^T\beta(x) = tr\left(\widetilde{W}^T\beta(x)e^T PB\right)$. (27) can be written as

$$\dot{V}\left(t, e, \widetilde{W}\right) = -\frac{1}{2}e^T Qe - tr\left(\widetilde{W}^T\sum_{j=1}^{p}\beta(x_j)\beta^T(x_j)\widetilde{W}\right). \tag{28}$$

To analyze the second term on the right hand side of (28), define the following matrix

$$\eta = \sum_{j=1}^{p} \beta(x_j)\beta^T(x_j). \tag{29}$$

*Claim*: If Condition 1 is satisfied, then $\eta = \eta^T \succ 0$.

*Proof*: Note that $\sum_{j=1}^{p} \beta(x_j)\beta^T(x_j) = ZZ^T,\ \ Z \in R^{s \times p}$, then

$$\eta = ZZ^T,\ \ \eta \in R^{s \times s}. \tag{30}$$

Symmetry arises from the fact that $\eta^T = ZZ^T = \eta$. To show that $\eta$ is positive-definite, we pick an arbitrary vector $\omega \in R^s$ and compute the following inner product

$$< \omega, \eta\omega > = \omega^T\eta\omega = \omega^T ZZ^T\omega = <\ Z^T\omega, Z^T\omega > =\ \|Z^T\omega\|^2. \tag{31}$$

$\|Z^T\omega\|$ is positive unless $Z^T\omega = 0$. Due to Condition 1, $rank(Z^T) = s$. Therefore, $null(Z^T) = \{0\}$. It implies that $Z^T\omega = 0$ if and only if $\omega = 0$. □

For conformable matrices $E, F$, and $G$, $tr(EFG) = vec(E^T)^T(I \otimes F)vec(G)$ [26]. By using the mentioned fact, (28) can be rewritten as

$$\dot{V}(t, e, \widetilde{W}) = -\frac{1}{2}e^T Qe - vec(\widetilde{W})^T \tilde{\eta} vec(\widetilde{W}), \tag{32}$$

where $\tilde{\eta} = diag[\eta,\ \eta,\ \ldots,\ \eta],\ \tilde{\eta} \in R^{(s \times m) \times (s \times m)}$. Hence, we have the following inequalities

$$\dot{V}(t, e, \widetilde{W}) \leq -\frac{1}{2}\lambda_{min}(Q)e^T e - \lambda_{min}(\eta)vec(\widetilde{W})^T vec(\widetilde{W}), \tag{33}$$

$$\dot{V}(t, \xi) \leq -\min\left\{\frac{1}{2}\lambda_{min}(Q), \lambda_{min}(\eta)\right\}\|\xi\|^2. \tag{34}$$

From (34), define the following positive constant

$$k_3 \coloneqq \min\left\{\frac{1}{2}\lambda_{min}(Q), \lambda_{min}(\eta)\right\}. \tag{35}$$

By (22), (34) with $\alpha$ in (23), $k_1$ in (24), $k_2$ in (25), $k_3$ in (35), and Theorem 4.10 in [9], the origin, i.e. $\xi = 0$, of the system given by (17) and (19) is exponentially stable. If Assumption 1 holds globally, i.e. $\Omega_x = R^n$, then $\xi = 0$ is globally exponentially stable. ■

**Remark 2** From the proof of Theorem 4.10 in [9], we know that $\|\xi(t)\|$ is bounded from above by exponentially decaying function such that

$$\|\xi(t)\| \leq \sqrt{\frac{k_2}{k_1}}\|\xi(t_0)\|\mathrm{e}^{-\lambda(t-t_0)}, \quad \forall\, t \geq t_0 \geq 0, \tag{36}$$

where $\lambda = k_3/(\alpha k_2) = \min\left\{\frac{1}{2}\lambda_{min}(Q), \lambda_{min}(\eta)\right\} / \max\{\lambda_{max}(P), \Gamma^{-1}\}$. It is obviously seen that the rate of convergence is dependent on the spectral properties of $Q$, $P$, Γ, and $\eta$. $Q$ and $P$ are determined by the reference model (nominal controller) and Γ is the positive constant learning rate in (13). On the other hand, $\eta$ is specified by the choice of recorded data.

**Remark 3** The static history-stack assumption of Theorem 1 can be relaxed if

$$\lambda_{min}(\eta(t)) \geq \bar{\lambda} > 0, \quad \forall\, t \geq t_0 \geq 0. \tag{37}$$

Then, (34) becomes

$$\dot{V}(t,\xi) \leq -\min\left\{\frac{1}{2}\lambda_{min}(Q), \bar{\lambda}\right\}\|\xi\|^2. \tag{38}$$

The online removal or inclusion of data points in (13) does not affect the inequalities (22) and (38) as long as (37) holds. Therefore, $\xi = 0$ is still exponentially stable according to Theorem 4.10 in [9]. If the imposed condition in (37) is queried, one should review the Nonautonomous Systems part of Chapter 4 in [9] or Example 2.1 in [24].

**Remark 4** In cases where a pre-recorded data is not available at $t = t_0$, the second sentence of Theorem 1 should be replaced with the following one:

i. Consider a data recording algorithm which selects data points $\beta(x_j)$ and the associated model error $\Delta(x_j)$, then the origin, i.e. $\left(e(t),\ \widetilde{W}(t)\right) \equiv 0$ of the closed-loop system given by (17) and (19) is uniformly stable.

ii. In addition to i, if $r(t)$ is such that $\beta(x(t))$ is exciting over a finite interval $(t_0, T)$, such that, for $T$, Condition 1 is satisfied by a data recording algorithm, and (37) is satisfied for all $t \geq T$, then the origin, i.e. $\left(e(t),\ \widetilde{W}(t)\right) \equiv 0$ of the closed-loop system given by (17) and (19) is exponentially stable for all $t \geq T$.

The effects of the new statement on the proof of Theorem 1 are examined as follows:

i. Now, $\eta(t)$ is positive-semidefinite for all $t \geq t_0$. Hence, (33) can be written as

$$\dot{V}(t, e, \widetilde{W}) \leq -\frac{1}{2}\lambda_{min}(Q)\|e\|^2 \leq 0. \tag{39}$$

(39) implies that the origin of the system given by (17) and (19) is uniformly stable.

ii. In addition to the first part, assume that $r(t)$ is such that $\beta(x(t))$ is exciting over a finite interval $(t_0, T)$. Then, a data recording algorithm guarantees that the history-stack contains as many linearly independent columns as the dimension of the basis vector for all $t \geq T$ and (37) holds: $\lambda_{min}(\eta(t)) \geq \bar{\lambda} > 0$ for all $t \geq T$. Now, the inequality (38) is valid for all $t \geq T$. Therefore, $\xi = 0$ is exponentially stable for all $t \geq T$.

**Remark 5** In [20], the performance of three different data point selection methods, namely static history-stack, cyclic history-stack, and singular value maximizing, were compared. Among them, singular value maximizing approach provides the fastest parameter convergence. The idea behind the singular value maximizing approach is the following. From (36), it is known that rate of convergence is directly proportional to the minimum eigenvalue of $\eta$. We also know that

$$\sigma_{min}(Z) = [\lambda_{min}(ZZ^T)]^{1/2} = [\lambda_{min}(\eta)]^{1/2}. \quad (40)$$

Hence, the history-stack is populated to maximize the minimum singular value of it.

In the simulations, we will also utilize the singular value maximizing algorithm for recording data points. Thus, the algorithm used in [17], [7], [20] is described here.

**Algorithm 1**

**if** $p = 0$ **then**
  $p = p + 1$
  $Z_t(:, p) = \beta(x(t))$
  $\Delta_t(:, p) = (B^T B)^{-1} B^T [\dot{x}(t) - Ax(t) - Bu(t)]$
**else if** $\frac{\|\beta(x(t)) - \beta(x_{p^-})\|^2}{\|\beta(x(t))\|} \geq \varepsilon$ **or** $rank([Z_t, \beta(x(t))]) > rank(Z_t)$ **then**
  **if** $p < \bar{p}$ **then**
    $p = p + 1$
    $Z_t(:, p) = \beta(x(t))$
    $\Delta_t(:, p) = (B^T B)^{-1} B^T [\dot{x}(t) - Ax(t) - Bu(t)]$
  **else**
    $T = Z_t$
    $SV_{old} = \sigma_{min}(Z_t)$
    **for** $j = 1$ to $p$ **do**
      $Z_t(:, j) = \beta(x(t))$
      $SV(j) = \sigma_{min}(Z_t)$
      $Z_t = T$
    **end for**
    find max $SV$ and let $k$ denote the corresponding column index
    **if** max $SV > SV_{old}$ **then**
      $Z_t(:, k) = \beta(x(t))$
      $\Delta_t(:, k) = (B^T B)^{-1} B^T [\dot{x}(t) - Ax(t) - Bu(t)]$
    **end if**
  **end if**
**end if**
**end if**

In Algorithm 1, $p \, \epsilon \, N$ and $p^- \epsilon \, N$ represent the number of stored points and the stored last point respectively. $Z_t$ denotes the history-stack at time $t$. Similar to $Z_t$, $\Delta_t$ denotes the matrix containing the associated model error information. The $p^{th}$ column of $Z_t$ and $\Delta_t$ are denoted by $Z_t(:, p)$ and $\Delta_t(:, p)$ respectively. $\varepsilon$ is a positive constant and $\bar{p} \, \epsilon \, N$ is the maximum allowable number of recorded data points. Furthermore, the first condition

of $else\ if$ should be modified to avoid numerical problems if $\|\beta(x(t))\|$ has a possibility of being around zero.

**Remark 6** After $p = \bar{p}$, the minimum singular value of $Z_t$ is nondecreasing because one of the old data points is replaced with the new data point such that the minimum singular value of $Z_t$ is increased, if possible. Now, suppose that $rank(Z_t) = s$ when $p = s$. Is the minimum singular of $Z_t$ nondecreasing for $p \in [s,\ \bar{p}]$? Yes, because

$$0 < \lambda_{min}(\eta(t)) \leq \lambda_{min}\left(\eta(t) + \beta(x_p)\beta^T(x_p)\right), \quad \forall\, p \in [s,\ \bar{p}] \tag{41}$$

from the special application of Theorem 10.3.1, one of the monotonicity theorems, in [25]. Hence, it can be concluded that (37) holds after $rank(Z_t) = s$.

## 2.4 Robustness of CL-MRAC to Switching in Ideal Weights

If the ideal weights in (3) switch in an unknown or undetectable manner, then Assumption 1 is violated. In that case, two questions arise:

i. What happens if irrelevant data points are not replaced with the relevant ones after a switch in the ideal weights?
   It is proved in [7] that the origin of the new system is ultimately bounded.
ii. How do we modify Algorithm 1 to remove irrelevant recorded data?
   Proposed algorithm for switched linear systems in [27] can also be used for the uncertain system given in (1). This algorithm is described in Algorithm 2.

In Algorithm 2, entire recorded data points are removed or added according to the switching surface determined by $g_1$, $g_2$, $g_3$, $\bar{t}$, $Z_{rec}$, and $Z_{use}$. We utilize $Z_{use}$, $\Delta_{use}$, and $p_{use}$ for concurrent learning adaptive law in (13). Note that $g_1$, $g_2$, and $g_3$ are positive constants. $Count$ is initialized to 0 and any data for use is equal to the recorded one until the singular value inequality is satisfied for the first time. Then, $g_3 > 0$ ensures the positive-definiteness of $Z_{use}{Z^T}_{use}$.

**Algorithm 2**

Use Algorithm 1 (replace $Z_t$ and $\Delta_t$ with $Z_{rec}$ and $\Delta_{rec}$ respectively)
**if** $Count = 0$ **then**
  $Z_{use} = Z_{rec}$
  $\Delta_{use} = \Delta_{rec}$
  $p_{use} = p$
**end if**
**if** $\sigma_{min}(Z_{rec}) > \sigma_{min}(Z_{use}) g_1 e^{-g_2(t-\bar{t})} + g_3$ **then**
  $Count = 1$
  $Z_{use} = Z_{rec}$
  $\Delta_{use} = \Delta_{rec}$
  $p_{use} = p$

  $Z_{rec} = 0$
  $\Delta_{rec} = 0$
  $p = 0$
  $\bar{t} = t$
**end if**

## 2.5 Simulation Example

We compare the effectiveness of Algorithm 1 with Algorithm 2 on the following simple system:

$$\begin{bmatrix} \dot{x}_1 \\ \dot{x}_2 \end{bmatrix} = \begin{bmatrix} 0 & 1 \\ 0 & 0 \end{bmatrix} \begin{bmatrix} x_1 \\ x_2 \end{bmatrix} + \begin{bmatrix} 0 \\ 1 \end{bmatrix} [u + W^T(t)\beta(x)], \tag{42}$$

where the ideal weights of the system switch at an unknown time

$$W^T(t) = \begin{cases} [0 \quad 1 \quad 2.5], & if\ 0 \le t < 50\ sec \\ [-0.5 \quad 4 \quad -0.5], & if\ 50 \le t \le 100\ sec \end{cases}, \tag{43}$$

and $\beta(x) = [1,\ x_1,\ x_2]^T$. Furthermore, $A \coloneqq \begin{bmatrix} 0 & 1 \\ 0 & 0 \end{bmatrix}$ and $B \coloneqq \begin{bmatrix} 0 \\ 1 \end{bmatrix}$.

System and input matrix of the reference model are selected as

$$A_m = \begin{bmatrix} 0 & 1 \\ -\omega_n^2 & -2\zeta\omega_n \end{bmatrix}, \quad B_m = \begin{bmatrix} 0 \\ \omega_n^2 \end{bmatrix} \tag{44}$$

with a pair of complex conjugate eigenvalues which have natural frequency $\omega_n = 2$ and damping ratio $\zeta = 0.7$. From the matching condition given in Assumption 2, nominal controller gains are $K_1 = [4,\ \ 2.8]$ and $K_2 = 4$.

In the simulations, three adaptive controllers are tested. These are the baseline adaptive law in (12), concurrent learning adaptive law in (13) with Algorithm 1 and Algorithm 2. For all adaptive controllers, the learning rate $\Gamma$ is set to 2 and $Q = diag[1,\ \ 1]$. In the concurrent learning cases, maximum number of recorded data points $\bar{p}$ is 15 and $\varepsilon$ used in data recording algorithms is 0.08. The switching surface parameters of Algorithm 2 are chosen as $g_1 = 1$, $g_2 = 0.02$, $g_3 = 10^{-3}$, and $\bar{t} = -10^3$. We run the simulations with a 0.005 sec time step using Euler integration.

Figure 1 shows the reference model tracking performance of the nominal controller and Figure 2 shows the control input. It is obviously seen that nominal controller cannot achieve reference model tracking. Moreover, bounded input yields unbounded state after switching in ideal weights at $t = 50\ sec$. Consider the system in (42) with nominal controller after switching in ideal weights, i.e. $50 \le t \le 100\ sec$

$$\begin{aligned} \dot{x} &= A_m x + B_m r + \begin{bmatrix} 0 \\ 1 \end{bmatrix} [-0.5 \quad 4 \quad -0.5] \begin{bmatrix} 1 \\ x_1 \\ x_2 \end{bmatrix} \\ &= A_m x + \begin{bmatrix} 0 & 0 \\ 4 & -0.5 \end{bmatrix} x + B_m r + \begin{bmatrix} 0 \\ -0.5 \end{bmatrix} \\ &= \begin{bmatrix} 0 & 1 \\ 0 & -3.3 \end{bmatrix} x + B_m \left( r - \frac{0.5}{4} \right). \end{aligned} \tag{45}$$

(45) is a linear time-invariant system with system matrix $A_{cl} := \begin{bmatrix} 0 & 1 \\ 0 & -3.3 \end{bmatrix}$ and input matrix $B_m$. For the ongoing analysis, let initial condition be zero and $x_1$ be measured. Then, output matrix is $C = [1 \quad 0]$. Since the pair $(A_{cl}, B_m)$ is controllable and the pair

$(A_{cl}, C)$ is observable, the realization is minimal. In this case, the characteristic polynomial of $A_{cl}$ is equal to the pole polynomial $d(s)$ of the transfer function from input to output. Therefore, we can directly conclude that (45) with output matrix $C$ is not bounded-input, bounded-output (BIBO) stable because $A_{cl}$ is not Hurwitz [28].

If we had known the ideal weights of the system during the nominal controller synthesis, we would have realized and solved the instability problem described in the foregoing analysis. However, we do not know the ideal weights. Thus, it explains why we use adaptive controllers to suppress or cancel the effects of the matched uncertainty.

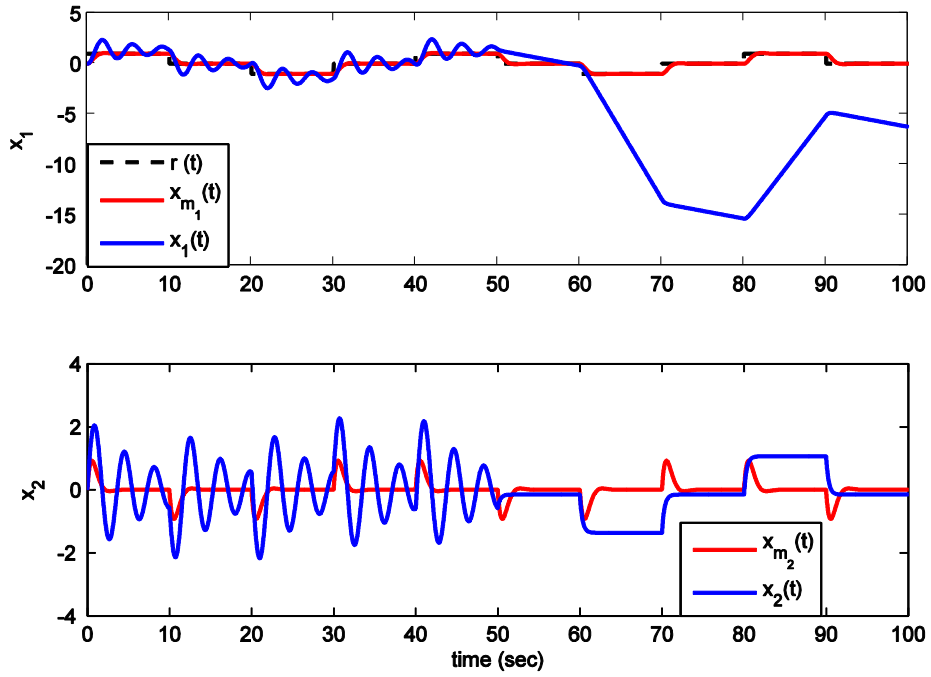


**Figure 1 Responses with nominal controller**

In Figure 3, the tracking performance of the baseline adaptive law is demonstrated and it is clearly better than nominal controller. Figure 4 shows the control input and uncertainty estimation. Note that uncertainty estimation does not uniformly cancel the matched uncertainty because the estimated weights do not converge to their ideal values as it is seen in Figure 5. It is the well-known issue of the baseline adaptive law because for weight convergence, basis vectors must be PE.

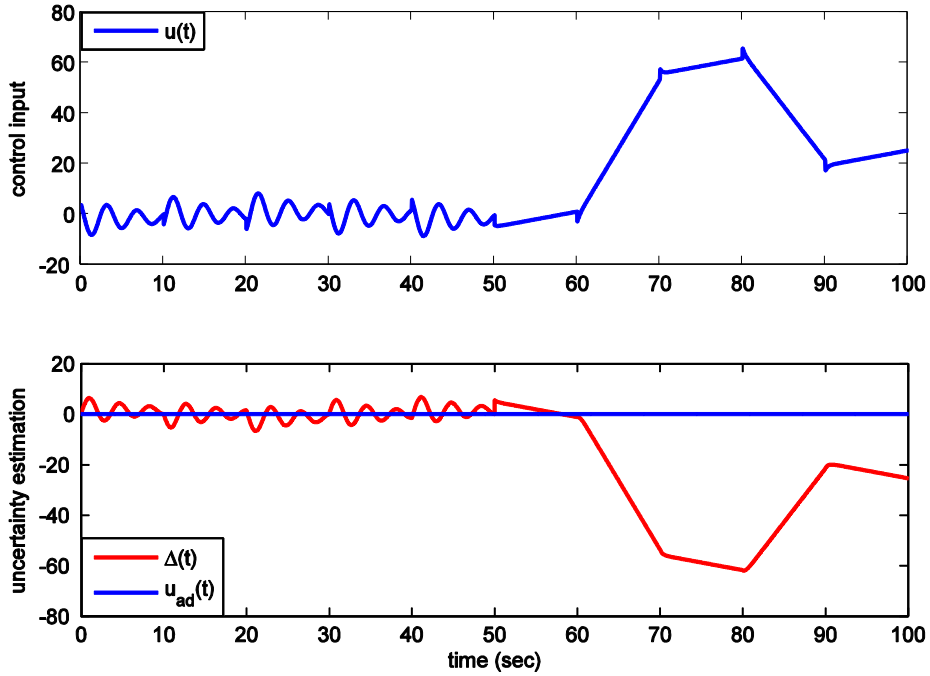


**Figure 2 Control input with nominal controller**

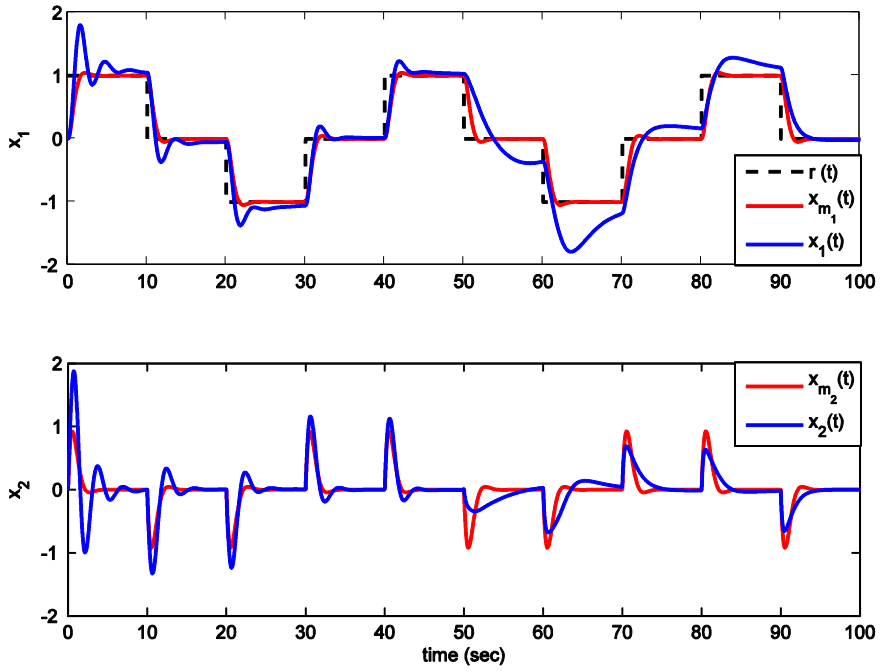


**Figure 3 Responses with baseline MRAC**

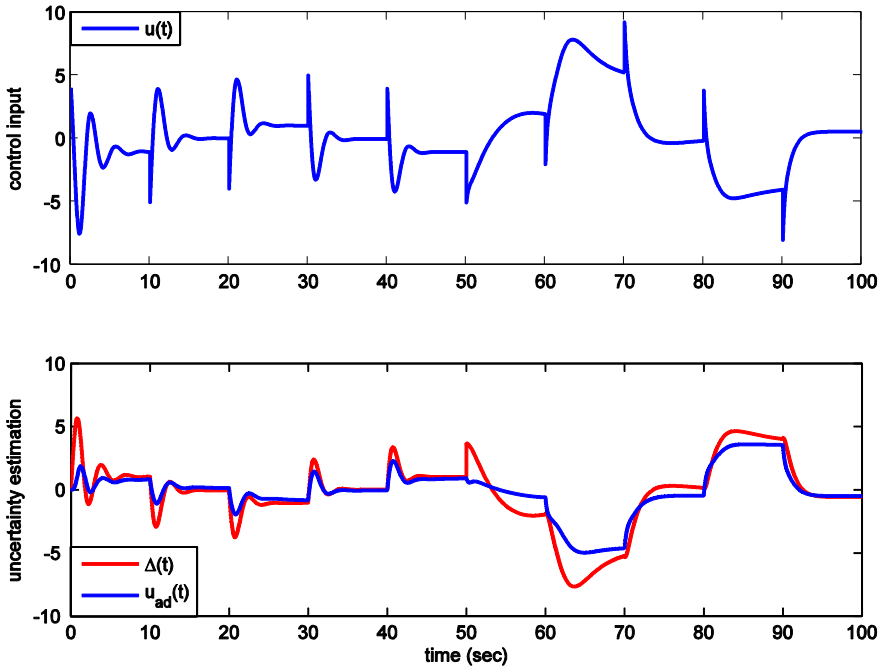


**Figure 4 Control input and uncertainty estimation with baseline MRAC**

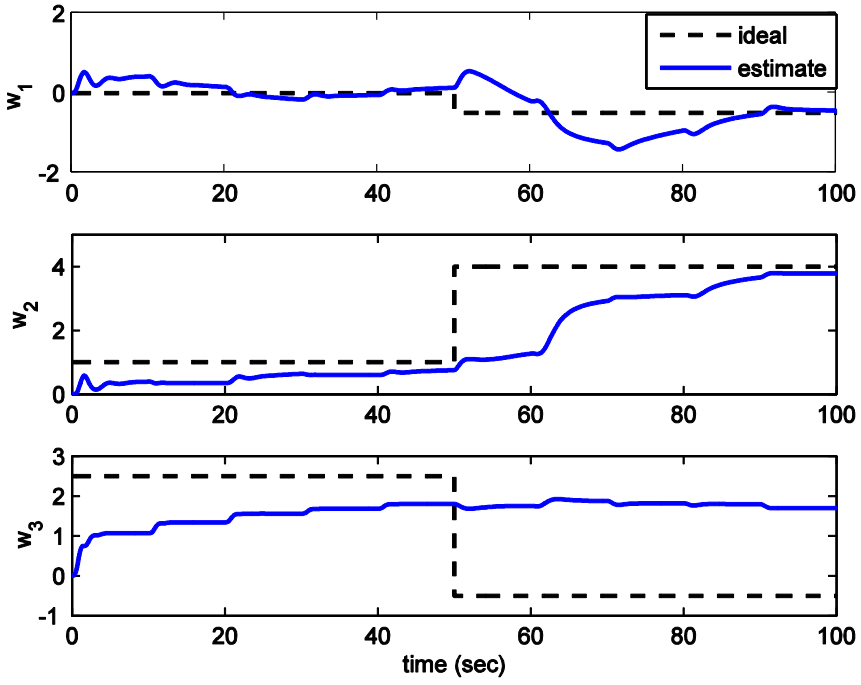


**Figure 5 Estimate of the ideal weights with baseline MRAC**

After the introductory simulation results with nominal controller and MRAC, it is time to present the outcomes of CL-MRAC. Figure 6 and Figure 10 demonstrate the tracking performance of CL-MRAC with Algorithm 1 and Algorithm 2 respectively. Their performance evaluation is divided into two parts:

i. Before the Switch in Ideal Weights, i.e. $t < 50\ sec$

In this part, ideal weights can be considered constant. Therefore, weight convergence is expected. As it is seen in Figure 8 and Figure 12, CL-MRAC with Algorithm 1 and Algorithm 2 achieve weight convergence. Thus, adaptive control inputs are very close to the matched uncertainty as it is seen in Figure 7 and Figure 11. At this point, it should be noted that Algorithm 1 provides faster parameter convergence than Algorithm 2. The difference in convergence rate is due to the difference in minimum singular value evolution; see Figure 9 and Figure 13. The history-stack of Algorithm 1 reaches higher minimum singular value. For example, $\sigma_{min}(Z_t) \cong 1.2$ by Algorithm 1, $\sigma_{min}(Z_{use}) \cong 0.1$ by Algorithm 2 at $t = 1.5\ sec$. The following explanation clarifies this difference. Algorithm 1 does not remove relevant data. However, Algorithm 2 replaces data with the recent ones though ideal weights do not vary. In other words, it causes unnecessary removal of relevant data because of the switching surface, thus limited time periods can be devoted to minimum singular value maximization. The fast convergence property of Algorithm 1 is also seen in the tracking performance when Figure 6 is compared with Figure 10. Furthermore, tracking performance and parameter convergence superiority of CL-MRAC over MRAC is clearly demonstrated in this part.

ii. After the Switch in Ideal Weights, i.e. $t \geq 50\ sec$

In contrast to previous part, weight convergence is not guaranteed in theory but ultimate boundedness is expected. If the minimum singular value evolution is evaluated to figure out the algorithm which provides faster convergence, one can draw wrong conclusion. Although the minimum singular values with Algorithm 1 is higher than the ones with Algorithm 2; see Figure 9 and Figure 13, one third of the data points, i.e. $5/15$ are irrelevant even at $t = 100\ sec$ when Algorithm

1 is used. As it is seen in Figure 8, estimated weights do not converge to ideal values. Tracking performance of Algorithm 1 improves gradually but adaptive control input cannot uniformly cancel the matched uncertainty due to lack of parameter convergence; see Figure 6 and Figure 7. On the other hand, Figure 13 shows that Algorithm 2 gets rid of irrelevant data points at $t = 57.665\, sec$. Therefore, Algorithm 2 achieves parameter convergence, see Figure 12. However, during the period from switching in ideal weights to irrelevant data removal, except one recent data point, Algorithm 2 uses irrelevant data points. Hence, it degrades the tracking performance and the uncertainty estimation in this period compared to Algorithm 1. With the removal of irrelevant data points, the tracking performance and the uncertainty estimation are immediately improved because of the parameter convergence; see Figure 10 and Figure 11. Moreover, both concurrent learning adaptive controllers perform better than baseline adaptive controller except the mentioned period encountered in Algorithm 2.

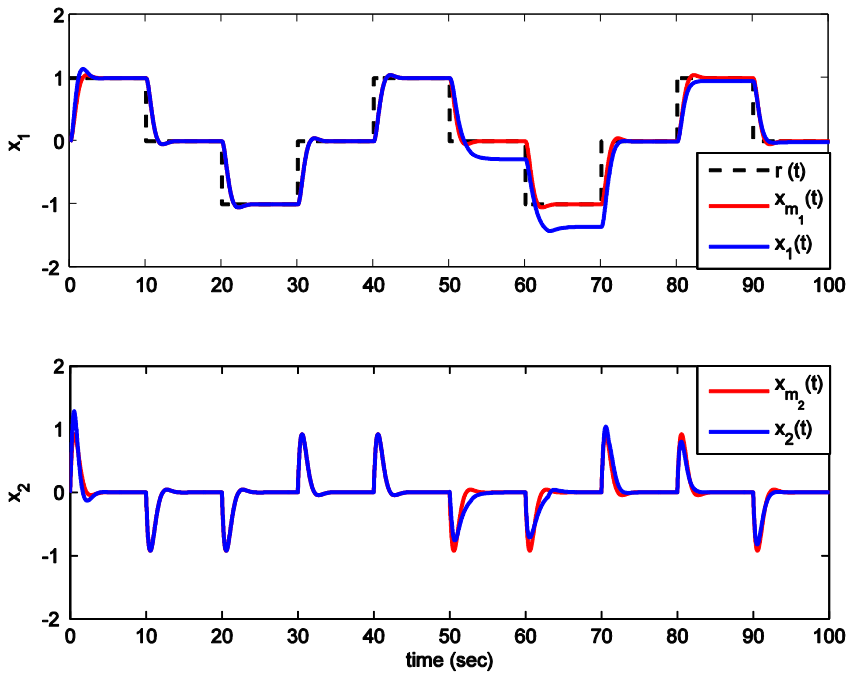


**Figure 6 Responses with CL-MRAC & Algorithm 1**

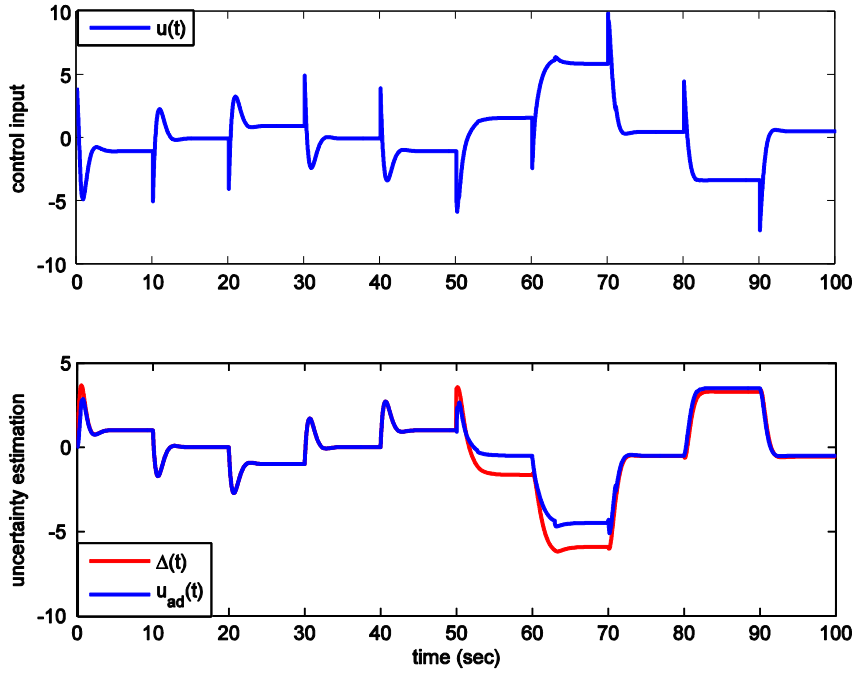


**Figure 7 Control input and uncertainty estimation with CL-MRAC & Algorithm 1**

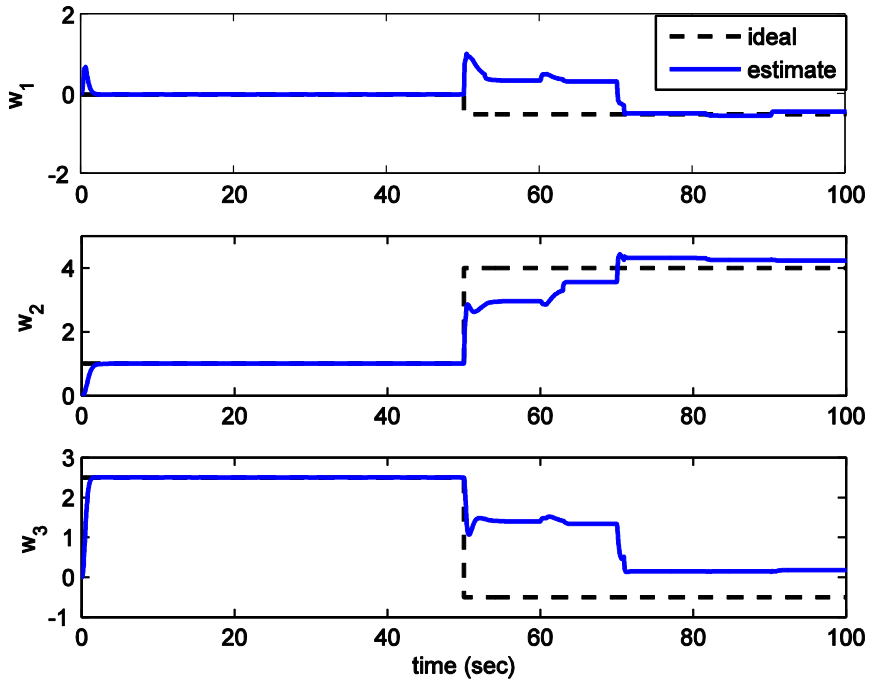


**Figure 8 Estimate of the ideal weights with CL-MRAC & Algorithm 1**

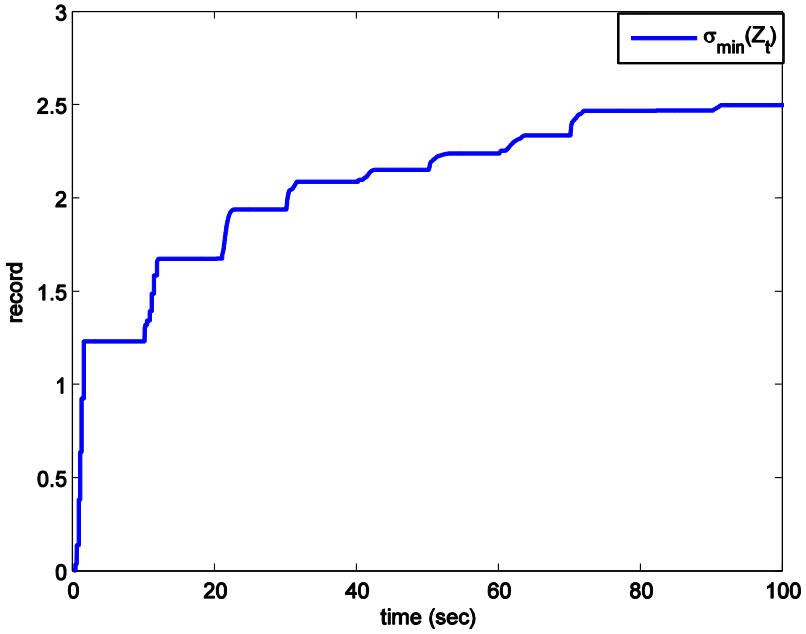


**Figure 9 Minimum singular value of the history-stack with CL-MRAC & Algorithm 1**

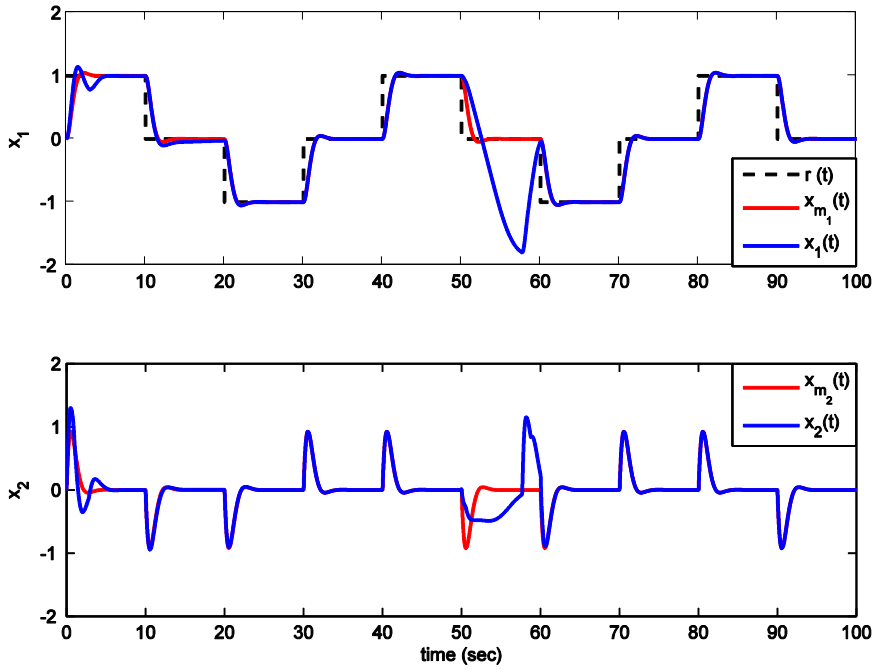


**Figure 10 Responses with CL-MRAC & Algorithm 2**

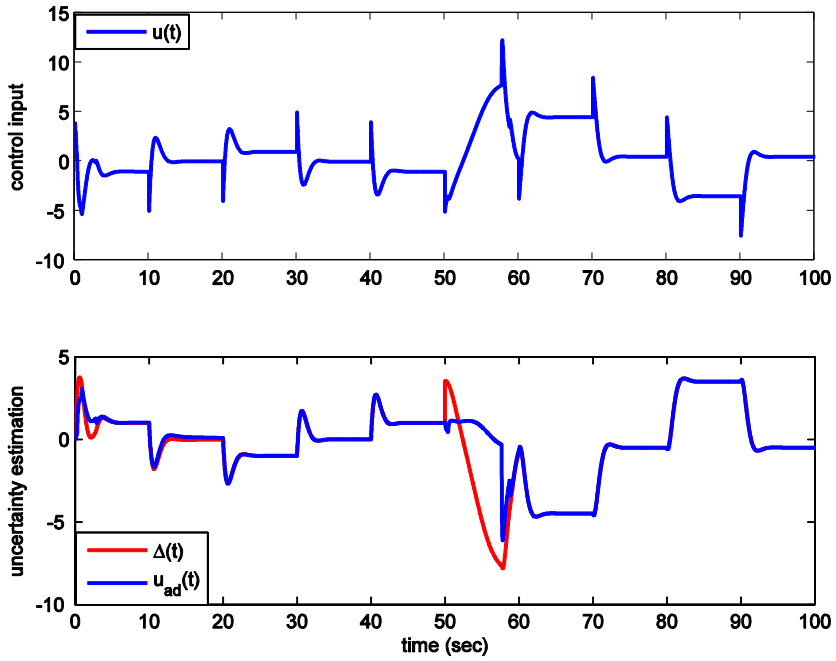


**Figure 11 Control input and uncertainty estimation with CL-MRAC & Algorithm 2**

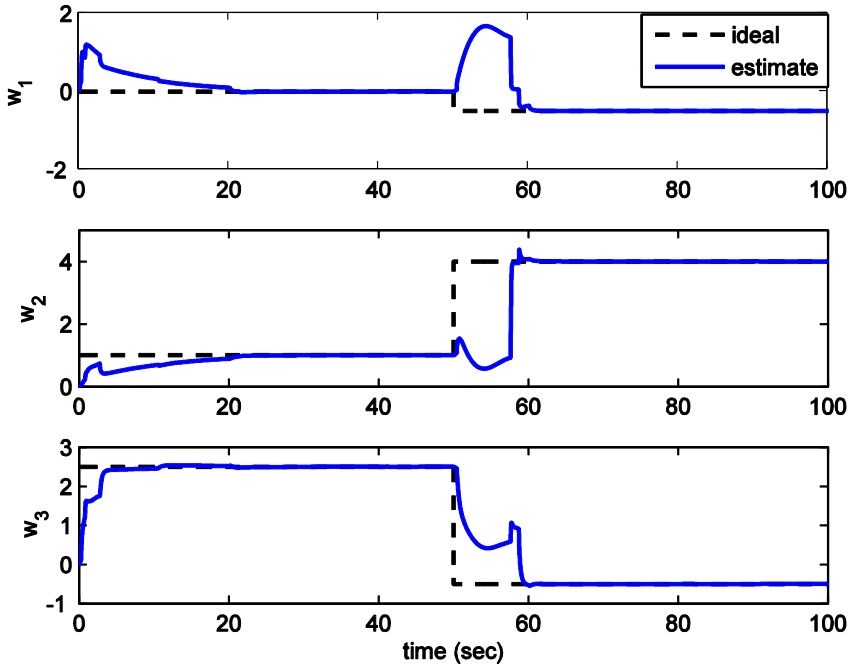


**Figure 12 Estimate of the ideal weights with CL-MRAC & Algorithm 2**

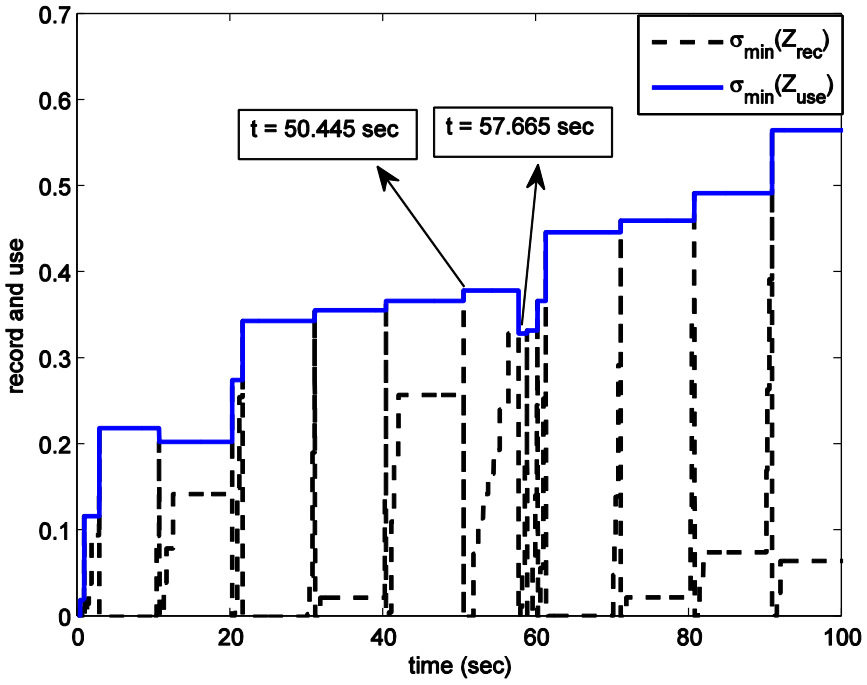


**Figure 13 "Record" and "Use" minimum singular value of the history-stack with CL-MRAC & Algorithm 2**

In Algorithm 2, we have supplementary tuning parameters, $g_1$, $g_2$, $g_3$, due to the switching surface. $\sigma_{min}(Z_{use})$ can be considered a norm of an initial condition of exponentially stable system. Then, $g_1$ and $g_2$ determine the amplitude and decay rate of the exponential decaying function, which bounds the solution of exponentially stable system, respectively. On the other hand, $g_3$ is treated as a small bias just to guarantee positive-definiteness of $Z_{use}Z^T{}_{use}$.

In Figure 14, for three different $g_1$ values, the tracking performances of CL-MRAC are seen. Since these responses differ from each other approximately for 15 seconds after switching in ideal weights, we present the simulation results from $t = 40\,sec$ to $t = 70\,sec$. By looking Figure 14 over, it is hard to understand the effects of $g_1$ variation. Thus, after switching in ideal weights, we should check the first and second time that singular value inequalities are satisfied. Furthermore, the ratio of the relevant

data points in "use" to the total data points in "use" between the first and second time should be figured out.

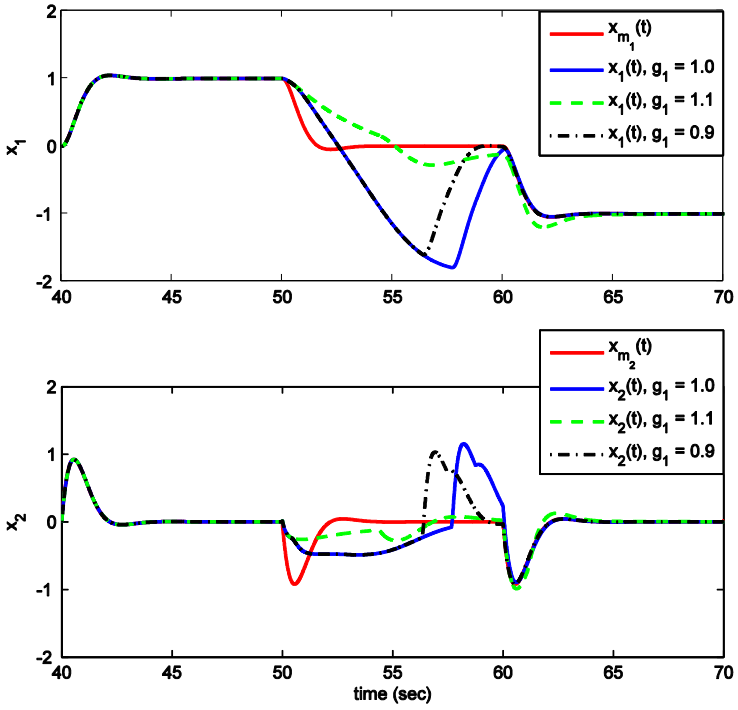


**Figure 14 Responses with CL-MRAC & Algorithm 2 & $g_2 = 0.02$, $g_3 = 10^{-3}$, $\bar{t} = -10^3$**

In Table 1, demanded useful information is given. For all given $g_1$ values, every irrelevant data point is replaced with the relevant one at the second time. From the second time values, we can deduce that the time required for removal of irrelevant data points decreases as $g_1$ decreases. Therefore, $g_1 = 0.9$ converges to reference model fast, see Figure 14. However, $g_1 = 1.1$ performs better than $g_1 = 1.0$ & $g_1 = 0.9$ cases until the removal of irrelevant data points. It may be explained by the ratio of the relevant data points in "use" to the total data points in "use" between the first and second time. That is, $g_1 = 1.1$ has more relevant data points than $g_1 = 1$ and $g_1 = 0.9$ cases.

Figure 15 shows the tracking performances of CL-MRAC for three different $g_2$ values. Similar to the previous case, the responses differ from each other approximately for 15

**Table 1: 1st & 2nd time that singular value inequality is satisfied and ratio between relevant and total data points in "use" during this time interval when $g_1$ changes**

| $g_1$ | 1st time (sec) | Ratio of relevant data points in "use" to total data points in "use" | 2nd time (sec) |
|---|---|---|---|
| 1.0 | 50.445 | 1/8 | 57.665 |
| 1.1 | 54.385 | 4/8 | 61.105 |
| 0.9 | 50.445 | 1/8 | 56.340 |

seconds after switching in ideal weights. Thus, we present the simulation results from $t = 40\ sec$ to $t = 70\ sec$. To evaluate the responses, consider the useful information given in Table 2. From the second time values, we can deduce that the time required for removal of irrelevant data points decreases as $g_2$ increases. Therefore, $g_2 = 0.04$ converges to reference model fast, see Figure 15. However, $g_2 = 0.01$ performs better than $g_2 = 0.02$ & $g_2 = 0.04$ cases until the removal of irrelevant data points. It may be again due to the ratio between the relevant and the total data points.

Before the simulation results were obtained, we intuitively expected that decreasing amplitude $g_1$ or increasing decay rate $g_2$ could result in reduction of the required time for irrelevant data removal. The inferences, especially about the required time for irrelevant data removal, we drew from the simulation results are consistent with the expectations. On the other hand, we have observed that high amplitude or low decay rate could yield better tracking performance until the removal of irrelevant data points. In conclusion, tuning the switching surface parameters is not trivial even in this simple example. We have trade-off between the time required for removal of irrelevant data points and the performance up to the removal of them.

**Table 2: 1st & 2nd time that singular value inequality is satisfied and ratio between relevant and total data points in "use" during this time interval when $g_2$ changes**

| $g_2$ | 1st time (sec) | Ratio of relevant data points in "use" to total data points in "use" | 2nd time (sec) |
|---|---|---|---|
| 0.02 | 50.445 | 1/8 | 57.665 |
| 0.04 | 51.610 | 2/7 | 55.550 |
| 0.01 | 54.185 | 4/8 | 61.170 |

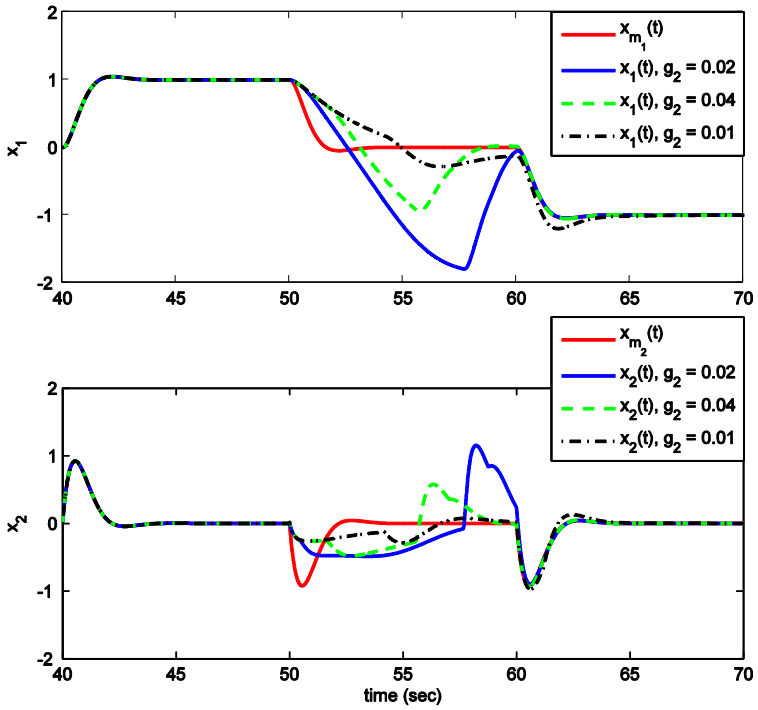


**Figure 15 Responses with CL-MRAC & Algorithm 2 & $g_1 = 1$, $g_3 = 10^{-3}$, $\bar{t} = -10^3$**

## 2.6 Robustness of CL-MRAC to Time-Varying Ideal Weights

In this section, time-varying ideal weights are allowed in the matched uncertainty. Thus, the uncertainty is changed from $\Delta(x(t))$ to $\Delta(t, x(t))$. Now, (1) is replaced with the following system

$$\dot{x}(t) = Ax(t) + B\left[u(t) + \Delta(t, x(t))\right] \tag{46}$$

**Assumption 3** The matched uncertainty in (46) can be linearly parameterized as

$$\Delta(t, x) = W^T(t)\beta(x), \qquad x \in \Omega_x, \tag{47}$$

where $W(t)\,\epsilon\,R^{s\,x\,m}$ is the unknown time-varying weight matrix that satisfies $\|W(t)\|_F \le w$ and $\left\|\dot{W}(t)\right\|_F \le \dot{w}$ with positive constants $w$ and $\dot{w}$, $\beta\big(x(t)\big) : R^n \to R^s$ is a vector of known basis functions $\beta(x) = [\beta_1(x),\ \beta_2(x),\ \dots,\ \beta_s(x)]^T\,\epsilon\,R^s$ and $\Omega_x$ is a sufficiently large compact subset of $R^n$.

*An example of (47)*:

$$\Delta(t,x) = \cos(t)\sin(x) + (1-e^{-t})\cos(x) + x^2, \qquad x\,\epsilon\,R,$$

where $W(t) = [\cos(t)\,,\ 1-e^{-t},\ 1]^T,\ \beta(x) = [\sin(x)\,,\ \cos(x)\,,\ x^2]^T$.

For time-varying ideal weights, the weight error is defined as

$$\widetilde{W}(t) \coloneqq W(t) - \widehat{W}(t), \tag{48}$$

and thus

$$\dot{\widetilde{W}}(t) = \dot{W}(t) - \dot{\widehat{W}}(t). \tag{49}$$

(14) can be written as

$$\varepsilon_j(t) = \Big(W\big(t_j\big) - \widehat{W}(t)\Big)^T \beta\big(x_j\big). \tag{50}$$

Using (49) and (50), the weight error dynamics can be obtained from (13):

$$\begin{aligned}\dot{\widetilde{W}}(t) = \dot{W}(t) &- \Gamma\beta\big(x(t)\big)e^T(t)PB \\ &-\Gamma\sum_{j=1}^{p}\beta\big(x_j\big)\beta^T\big(x_j\big)\Big(W\big(t_j\big) - \widehat{W}(t)\Big).\end{aligned} \tag{51}$$

Using (29) and (48), $\dot{\widetilde{W}}(t)$ can be written as

$$\begin{aligned}\dot{\widetilde{W}}(t) = \dot{W}(t) &- \Gamma\beta\big(x(t)\big)e^T(t)PB - \Gamma\,\eta(\widetilde{W}(t) - W(t)) \\ &-\Gamma\sum_{j=1}^{p}\beta\big(x_j\big)\beta^T\big(x_j\big)W\big(t_j\big).\end{aligned} \tag{52}$$

The weight error dynamics for time-varying ideal weights is obviously different from the one for constant ideal weights; see (52) and (19). On the other hand, there is no variation in the state tracking error dynamics given in (17).

In this section, we aim to show that the solutions of the system given by (17) and (52) are uniformly ultimately bounded (UUB) under Assumption 3. Consider the error vector $\xi \coloneqq \left[e^T,\ vec\left(\widetilde{W}\right)^T\right]^T$, the Lyapunov function in (21), and

$$B_r = \left\{\xi \in R^{n+(s\times m)} \middle| \|\xi\| \leq r\right\} \subset \Omega_\xi, \tag{53}$$

where $\Omega_\xi$ is a sufficiently large compact set. Let $c$ be the minimum value of $V(\xi)$ on the boundary of $B_r$. Using (22) and (24),

$$c = min_{\|\xi\|=r} V(\xi) = k_1 r^2. \tag{54}$$

Define

$$\Omega_c = \{\xi \in B_r | V(\xi) \leq c\}, \tag{55}$$

and notice that (54) ensures that $\Omega_c \subset B_r$. These sets are presented in Figure 16.

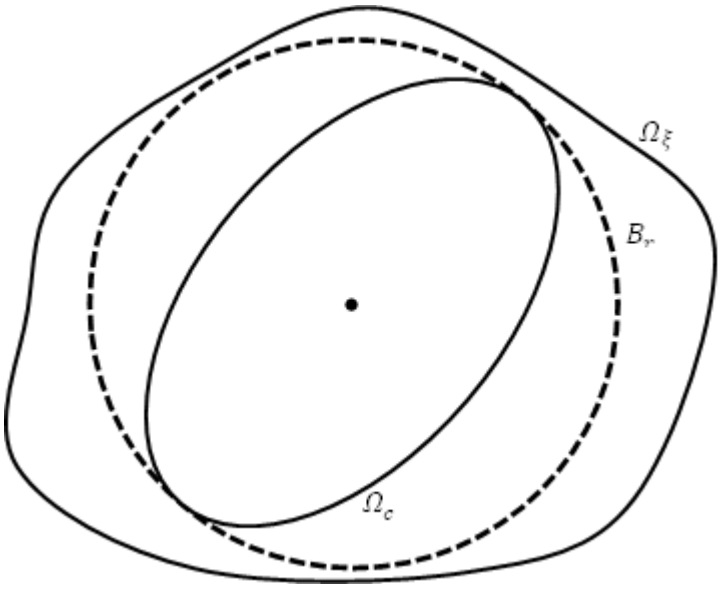


**Figure 16 Geometric representation of the sets $\Omega_\xi$, $\Omega_c$ (solid) and $B_r$ (dashed)**

**Assumption 4** Assume

$$r > \sqrt{\frac{k_2}{k_1}}\mu \geq \mu, \tag{56}$$

$\mu$ is defined as

$$\mu = \frac{\Gamma^{-1}\dot{w} + w(\|\eta\|_F + p\|\eta\|_2)}{\theta\lambda_{min}(\eta)} \tag{57}$$

where $0 < \theta < 1$.

**Theorem 2** Consider the system in (46) subject to Assumption 3, the reference model in (2), and the tracking control law in (4), with the nominal control component given by (5) subject to Assumption 2 and the adaptive feedback control component given by (6) which has the concurrent learning weight update law in (13). It is also assumed that the recorded data points satisfy Condition 1 at $t = t_0$ and the history-stack is static, i.e. it is not overwritten. Furthermore, let Assumption 4 hold. Then, $\Omega_c$ is positively invariant and $\forall\ \xi(t_0) \in \Omega_c$, there exists $T = T(\xi(t_0), \mu) \geq 0$ such that

$$\|\xi(t)\| \leq \sqrt{\frac{k_2}{k_1}}\|\xi(t_0)\|e^{-\lambda(t-t_0)}, \quad \forall\ t_0 \leq t \leq t_0 + T, \tag{58}$$

where $\lambda = c_3/(2k_2) = \min\left\{\frac{1}{2}\lambda_{min}(Q), (1-\theta)\lambda_{min}(\eta)\right\} / \max\{\lambda_{max}(P), \Gamma^{-1}\}$, $c_3$ is defined in the proof,

$$\|\xi(t)\| \leq \sqrt{\frac{k_2}{k_1}}\mu, \quad \forall\ t \geq t_0 + T, \tag{59}$$

If Assumption 3 holds globally, i.e. $\Omega_x = R^n$, then (58) and (59) hold $\forall\ \xi(t_0)$, without limitation on how large μ is.

**Proof:** To keep the formulas short, drop the argument $t$ in the proof.

Consider the Lyapunov function given in (20). The time derivative of (20) along trajectories (17) and (52) can be expressed as

$$\begin{aligned}\dot{V}\left(t,e,\widetilde{W}\right) &= \frac{1}{2}e^T[A_m^TP + PA_m]e + e^TPB\widetilde{W}^T\beta(x) + \Gamma^{-1}tr\left(\widetilde{W}^T\dot{\widetilde{W}}\right)\\ &= \frac{1}{2}e^T[A_m^TP + PA_m]e + e^TPB\widetilde{W}^T\beta(x) \ + \Gamma^{-1}tr\left(\widetilde{W}^T\dot{W}\right)\\ &\quad -tr\left(\widetilde{W}^T\beta(x)e^TPB\right) - tr\left(\widetilde{W}^T\eta\left(\widetilde{W}-W\right)\right)\\ &\quad -tr\left(\widetilde{W}^T\sum_{j=1}^{p}\beta\left(x_j\right)\beta^T\left(x_j\right)W\left(t_j\right)\right).\end{aligned} \tag{60}$$

Define the following matrix

$$\Theta \coloneqq \sum_{j=1}^{p}\beta\left(x_j\right)\beta^T\left(x_j\right)W\left(t_j\right). \tag{61}$$

Noting that $e^TPB\widetilde{W}^T\beta(x) = tr\left(\widetilde{W}^T\beta(x)e^TPB\right)$ and using the Lyapunov equation in (11), we have

$$\begin{aligned}\dot{V}\left(t,e,\widetilde{W}\right) &= -\frac{1}{2}e^TQe - tr\left(\widetilde{W}^T\eta\widetilde{W}\right) + tr\left(\widetilde{W}^T\eta W\right) + \Gamma^{-1}tr\left(\widetilde{W}^T\dot{W}\right)\\ &\quad -tr\left(\widetilde{W}^T\Theta\right)\end{aligned} \tag{62}$$

Revisit the equalities and inequality used in the proof of Theorem 1: $-tr\left(\widetilde{W}^T\eta\widetilde{W}\right) = -vec\left(\widetilde{W}\right)^T\tilde{\eta}vec\left(\widetilde{W}\right) \le -\lambda_{min}(\eta)vec\left(\widetilde{W}\right)^Tvec\left(\widetilde{W}\right) = -\lambda_{min}(\eta)\left\|\widetilde{W}\right\|_F^2$. Hence, we have the following inequality

$$\begin{aligned}\dot{V}\left(t,e,\widetilde{W}\right) &\le -\frac{1}{2}\lambda_{min}(Q)\|e\|^2 - \lambda_{min}(\eta)\left\|\widetilde{W}\right\|_F^2 + tr\left(\widetilde{W}^T\eta W\right)\\ &\quad +\Gamma^{-1}tr\left(\widetilde{W}^T\dot{W}\right) - tr\left(\widetilde{W}^T\Theta\right).\end{aligned} \tag{63}$$

From Cauchy-Bunyakovskii-Schwarz (CBS) inequality, we know that for any arbitrary matrices $M,\ N \epsilon R^{s\times m}$, $|< M, N >| \leq \|M\|_F \|N\|_F$. Using CBS, (63) becomes

$$\begin{aligned}\dot{V}\left(t, e, \widetilde{W}\right) \leq & -\frac{1}{2}\lambda_{min}(Q)\|e\|^2 - \lambda_{min}(\eta)\left\|\widetilde{W}\right\|_F^2 \\ & +(\|W\|_F\|\eta\|_F + \Gamma^{-1}\left\|\dot{W}\right\|_F + \|\Theta\|_F)\left\|\widetilde{W}\right\|_F.\end{aligned} \tag{64}$$

With the upper bounds given in Assumption 3, (64) can be upper bounded as

$$\begin{aligned}\dot{V}\left(t, e, \widetilde{W}\right) \leq & -\frac{1}{2}\lambda_{min}(Q)\|e\|^2 - \lambda_{min}(\eta)\left\|\widetilde{W}\right\|_F^2 \\ & +(w\|\eta\|_F + \Gamma^{-1}\dot{w} + \|\Theta\|_F)\left\|\widetilde{W}\right\|_F.\end{aligned} \tag{65}$$

In order to complete the proof, we require an upper bound on $\|\Theta\|_F$. It can be established as follows:

$$\begin{aligned}\|\Theta\|_F &= \left\|\beta(x_1)\beta^T(x_1)W(t_1) + \cdots + \beta\left(x_p\right)\beta^T\left(x_p\right)W\left(t_p\right)\right\|_F \\ &\leq \|\beta(x_1)\beta^T(x_1)W(t_1)\|_F + \cdots + \left\|\beta\left(x_p\right)\beta^T\left(x_p\right)W\left(t_p\right)\right\|_F \\ &\leq \|\beta(x_1)\beta^T(x_1)\|_F\|W(t_1)\|_F + \cdots + \left\|\beta\left(x_p\right)\beta^T\left(x_p\right)\right\|_F\left\|W\left(t_p\right)\right\|_F.\end{aligned} \tag{66}$$

With the upper bound in Assumption 3, we can further upper bound (66) as

$$\|\Theta\|_F \leq w(\|\beta(x_1)\beta^T(x_1)\|_F + \cdots + \left\|\beta\left(x_p\right)\beta^T\left(x_p\right)\right\|_F) \tag{67}$$

*Claim*: $\left\|\beta\left(x_\rho\right)\beta^T\left(x_\rho\right)\right\|_F \leq \|\eta\|_2, \qquad \rho = 1, \ldots, p$

*Proof*: The Frobenius norm of $\beta\left(x_\rho\right)\beta^T\left(x_\rho\right)$ can be written as

$$\left\|\beta\left(x_\rho\right)\beta^T\left(x_\rho\right)\right\|_F = \sqrt{\sum_{i=1}^{s}\sigma_i\left[\beta\left(x_\rho\right)\beta^T\left(x_\rho\right)\right]^2}. \tag{68}$$

Since $\beta(x_\rho)\beta^T(x_\rho)$ is a symmetric positive-semidefinite matrix, we have

$$\sigma_i[\beta(x_\rho)\beta^T(x_\rho)] = \sqrt{\lambda_i\left[\left(\beta(x_\rho)\beta^T(x_\rho)\right)^2\right]}, \tag{69}$$

where $\sqrt{\lambda_i\left[\left(\beta(x_\rho)\beta^T(x_\rho)\right)^2\right]} = \sqrt{\lambda_i[\beta(x_\rho)\beta^T(x_\rho)]^2} = \lambda_i[\beta(x_\rho)\beta^T(x_\rho)]$. Thus, (68) can be rewritten as

$$\left\|\beta(x_\rho)\beta^T(x_\rho)\right\|_F = \sqrt{\sum_{i=1}^{s}\lambda_i\left[\beta(x_\rho)\beta^T(x_\rho)\right]^2}. \tag{70}$$

Define $v_1 \coloneqq \beta(x_\rho)$ and $H \coloneqq v_1 v_1^T$. If $v_1 = 0$, it is clear that $\|H\|_F = 0$. Now, suppose that $v_1 \neq 0$ and let $\{v_1, v_2, \dots, v_s\}$ be an orthogonal basis for $R^s$, that is, $v_i^T v_i = \alpha_i > 0$ and $v_i^T v_j = 0$ for $i \neq j$. $Hv_i = 0$ for $i = 2, \dots, s$. Thus, $null(H) = \{v_2, \dots, v_s\}$ and $\dim[null(H)] = s - 1$. Note that $H^2 = v_1 v_1^T v_1 v_1^T = \alpha_1 H$. Then, $H^2 - \alpha_1 H = 0$. Thus, the minimal polynomial of $H$ is $m(\lambda) = \lambda^2 - \alpha_1\lambda = \lambda(\lambda - \alpha_1)$. The minimal polynomial directly implies that the eigenvalues of $H$ are $\lambda(H) = \{0, \alpha_1\}$. We have $R^s = null(H) \oplus null(H - \alpha_1 I)$ and thus $\dim[null(H - \alpha_1 I)] = 1$. Finally, we get the characteristic polynomial of $H$: $d(\lambda) = \lambda^{s-1}(\lambda - \alpha_1)$.

Using the result of the foregoing analysis, (70) is rewritten as

$$\left\|\beta(x_\rho)\beta^T(x_\rho)\right\|_F = \lambda_{max}[\beta(x_\rho)\beta^T(x_\rho)]. \tag{71}$$

One can quickly realize $\left\|\beta(x_\rho)\beta^T(x_\rho)\right\|_F = \left\|\beta(x_\rho)\beta^T(x_\rho)\right\|_2$. Similar to (69), the following equality can be easily shown in few steps

$$\|\eta\|_2 = \|ZZ^T\|_2 = \lambda_{max}[ZZ^T]. \tag{72}$$

Let the eigenvalues be labeled in nondecreasing order, i.e. $\lambda_1 \leq \lambda_2 \leq \cdots \leq \lambda_s$. From Theorem 10.3.1 in [25], we know that for any symmetric matrices $H$, $Y \in R^{s\times s}$,

$$\lambda_i(H) + \lambda_j(Y) \leq \lambda_{i+j-1}(H+Y), \qquad 1 \leq i+j-1 \leq s \tag{73}$$

Let $Y \coloneqq ZZ^T - H$ . Recall that $H$ is positive-semidefinite, $Y$ is either positive-semidefinite or positive-definite, and $H+Y$ is positive-definite. Then, we can lower bound (73) as

$$0 \leq \lambda_i(H) + \lambda_j(Y) \leq \lambda_{i+j-1}(H+Y), \qquad 1 \leq i+j-1 \leq s \tag{74}$$

Let $j = 1$, we have the following inequalities

$$0 \leq \lambda_i(H) + \lambda_1(Y) \leq \lambda_i(H+Y), \qquad 1 \leq i \leq s, \tag{75}$$

$$0 \leq \lambda_i(H) \leq \lambda_i(H) + \lambda_1(Y) \leq \lambda_i(H+Y), \qquad 1 \leq i \leq s, \tag{76}$$

$$0 \leq \lambda_i(H) \leq \lambda_i(H+Y), \qquad 1 \leq i \leq s. \tag{77}$$

The following inequality is obtained from (77)

$$\lambda_{max}\left[\beta(x_\rho)\beta^T(x_\rho)\right] \leq \lambda_{max}[ZZ^T], \tag{78}$$

Recalling (71) & (72), and noting (78), the target inequality in the claim is met. □

In the light of this discussion, (67) is upper bounded as

$$\|\Theta\|_F \leq wp\|\eta\|_2. \tag{79}$$

Now, we are ready to continue Lyapunov analysis. Using (79), we upper bound (65) as

$$\begin{aligned} \dot{V}\left(t, e, \widetilde{W}\right) \leq & -\frac{1}{2}\lambda_{min}(Q)\|e\|^2 - \lambda_{min}(\eta)\left\|\widetilde{W}\right\|_F^2 \\ & +\left(\Gamma^{-1}\dot{w} + w(\|\eta\|_F + p\|\eta\|_2)\right)\left\|\widetilde{W}\right\|_F. \end{aligned} \tag{80}$$

The foregoing inequality can be rewritten as

$$\begin{aligned} \dot{V}\left(t, e, \widetilde{W}\right) \leq & -\frac{1}{2}\lambda_{min}(Q)\|e\|^2 - (1-\theta)\lambda_{min}(\eta)\left\|\widetilde{W}\right\|_F^2 \\ & -\theta\lambda_{min}(\eta)\left\|\widetilde{W}\right\|_F^2 + \left(\Gamma^{-1}\dot{w} + w(\|\eta\|_F + p\|\eta\|_2)\right)\left\|\widetilde{W}\right\|_F, \end{aligned} \tag{81}$$

where $0 < \theta < 1$. Then, we get

$$\dot{V}(t,\xi) \leq -\min\left\{\frac{1}{2}\lambda_{min}(Q), (1-\theta)\lambda_{min}(\eta)\right\}\|\xi\|^2, \forall\, \|\xi\| \geq \left\|\widetilde{W}\right\|_F \geq \mu, \tag{82}$$

where $\mu = \left(\Gamma^{-1}\dot{w} + w(\|\eta\|_F + p\|\eta\|_2)\right)/(\theta\lambda_{min}(\eta))$. From (82), define the following positive constant

$$c_3 \coloneqq \min\left\{\frac{1}{2}\lambda_{min}(Q), (1-\theta)\lambda_{min}(\eta)\right\}. \tag{83}$$

Define the compact set

$$B_\mu = \{\xi \in B_r | \|\xi\| \leq \mu\}. \tag{84}$$

It should be noted that (56) ensures that $B_\mu \subset B_r$. Let $d$ be the maximum value of $V(\xi)$ on the boundary of $B_\mu$. Using (22) and (25),

$$d = max_{\|\xi\|=\mu} V(\xi) = k_2\mu^2. \tag{85}$$

Define

$$\Omega_d = \{\xi \in B_r | V(\xi) \leq d\}. \tag{86}$$

(85) guarantees that $B_\mu \subset \Omega_d$ and from the condition in (56), we ensure that $\Omega_d \subset \Omega_c$. All sets used in the proof are presented in Figure 17.

By (22), (82) with $k_1$ in (24), $k_2$ in (25), $c_3$ in (83), Assumption 4, and Theorem 4.5 in [29], $\Omega_c$ is positively invariant and for all initial errors $\xi(t_0)$ belong to $\Omega_c$, there exists $T = T(\xi(t_0), \mu) \geq 0$ such that (58) and (59) are satisfied. ■

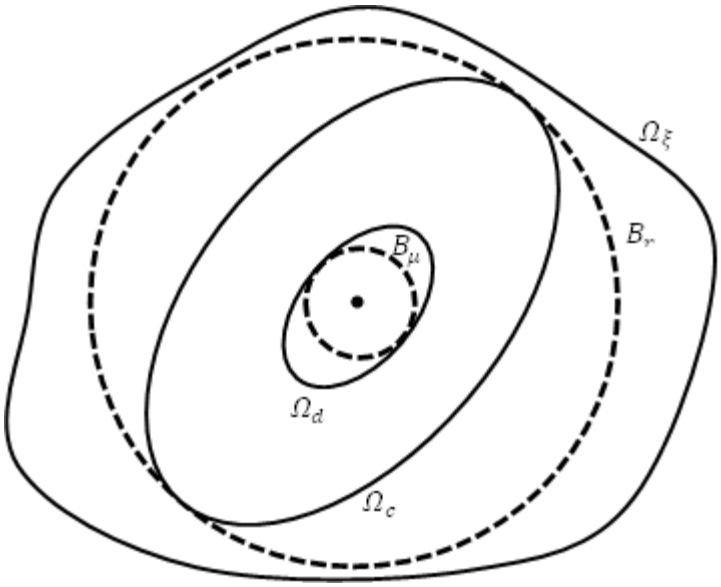


**Figure 17 Geometric representation of the sets $\Omega_\xi$, $\Omega_c$, $\Omega_d$ (solid) and $B_r$, $B_\mu$ (dashed)**

**Remark 7** Theorem 2 provides not only UUB solutions of the system given by (17) and (52) but also estimates for the ultimate bound and the exponential convergence rate to that bound. When (58) is compared with (36), it is noticed that there is no variation in the convergence rate $\lambda$ except the new term $\theta$. Since $\theta$ is not a design parameter and it is restricted to $0 < \theta < 1$ in the proof, the discussions we had in Remark 2 are still valid. It should also be kept in mind that $\lambda$ is the convergence rate to the origin in constant ideal weight case, while it is the convergence rate to the ultimate bound in time-varying ideal weight case. Moreover, consider the ultimate bound given in (59). It is rewritten as

$$b = \sqrt{\frac{k_2}{k_1}}\mu = \sqrt{\frac{\max\{\lambda_{max}(P), \Gamma^{-1}\}}{\min\{\lambda_{min}(P), \Gamma^{-1}\}}}\left(\frac{\Gamma^{-1}\dot{w} + w(\|\eta\|_F + p\|\eta\|_2)}{\theta\lambda_{min}(\eta)}\right). \tag{87}$$

From (87), we can deduce that ultimate bound $b$ is dependent on the spectral properties of $P$, $\Gamma$, $\eta$, the number of recorded data points $p$, and the upper bounds on the ideal weight and its derivative, i.e. $w$, $\dot{w}$. Note that $P$, $\Gamma$, $\eta$, and $p$ are controller design parameters, while $w$ and $\dot{w}$ are the inherent properties of the system. It should also be noted that high learning rate $\Gamma$ decreases the effect of $\dot{w}$ but it can amplify $\sqrt{k_2/k_1}$ in $b$.

**Remark 8** The static history-stack assumption of Theorem 2 can be relaxed if (37) and the following inequality hold

$$\|\eta(t)\|_F \leq \bar{\eta}, \quad \forall\, t \geq t_0 \geq 0, \tag{88}$$

where $\bar{\eta}$ is a positive constant. Note that $\|\eta(t)\|_2 \leq \|\eta(t)\|_F$. Then, (82) becomes

$$\dot{V}(t,\xi) \leq -\min\left\{\frac{1}{2}\lambda_{min}(Q), (1-\theta)\bar{\lambda}\right\}\|\xi\|^2, \;\; \forall \;\|\xi\| \geq \left\|\widetilde{W}\right\|_F \geq \mu, \tag{89}$$

where $\mu = (\Gamma^{-1}\dot{w} + w(1+\bar{p})\bar{\eta})/(\theta\bar{\lambda})$. In time-varying history-stack case, the remaining part of the proof of Theorem 2 is completely same.

**Remark 9** When we use baseline adaptive law in (12) instead of concurrent learning adaptive law in (13), weight error dynamics can be written as

$$\dot{\widetilde{W}}(t) = \dot{W}(t) - \Gamma\beta\big(x(t)\big)e^T(t)PB, \tag{90}$$

and the following inequality is obtained after Lyapunov analysis

$$\dot{V}\big(t,e,\widetilde{W}\big) \leq -\frac{1}{2}\lambda_{min}(Q)\|e\|^2 + \Gamma^{-1}\dot{w}\left\|\widetilde{W}\right\|_F. \tag{91}$$

From (91), we cannot conclude that the solutions of the system given by (17) and (90) are UUB. Actually, it is well known that baseline adaptive law suffers from the parameter drift, which is one of the instability phenomena in adaptive systems. Therefore, the baseline adaptive control is not appropriate for practical applications [11], [3].

## 2.7 Data Point Selection Methods

In this section, we intend to share data recording algorithms which can be used for time-varying ideal weights. All algorithms, which are going to be presented, take account of the constraints mentioned in Remark 10.

**Remark 10** The following constraints on algorithms are quite simple**:**

i. Pre-recorded data which satisfies Condition 1 is required due to Theorem 2.

ii. From Remark 8, we know that the inequalities in (37) and (88) are also required.

The efficiency of singular value maximizing algorithm for constant ideal weights is known from Remark 5. However, its performance in time-varying ideal weights has not been investigated yet. Moreover, is there any reason for maximizing the minimum singular value of the history-stack? The answer is still "yes" because the convergence rate to the ultimate bound is directly proportional to the minimum singular value of the history-stack, see (58). Thus, Algorithm 1 is modified and the modified version is given in Algorithm 3. Since the first constraint given in Remark 10 implies that $p$ cannot be initialized to 0, the first $if$ condition in Algorithm 1 is removed. Furthermore, additional $if$ condition is included to ensure that (88) holds. On the other hand, as it is described in Remark 6, (37) holds without any modification.

In Algorithm 3, the upper bound of $\|\eta(t)\|_F$, i.e. $\bar{\eta}$ is a new parameter which should be selected by considering the pre-recorded data, i.e. $\|\eta(t_0)\|_F$.

We aimed to increase the convergence rate to the ultimate bound in Algorithm 3. Now, consider also the ultimate bound given in (87). Note that the ultimate bound is directly proportional to $\mu$. Then, we separate $\mu$ into two parts:

$$\mu = \mu_1 + \mu_2, \tag{92}$$

where $\mu_1 = \Gamma^{-1}\dot{w}/(\theta\lambda_{min}(\eta))$ and $\mu_2 = w(\|\eta\|_F + p\|\eta\|_2)/(\theta\lambda_{min}(\eta))$. It is clear that increasing the minimum singular value of the history-stack decreases $\mu_1$. On the other hand, $\mu_2$ is directly proportional to $(\|\eta\|_F + p\|\eta\|_2)/\lambda_{min}(\eta)$. This ratio can be upper and lower bounded as

$$\frac{(\sqrt{s}+p)\|\eta\|_2}{\lambda_{min}(\eta)} \geq \frac{\|\eta\|_F + p\|\eta\|_2}{\lambda_{min}(\eta)} \geq \frac{(1+p)\|\eta\|_2}{\lambda_{min}(\eta)}. \tag{93}$$

In order to decrease $\mu_2$, it seems reasonable to minimize $\|\eta\|_2/\lambda_{min}(\eta)$ for constant $p$. It is nothing but the squared condition number of the history-stack as follows:

$$\frac{\|\eta\|_2}{\lambda_{min}(\eta)} = \frac{\sigma_{max}(\eta)}{\lambda_{min}(\eta)} = \frac{\lambda_{max}(\eta)}{\lambda_{min}(\eta)} = \left(\frac{\sigma_{max}(Z)}{\sigma_{min}(Z)}\right)^2. \quad (94)$$

In the light of this discussion, we can populate the history-stack such that not only its minimum singular value is maximized but also its condition number is minimized. Hence, Algorithm 3 is modified and modified version is called Algorithm 4. Only the modified part of Algorithm 3 is demonstrated in Algorithm 4.

**Algorithm 3**

**if** $\frac{\|\beta(x(t))-\beta(x_{p^-})\|^2}{\|\beta(x(t))\|} \geq \varepsilon$ **then**
  **if** $p < \bar{p}$ **then**
    $p = p + 1$
    $Z_t(:, p) = \beta(x(t))$
    $\eta_{temp} = \|Z_t Z_t^T\|_F$
    **if** $\eta_{temp} \leq \bar{\eta}$ **then**
      $\Delta_t(:, p) = (B^T B)^{-1} B^T [\dot{x}(t) - Ax(t) - Bu(t)]$
    **else**
      $Z_t(:, p) = 0$
      $p = p - 1$
    **end if**
  **else**
    $T = Z_t$
    $SV_{old} = \sigma_{min}(Z_t)$
    **for** $j = 1$ to $p$ **do**
      $Z_t(:, j) = \beta(x(t))$
      $SV(j) = \sigma_{min}(Z_t)$
      $Z_t = T$
    **end for**
    find max $SV$ and let $k$ denote the corresponding column index
    $Z_t(:, k) = \beta(x(t))$
    $\eta_{temp} = \|Z_t Z_t^T\|_F$
    **if** max $SV > SV_{old}$ **and** $\eta_{temp} \leq \bar{\eta}$ **then**
      $\Delta_t(:, k) = (B^T B)^{-1} B^T [\dot{x}(t) - Ax(t) - Bu(t)]$
    **else**
      $Z_t = T$
    **end if**
  **end if**
**end if**

**Algorithm 4**

⋮

$T = Z_t$
$SV_{old} = \sigma_{min}(Z_t)$
$CN_{old} = \sigma_{max}(Z_t)/\sigma_{min}(Z_t)$
**for** $j = 1$ to $p$ **do**
  $Z_t(:, j) = \beta(x(t))$
  $SV(j) = \sigma_{min}(Z_t)$
  $CN(j) = \sigma_{max}(Z_t)/\sigma_{min}(Z_t)$
  $Z_t = T$
**end for**
find max $SV$ and let $k$ denote the corresponding column index
find min $CN$ and let $kk$ denote the corresponding column index
**if** $k = kk$
  $Z_t(:, k) = \beta(x(t))$
  $\eta_{temp} = \|Z_t Z_t^T\|_F$
  **if** $\max SV > SV_{old}$ **and** $min\, CN < CN_{old}$ **and** $\eta_{temp} \leq \bar{\eta}$ **then**
    $\Delta_t(:, k) = (B^T B)^{-1} B^T [\dot{x}(t) - Ax(t) - Bu(t)]$
  **else**
    $Z_t = T$
  **end if**
**end if**

⋮

Instead of Algorithm 4, one can use another algorithm which maximizes minimum singular value and minimizes condition number of the history-stack.

**Remark 11** The estimate of the ultimate bound given in (87) would lead to conservative bounds because of norm inequalities. Therefore, Algorithm 4 may not improve the performance of the controller significantly, although it decreases the ultimate bound.

Due to Remark 11, it makes sense to look for an alternative algorithm which uses recent data points mostly. Similar to Algorithm 1, one can modify Algorithm 2 to use it for time-varying ideal weights. Since Algorithm 2 has additional three tuning parameters and tuning them is not trivial issue, instead of modifying Algorithm 2, we will use cyclic history-stack approach, simpler than Algorithm 2, to record the most recent data points. As mentioned in Remark 5, cyclic history-stack approach does not perform as well as singular value maximizing method for constant ideal weights. However, for time-

varying ideal weights, it gives us a chance to record data points such that new data point is replaced with the oldest one after $p = \bar{p}$. Thus, we modify Algorithm 3 and call it Algorithm 5. In contrast to Algorithm 3 and Algorithm 4, (37) does not hold automatically after $p = \bar{p}$. To satisfy (37), it is included in $if$ condition in Algorithm 5. The lower bound of $\lambda_{min}(\eta(t))$, i.e. $\bar{\lambda}$ is a new parameter which should be selected by considering the pre-recorded data, i.e. $\lambda_{min}(\eta(t_0))$.

**Algorithm 5**

⋮

$T = Z_t$
$Z_t(:, 1:p-1) = Z_t(:, 2:p)$
$Z_t(:, p) = \beta\big(x(t)\big)$
$\eta_{temp} = \|Z_t Z_t^T\|_F$
$\lambda_{temp} = \lambda_{min}(Z_t Z_t^T)$
**if** $\eta_{temp} \leq \bar{\eta}$ **and** $\lambda_{temp} \geq \bar{\lambda}$ **then**
  $\Delta_t(:, 1:p-1) = \Delta_t(:, 2:p)$
  $\Delta_t(:, p) = (B^T B)^{-1} B^T [\dot{x}(t) - Ax(t) - Bu(t)]$
**else**
  $Z_t = T$
**end if**

⋮

## 2.8 Simulation Examples

In this section, we evaluate the performance of Algorithm 3, Algorithm 4, and Algorithm 5 through simulations. For the evaluation, one regulation and one tracking problem are considered.

### 2.8.1 Regulation Problem

Consider the scalar system:

$$\dot{x} = u + w_2 x + d(t), \tag{95}$$

where $w_2$ is an unknown constant and $d(t)$ is a time-varying disturbance such that it is uniformly bounded, continuously differentiable, and its derivative is uniformly bounded. Recall that Theorem 2 allows time-varying ideal weights in the matched uncertainty. Therefore, (95) can be rewritten by including a bias term in the basis function

$$\dot{x} = u + W^T(t)\beta(x), \tag{96}$$

where $W^T(t) = [d(t),\ w_2]$ and $\beta(x) = [1,\ x]^T$. Note that $A \coloneqq 0$ and $B \coloneqq 1$. In the simulations, $d(t) = w_1(t) = \sin(0.1t)$ and $w_2 = 1$.

System and input constants of the reference model are selected as

$$A_m = -\frac{1}{T_c}, \quad B_m = \frac{1}{T_c} \tag{97}$$

with an eigenvalue which has time constant $T_c = 2$. From the matching condition given in Assumption 2, nominal controller gains are $K_1 = 0.5$ and $K_2 = 0.5$.

In the simulations, four adaptive controllers are tested. These are the baseline adaptive law in (12), concurrent learning adaptive law in (13) with Algorithm 3, Algorithm 4, and Algorithm 5. For all controllers, learning rate $\Gamma$ is set to 1 and $Q = 1$. In the concurrent learning cases, maximum number of recorded data points $\bar{p}$ is 4 and $\varepsilon$ used in data recording algorithms is $0.08$. Simulations are started with pre-recorded history-stack satisfying Condition 1. It has 2 linearly independent columns, i.e. $p = 2$ and $\|\eta(0)\|_F = 3.9$, $\lambda_{min}(\eta(0)) = 10^{-4}$, which are required to determine $\bar{\eta}$ and $\bar{\lambda}$. Considering these initial values, $\bar{\eta}$ and $\bar{\lambda}$ are set to 10 and $10^{-4}$ respectively. Furthermore, the responses of the closed-loop system are obtained with the initial conditions: $x(0) = 1$, $x_m(0) = 0$, and $\widehat{W}^T(0) = [0,\ 5]$ and we run the simulations with a $0.005$ sec time step using Euler integration.

In Figure 18, the regulation and the weight estimation performance of the baseline adaptive law is presented. Norm of the error vector $\xi$ is also given to discuss the boundedness of the closed-loop system. If we consider only the regulation performance, it may be satisfactory. However, it should be noted that $\widehat{w}_2(t)$ drifts to infinity. Thus,

the closed-loop system is unbounded. This example shows the parameter drift instability characteristics of the baseline adaptive law which is mentioned in Remark 9.

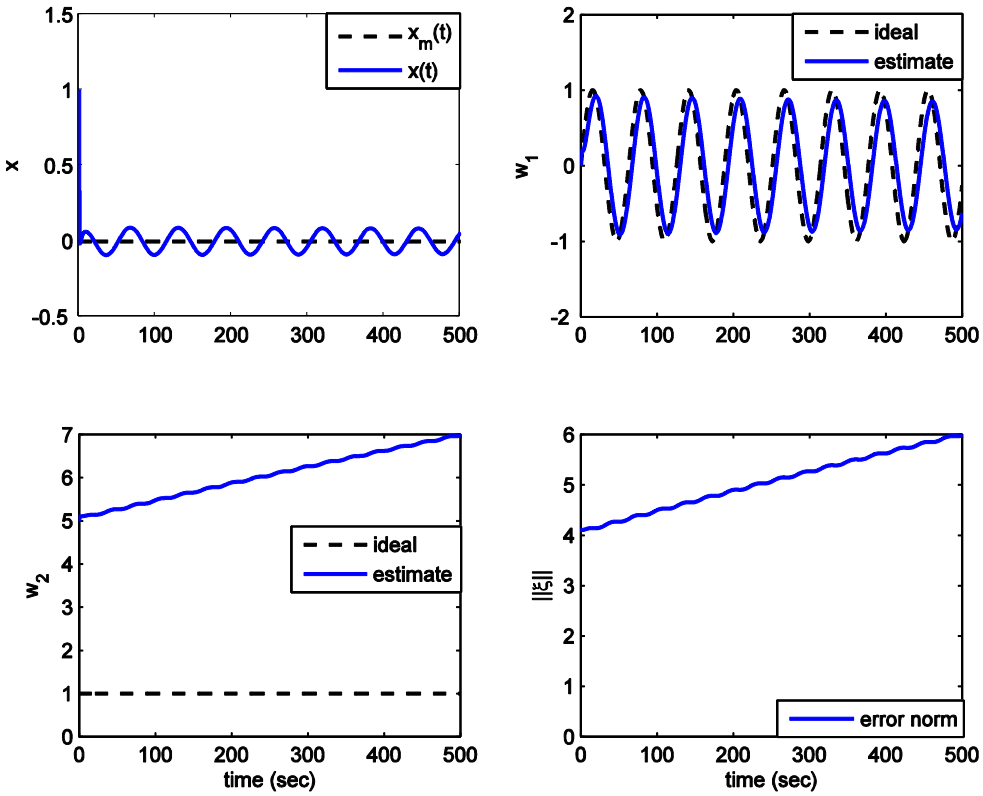


**Figure 18 Responses and error norm with baseline MRAC**

As it is described in [3], this parameter drift instability can also be explained by solving for the "quasi" steady state response of (96) and (12). Since $x_m(0) = 0$ and $r(t) = 0$ for all $t \geq 0$, $x_m(t) = 0$ for all $t \geq 0$ and thus $e(t) = x(t)$ for all $t \geq 0$. From (12), $x_{ss} \approx 0$. Moreover, we substitute $u$ into (96)

$$0 \approx -K_1 x_{ss} - \hat{w}_1 - \hat{w}_2 x_{ss} + d + w_2 x_{ss}, \tag{98}$$

and (98) can be rewritten as

$$x_{ss} \approx \frac{d - \hat{w}_1}{\hat{w}_2 - w_2 + K_1}. \tag{99}$$

It is clear from (99) that for given $d$, $w_2$, and $K_1$, $x_{ss}$ goes to zero when either $\hat{w}_1 \to d$ or $\hat{w}_2 \to \infty$. Since $d$ is unknown time-varying signal, $\hat{w}_1$ cannot converge to $d$. Thus, $\hat{w}_2 \to \infty$. This conclusion is consistent with the simulation result.

In Figure 19, the regulation and the weight estimation performances of CL-MRAC with Algorithm 3, Algorithm 4, and Algorithm 5 are demonstrated. Norms of the error vectors are also given. In contrast to baseline MRAC, it is obviously seen that closed-loop systems with CL-MRAC are bounded as Theorem 2 promises. Among three algorithms, Algorithm 5 has the best performance in terms of regulation. On the other hand, Algorithm 4 achieves the lowest error norm.

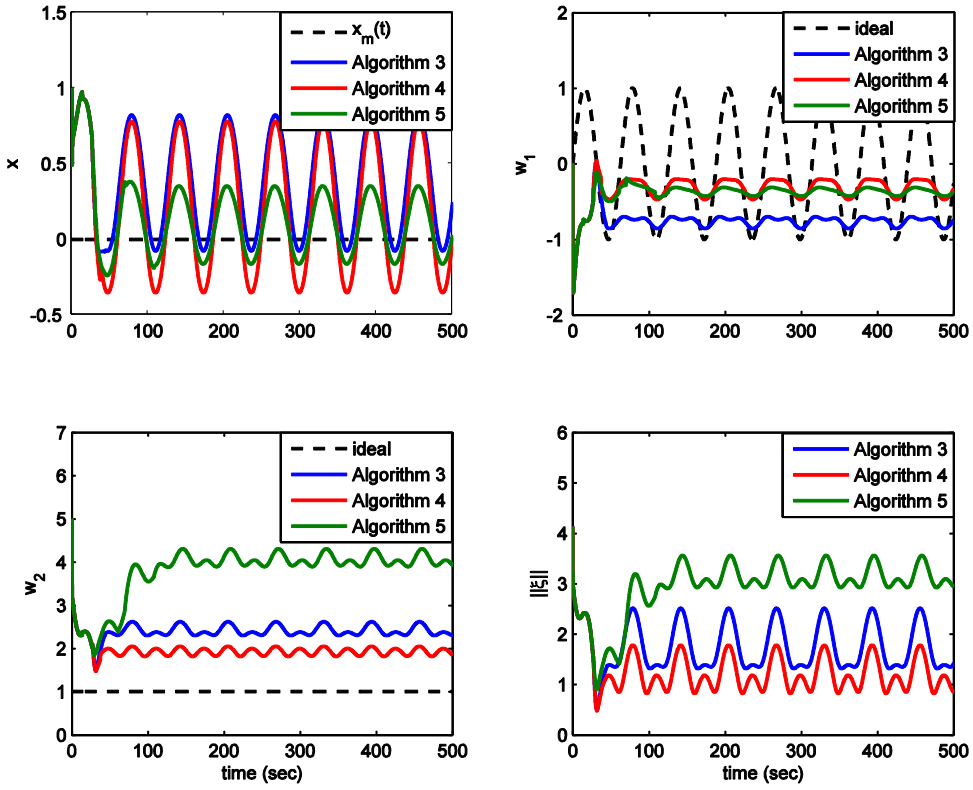


**Figure 19 Responses and error norm with CL-MRAC**

In Figure 20, the evolution of the minimum singular value and the condition number of the history-stacks is shown. In the left part of Figure 20, $p$ is less than $\bar{p}$ up to 13.72 sec

and thus algorithms are exactly the same algorithm. Although algorithms differ from each other after $t = 13.72\ sec$, difference in the evolution appears in the right part of the figure. Furthermore, since new data points were not recorded by algorithms from $t = 125.28\ sec$ to $t = 500\ sec$, that part is omitted from the figure.

Even though the only thing we expect from Algorithm 3 is minimum singular value maximization of the history-stack, it is clearly seen that the condition number of it also decreases. Algorithm 4 maximizes the minimum singular value and minimizes the condition number of the history-stack as it is desired and it achieves the maximum minimum singular value and the minimum condition number of the history-stack among three algorithms. Since Algorithm 5 records data in a cyclic manner, neither minimum singular value nor condition number behaves in a monotonic way.

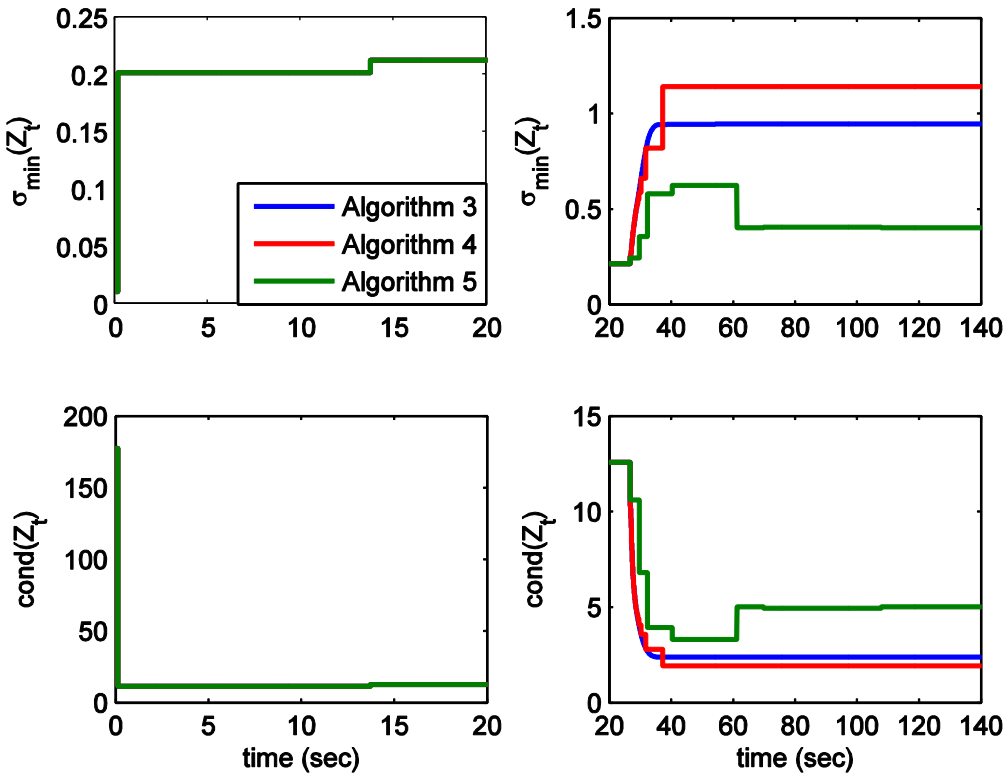


**Figure 20 Minimum singular value and condition number evolution of the history-stacks with CL-MRAC**

Algorithm 4 minimizes the condition number of the history-stack and thus the ultimate bound of the solution of the closed-loop system. It also maximizes the minimum singular value of the history-stack and thus the convergence rate to the ultimate bound. In the light of this information, the following question arises:

- When we quantify the estimate of the ultimate bound, does it give us practical information? In other words, is the estimated ultimate bound value of Algorithm 4 around 2, see Figure 19?

Instead of evaluating (87) throughout the simulation, we can answer this question just by calculating its lower bound. Since $P = 1$ and $\Gamma = 1$, $b = \mu$ for the given example. Using (93) and (94), $\mu$ can be conservatively lower bounded as

$$\mu = \frac{\dot{w} + w(\|\eta\|_F + p\|\eta\|_2)}{\theta\lambda_{min}(\eta)} > \frac{w(1+p)\|\eta\|_2}{\lambda_{min}(\eta)} \geq w(1+p). \tag{100}$$

Note that the upper bound on the ideal weight $w$ is $\sqrt{2}$ and the number of recorded data points $p$ is 4 after $t = 13.72\,sec$ for all algorithms used in the simulation. We can further lower bound (100) as

$$\mu > 7.07. \tag{101}$$

(101) implies that the ultimate bound lower than 7.07 cannot be guaranteed by (87). Therefore, without explicitly evaluating (87) we can conclude that the estimated ultimate bound overestimates the simulation result given in Figure 19, regardless of algorithm. It should be noted that this result is consistent with Remark 11.

When we evaluate (87) at $t = 0\,sec$, the estimated ultimate bound is very high, i.e. $\mu \cong 10^5$. As it is expected, Algorithm 4 attains the minimum value, $\mu = 26.1$, among three algorithms, see Figure 21. From the foregoing discussion, we know that the attained value is still high. However, even if the attained value does not give us practical information, it is meaningful because Algorithm 4 constantly improves the ultimate bound which we guarantee in theory.

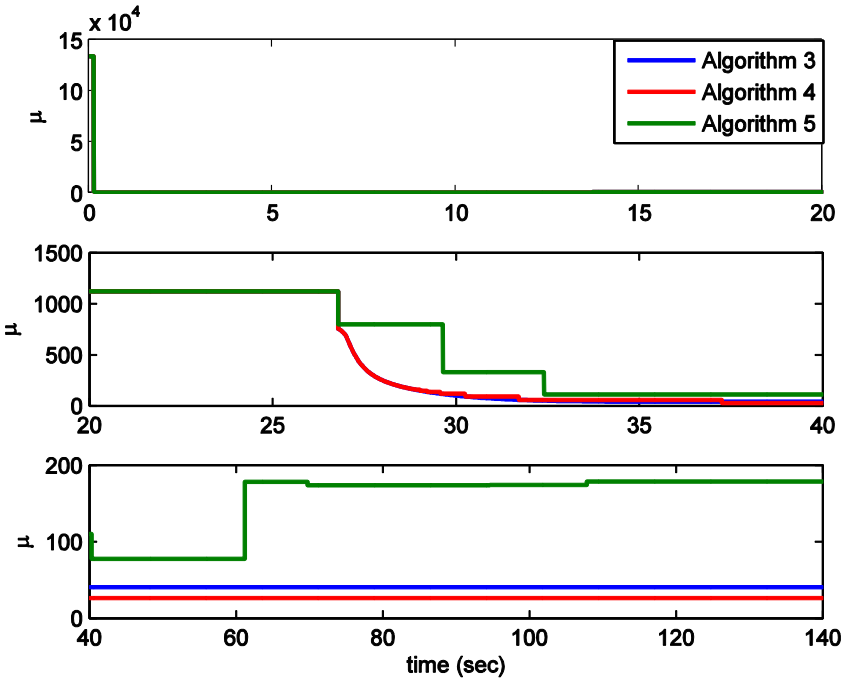


**Figure 21 Estimated ultimate bound evolution of the solution of the closed-loop system with CL-MRAC**

In order to use most recent data points, Algorithm 5 was proposed in the previous section. In Table 3, we see when the last data points were recorded by algorithms. That is, data points of history-stacks at $t = 500\ sec$ were recorded at given instants. Among three algorithms, Algorithm 5 has the most recent data points. However, it does not update its history-stack after $t = 125.28$ and variation in history-stack is not as frequent as it is desired for the given example.

**Table 3: The time when the last data points were recorded by algorithms in regulation problem**

| | Algorithm 3 | Algorithm 4 | Algorithm 5 |
|---|---|---|---|
| time (sec) | 0 | 0 | 69.755 |
| | 43.465 | 37.245 | 94.645 |
| | 43.470 | 37.250 | 107.83 |
| | 13.720 | 13.720 | 125.28 |

### 2.8.2 Tracking Problem

Consider the system given in (42) with the following ideal weights

$$W^T(t) = [w_1(t),\ w_2(t),\ w_3(t)], \tag{102}$$

where

$$w_1(t) = 0.1\sin(0.1t) - 0.05\sin(0.5t) - 0.5(1 - e^{-0.05t}), \tag{103}$$

$$w_2(t) = 4 - \frac{3}{1 + 0.1t}, \tag{104}$$

$$w_3(t) = \begin{cases} 2.5, & t < 20\ sec \\ -0.0025t^2 + 0.1t + 1.5, & 20 \le t < 40\ sec \\ 0.00125t^2 - 0.2t + 7.5, & 40 \le t < 80\ sec \\ -0.5, & t \ge 80\ sec \end{cases}. \tag{105}$$

In the simulations, three adaptive controllers are tested. These are the concurrent learning adaptive law in (13) with Algorithm 3, Algorithm 4, and Algorithm 5. We use the same reference model, nominal controller gains, and adaptive controller parameters as the section: 2.5 Simulation Example. The difference is in the algorithms and its parameters. The maximum number of recorded data points $\bar{p}$ is $6$. Simulations are started with pre-recorded history-stack satisfying Condition 1. It has 3 linearly independent columns, i.e. $p = 3$ and $\|\eta(0)\|_F = 3.1$, $\lambda_{min}(\eta(0)) = 10^{-6}$, which are required to determine $\bar{\eta}$ and $\bar{\lambda}$. Considering these initial values, $\bar{\eta}$ and $\bar{\lambda}$ are set to $20$ and $10^{-6}$ respectively. We run the simulations with a $0.005$ sec time step using Euler integration.

In Figure 22, the tracking performances of the concurrent learning adaptive controllers are presented and the ideal weight estimation performances of them are demonstrated in Figure 23. Norms of the error vectors $\xi$ are also shown in Figure 24. In contrast to the regulation problem in the previous section, Algorithm 5 achieves the lowest error norm after $t = 11\ sec$. Moreover, tracking and weight estimation performances of Algorithm 5 are better than Algorithm 3 and Algorithm 4.

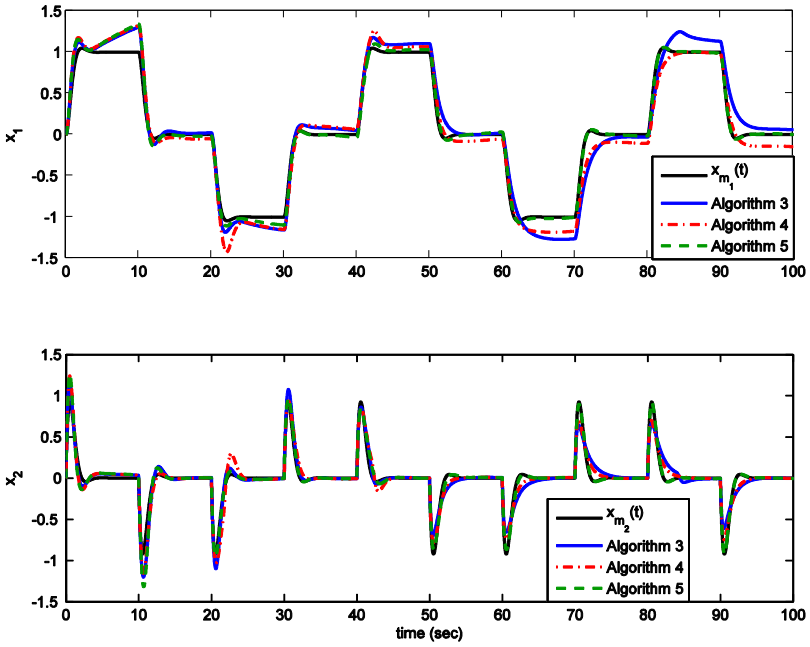


**Figure 22 Responses with CL-MRAC**

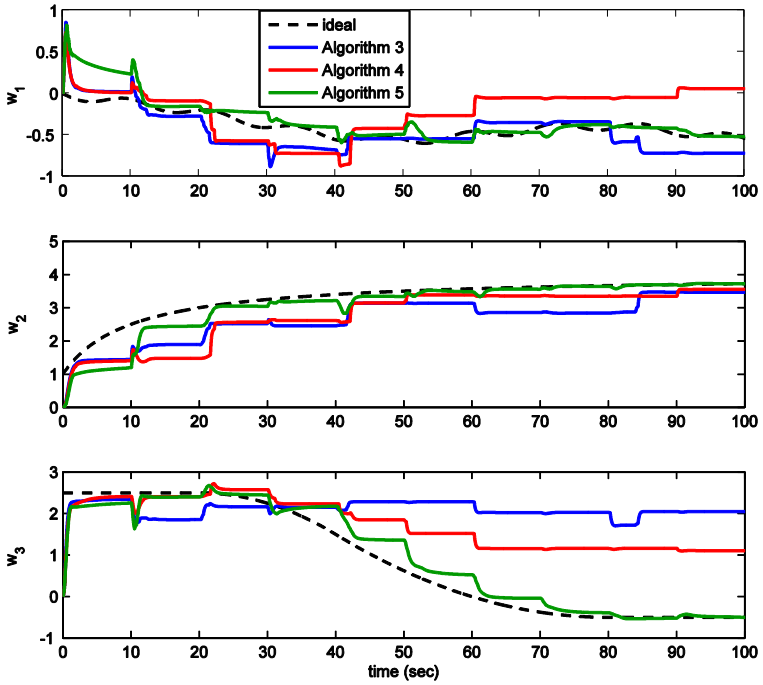


**Figure 23 Estimate of the ideal weights with CL-MRAC**

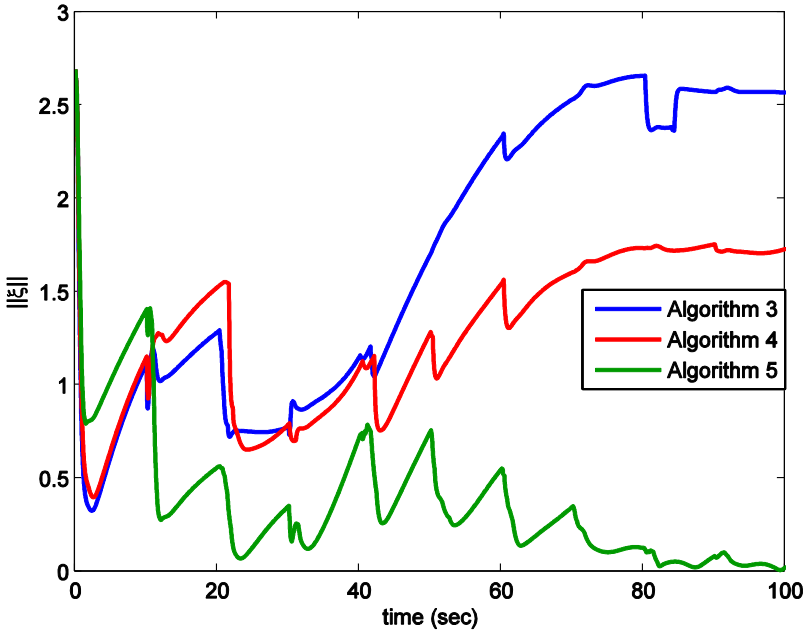


**Figure 24 Norm of the error vector with CL-MRAC**

The superiority of Algorithm 5 in this example is not very surprising because we know from Remark 11 and the previous regulation problem that even if the ultimate bound is minimized by Algorithm 4, this value will be still large. Actually, Algorithm 4 achieves the lowest condition number of the history-stack as it is desired. On the other hand, Algorithm 5 updates its history-stack frequently most probably due to the richness of the reference input. Therefore, it has the most current data points, see Table 4. Since the ideal weights vary slowly, this frequent update improves the weight estimation and thus the tracking performance.

**Table 4: The time when the last data points were recorded by algorithms in tracking problem**

| | Algorithm 3 | Algorithm 4 | Algorithm 5 |
|---|---|---|---|
| time (sec) | 80.365 | 50.655 | 90.200 |
| | 10.365 | 90.115 | 90.450 |
| | 31.130 | 31.070 | 90.810 |
| | 84.415 | 21.650 | 91.105 |
| | 84.405 | 60.555 | 91.425 |
| | 20.915 | 40.480 | 91.940 |

## 2.9 Derivative-Free Model Reference Adaptive Control (DF-MRAC)

Derivative-free weight update law uses both delayed weight estimates and current system states and errors to cancel the effects of the matched uncertainty which has time-varying ideal weights [5], [21]. In this section, we consider again the system given in (46). In contrast to derivative-based adaptive laws, derivative-free approach does not require continuous ideal weights in Lyapunov analysis. Therefore, Assumption 3 is relaxed as follows:

**Assumption 5** The matched uncertainty in (46) can be linearly parameterized as

$$\Delta(t,x) = W^T(t)\beta(x), \qquad x \in \Omega_x, \tag{106}$$

where $W(t) \in R^{s\times m}$ is the unknown time-varying weight matrix that satisfies $\|W(t)\|_F \leq w$ with positive constant $w$ and $\beta\big(x(t)\big) : R^n \to R^s$ is a vector of known basis functions $\beta(x) = [\beta_1(x),\ \beta_2(x),\ \dots,\ \beta_s(x)]^T \in R^s$ and $\Omega_x$ is a sufficiently large compact subset of $R^n$.

Derivative-free adaptive law has the following form

$$\widehat{W}(t) = \Omega_1\widehat{W}(t-\tau) + \widehat{\Omega}_2(t), \tag{107}$$

where $\tau > 0$,

$$0 \leq \Omega_1^2 < \kappa_1 < 1, \tag{108}$$

and

$$\widehat{\Omega}_2(t) = \kappa_2\beta(x(t))e^T(t)PB, \tag{109}$$

with $\kappa_2 > 0$. Using (107), define $\Omega_2$

$$\Omega_2(t) \coloneqq W(t) - \Omega_1 W(t-\tau). \tag{110}$$

With the upper bound given in Assumption 5 and (108), $\|\Omega_2(t)\|_F$ can be upper bounded as

$$\|\Omega_2(t)\|_F \leq \|W(t)\|_F + |\Omega_1|\|W(t-\tau)\|_F \leq w(1+\sqrt{\kappa_1}) \tag{111}$$

Using (107), (110) and the definition in (48), the weight error can be rewritten as

$$\widetilde{W}(t) = \Omega_1 \widetilde{W}(t-\tau) - \widehat{\Omega}_2(t) + \Omega_2(t). \tag{112}$$

On the other hand, there is no variation in the state tracking error dynamics given in (17). To keep the formulas short, we will drop the argument $t$ in the following analysis as long as explicit explanation is not required.

The following theorem and its proof can be found in [5], [21]. For the sake of completeness, the theorem with minor variations in its statement and correction in the corollary about convergence rate to the ultimate bound is proved here.

Define the error vector $\xi \coloneqq [e^T,\ \tilde{v}(t,\tau)]^T$, where $\tilde{v}^2(t,\tau) \coloneqq tr\left(\int_{t-\tau}^{t} \widetilde{W}^T(s)\widetilde{W}(s)ds\right)$ and consider the following continuously differentiable Lyapunov-Krasovskii function

$$V\left(e, \widetilde{W}_t\right) = e^T P e + \rho tr\left(\int_{t-\tau}^{t} \widetilde{W}^T(s)\widetilde{W}(s)ds\right), \tag{113}$$

where $\rho > 0$ and $\widetilde{W}_t$ represents $\widetilde{W}(t)$ over the time interval $t-\tau$ to $t$. (113) can be rewritten as

$$V(\xi) = \xi^T \tilde{P} \xi, \tag{114}$$

where $\tilde{P} = diag[P,\ \rho]$. Then, (114) can be lower and upper bounded as

$$\min\{\lambda_{min}(P), \rho\}\,\|\xi\|^2 \leq V(\xi) \leq \max\{\lambda_{max}(P), \rho\}\,\|\xi\|^2. \tag{115}$$

Note that $V(0) = 0$ and $V(\xi) > 0,\ \ \forall\, \xi \neq 0$.

From (115), define the following positive constants,

$$k_1 \coloneqq \min\{\lambda_{min}(P), \rho\}, \tag{116}$$

$$k_2 \coloneqq \max\{\lambda_{max}(P), \rho\}. \tag{117}$$

Consider the sets represented in Figure 16 with a variation in the dimension due to the new definition of the error vector. This variation is obviously seen in the following definition of $B_r$

$$B_r = \{\xi \in R^{n+1} | \|\xi\| \leq r\} \subset \Omega_\xi. \tag{118}$$

**Assumption 6** Assume

$$r > \sqrt{\frac{k_2}{k_1}}\mu \geq \mu, \tag{119}$$

$\mu$ is defined as

$$\mu = w\left(1 + \sqrt{\kappa_1}\right)\sqrt{\frac{1}{\theta\lambda_{min}(Q)\kappa_2(1 - q_2\kappa_1)}} \tag{120}$$

where $0 < \theta < 1$ and $1 < q_2 < \kappa_1^{-1}$.

**Theorem 3** Consider the system in (46) subject to Assumption 5, the reference model in (2), and the tracking control law in (4), with the nominal control component given by (5) subject to Assumption 2 and the adaptive feedback control component given by (6) which has the derivative-free weight update law in (107). Moreover, let Assumption 6 hold. Then, $\Omega_c$ is positively invariant and $\forall\, \xi(t_0) \in \Omega_c$, there exists $T = T(\xi(t_0), \mu) \geq 0$ such that

$$\|\xi(t)\| \leq \sqrt{\frac{k_2}{k_1}}\|\xi(t_0)\|\mathrm{e}^{-\lambda(t-t_0)}, \quad \forall\, t_0 \leq t \leq t_0 + T, \tag{121}$$

where $\lambda = k_3/(2k_2) = (1-\theta)\,\lambda_{min}(Q)/\,(2\max\{\lambda_{max}(P),\rho\}), k_3$ is defined in the proof,

$$\|\xi(t)\| \le \sqrt{\frac{k_2}{k_1}}\mu, \quad \forall\, t \ge t_0 + T, \tag{122}$$

If Assumption 5 holds globally, i.e. $\Omega_x = R^n$, then (121) and (122) hold $\forall\, \xi(t_0)$, without limitation on how large μ is.

**Proof:** Consider the Lyapunov-Krasovkii function given in (113). The time derivative of (113) along trajectories (17) and (112) can be expressed as

$$\begin{aligned}
\dot{V}\left(t, e, \widetilde{W}_t\right) &= e^T[A_m^T P + P A_m]e + 2e^T PB\widetilde{W}^T\beta(x) \\
&\quad +\rho tr\left(\widetilde{W}^T\widetilde{W} - \widetilde{W}^T(t-\tau)\widetilde{W}(t-\tau)\right) \\
&= e^T[A_m^T P + P A_m]e + 2\Omega_1 e^T PB\widetilde{W}^T(t-\tau)\beta(x) \\
&\quad -2e^T PB\widehat{\Omega}_2^T\beta(x) + 2e^T PB\Omega_2^T\beta(x) \\
&\quad +\rho tr\left(-q_1\widetilde{W}^T\widetilde{W} + q_2\widetilde{W}^T\widetilde{W} - \widetilde{W}^T(t-\tau)\widetilde{W}(t-\tau)\right),
\end{aligned} \tag{123}$$

where $q_2 - q_1 = 1$ and $q_1 > 0$. Thus, $q_2 > 1$.

Using the Lyapunov equation in (11) and expanding $tr(q_2\widetilde{W}^T\widetilde{W})$, we have

$$\begin{aligned}
\dot{V}\left(t, e, \widetilde{W}_t\right) &= -e^T Qe + 2\Omega_1 e^T PB\widetilde{W}^T(t-\tau)\beta(x) \\
&\quad -2e^T PB\widehat{\Omega}_2^T\beta(x) + 2e^T PB\Omega_2^T\beta(x) \\
&\quad +\rho tr\left(-q_1\widetilde{W}^T\widetilde{W} - \widetilde{W}^T(t-\tau)\widetilde{W}(t-\tau)\right) \\
&\quad +\rho tr\left(q_2\Omega_1^2\widetilde{W}^T(t-\tau)\widetilde{W}(t-\tau)\right) + \rho tr\left(q_2\widehat{\Omega}_2^T\widehat{\Omega}_2\right) \\
&\quad +\rho tr(q_2\Omega_2^T\Omega_2) - \rho tr\left(2q_2\Omega_1\widehat{\Omega}_2^T\widetilde{W}(t-\tau)\right) \\
&\quad +\rho tr\left(2q_2\Omega_1\widetilde{W}^T(t-\tau)\Omega_2\right) - \rho tr\left(2q_2\widehat{\Omega}_2^T\Omega_2\right).
\end{aligned} \tag{124}$$

For conformable matrices $A$ and $B$, $tr(A^TB) \le \gamma tr(A^TA) + tr(B^TB)/(4\gamma)$, where $\gamma > 0$. This inequality is obtained from Young's inequality in [5]. The following term in (124) can be upper bounded as

$$\begin{aligned}\rho tr\big(2q_2\Omega_1\widetilde{W}^T(t-\tau)\Omega_2\big) \le\ & \rho\gamma tr\left(\Omega_1^2\widetilde{W}^T(t-\tau)\widetilde{W}(t-\tau)\right) \\ & +\rho q_2^2 tr(\Omega_2^T\Omega_2)/\gamma.\end{aligned} \tag{125}$$

Using (109) with $\kappa_2 \coloneqq 1/(\rho q_2) > 0$, we have the following three equalities.

The first one is

$$2\Omega_1 e^T PB\widetilde{W}^T(t-\tau)\beta(x) = \rho tr\left(2q_2\Omega_1\widehat{\Omega}_2^T\widetilde{W}(t-\tau)\right) \tag{126}$$

because

$$\begin{aligned}2\Omega_1 e^T PB\widetilde{W}^T(t-\tau)\beta(x) &= 2\Omega_1 tr\left(\beta(x)e^T PB\widetilde{W}^T(t-\tau)\right) \\ &= \frac{2}{\kappa_2}\Omega_1 tr\left(\widehat{\Omega}_2\widetilde{W}^T(t-\tau)\right)\end{aligned} \tag{127}$$

and

$$\begin{aligned}\rho tr\left(2q_2\Omega_1\widehat{\Omega}_2^T\widetilde{W}(t-\tau)\right) &= \frac{2}{\kappa_2}\Omega_1 tr\left(\widehat{\Omega}_2^T\widetilde{W}(t-\tau)\right) \\ &= \frac{2}{\kappa_2}\Omega_1 tr\left(\widehat{\Omega}_2\widetilde{W}^T(t-\tau)\right).\end{aligned} \tag{128}$$

The second one is

$$-2e^T PB\widehat{\Omega}_2^T\beta(x) + \rho tr\big(q_2\widehat{\Omega}_2^T\widehat{\Omega}_2\big) = -\frac{1}{\kappa_2}tr\big(\widehat{\Omega}_2^T\widehat{\Omega}_2\big) \tag{129}$$

because

$$\begin{aligned}-2e^T PB\widehat{\Omega}_2^T\beta(x) &= -2tr\big(\beta(x)e^T PB\widehat{\Omega}_2^T\big) \\ &= -\frac{2}{\kappa_2}tr\big(\widehat{\Omega}_2\widehat{\Omega}_2^T\big) = -\frac{2}{\kappa_2}tr\big(\widehat{\Omega}_2^T\widehat{\Omega}_2\big)\end{aligned} \tag{130}$$

and

$$\rho tr\left(q_2\widehat{\Omega}_2^T\widehat{\Omega}_2\right) = \frac{1}{\kappa_2} tr\left(\widehat{\Omega}_2^T\widehat{\Omega}_2\right). \tag{131}$$

The third one is

$$2e^T PB\Omega_2^T\beta(x) = \rho tr\left(2q_2\widehat{\Omega}_2^T\Omega_2\right) \tag{132}$$

because

$$2e^T PB\Omega_2^T\beta(x) = 2tr(\beta(x)e^T PB\Omega_2^T) = \frac{2}{\kappa_2} tr\left(\widehat{\Omega}_2\Omega_2^T\right) = \frac{2}{\kappa_2} tr\left(\widehat{\Omega}_2^T\Omega_2\right) \tag{133}$$

and

$$\rho tr\left(2q_2\widehat{\Omega}_2^T\Omega_2\right) = \frac{2}{\kappa_2} tr\left(\widehat{\Omega}_2^T\Omega_2\right). \tag{134}$$

Using the inequality (125) and the equalities (126), (129), and (132), we upper bound (124) as

$$\begin{aligned}\dot{V}\left(t, e, \widetilde{W}_t\right) \leq & -e^T Qe \; - \frac{1}{\kappa_2} tr\left(\widehat{\Omega}_2^T\widehat{\Omega}_2\right) - \rho q_1 tr\left(\widetilde{W}^T\widetilde{W}\right) \\ & -\rho tr\left((1-(q_2+\gamma)\Omega_1^2)\widetilde{W}^T(t-\tau)\widetilde{W}(t-\tau)\right) \\ & +\rho tr\left(\left(q_2 + \frac{q_2^2}{\gamma}\right)\Omega_2^T\Omega_2\right).\end{aligned} \tag{135}$$

Letting $\kappa_1 \coloneqq 1/(q_2+\gamma)$ and using the inequality (108), we can easily show that $(1-(q_2+\gamma)\Omega_1^2) > 0$. Using positive-definiteness of $Q$, (111), and Frobenius norm properties, we can further upper bound (135) as

$$\dot{V}\left(t, e, \widetilde{W}_t\right) \leq \; -m_1\|e\|^2 - m_2\left\|\widetilde{W}\right\|_F^2 \; - m_3\left\|\widetilde{W}(t-\tau)\right\|_F^2 + \delta, \tag{136}$$

where

$$m_1 = \lambda_{min}(Q) > 0, \tag{137}$$

$$m_2 = \rho q_1 > 0, \tag{138}$$

$$m_3 = \rho(1 - \kappa_1^{-1}\Omega_1^2) > 0, \tag{139}$$

$$\delta = \rho\left(q_2 + \frac{q_2^2}{\gamma}\right)w^2\left(1 + \sqrt{\kappa_1}\right)^2 > 0 \tag{140}$$

In [5], it is claimed that the following inequality, i.e. (141), can be obtained by selecting $q_1$ such that $m_2 = m_1\tau$. Although we could not establish that inequality, we continue with the ongoing analysis by assuming that their claim is correct:

$$\dot{V}(t,\xi) \leq -m_1\|\xi\|^2 + \delta. \tag{141}$$

The foregoing inequality can be rewritten as

$$\dot{V}(t,\xi) \leq -(1-\theta)m_1\|\xi\|^2 - \theta m_1\|\xi\|^2 + \delta, \tag{142}$$

where $0 < \theta < 1$. Then, we get

$$\dot{V}(t,\xi) \leq -(1-\theta)m_1\|\xi\|^2, \forall\|\xi\| \geq \mu, \tag{143}$$

where $\mu = \sqrt{\delta/(\theta m_1)}$. Since $0 < \kappa_1 < 1$, $\gamma > 0$, $q_2 = \kappa_1^{-1} - \gamma$, and $q_2 > 1$, it is obvious that $q_2 \in (1, \kappa_1^{-1})$. Using $\kappa_2 = 1/(\rho q_2)$ and $\gamma = \kappa_1^{-1} - q_2$, $\mu$ can be rewritten as

$$\mu = w\left(1 + \sqrt{\kappa_1}\right)\sqrt{\frac{1}{\theta\lambda_{min}(Q)\kappa_2(1 - q_2\kappa_1)}}. \tag{144}$$

One can find an alternative representation for (144) if $m_2 = m_1\tau$ is used. From (143), define the following positive constant

$$k_3 \coloneqq (1-\theta)\lambda_{min}(Q). \tag{145}$$

The following steps are very similar to the steps in the proof of Theorem 2. Define the compact set

$$B_\mu = \{\xi \in B_r | \|\xi\| \leq \mu\}. \tag{146}$$

It should be noted that (119) ensures that $B_\mu \subset B_r$. Let $d$ be the maximum value of $V(\xi)$ on the boundary of $B_\mu$. Using (115) and (117),

$$d = max_{\|\xi\|=\mu} V(\xi) = k_2 \mu^2. \tag{147}$$

Define

$$\Omega_d = \{\xi \in B_r | V(\xi) \leq d\}. \tag{148}$$

(147) guarantees that $B_\mu \subset \Omega_d$ and from the condition in (119), we ensure that $\Omega_d \subset \Omega_c$. All sets used in the proof are presented in Figure 17.

By (115), (143) with $k_1$ in (116), $k_2$ in (117), $k_3$ in (145), Assumption 6, and Theorem 4.5 in [29], $\Omega_c$ is positively invariant and for all initial errors $\xi(t_0)$ belong to $\Omega_c$, there exists $T = T(\xi(t_0), \mu) \geq 0$ such that (121) and (122) are satisfied. ■

**Remark 12** In Theorem 3**,** it is proved that the error vector $\xi = [e^T, \ \tilde{v}(t,\tau)]^T$ is uniformly bounded. Does bounded $\xi$ imply bounded weight error $\widetilde{W}$? The answer is "yes". Since $e$ and $x_m$ are bounded, $x$ is bounded. Since $e$ and $x$ are bounded, $\widehat{\Omega}_2$ is bounded. (107) is a difference equation and it can be regarded as $s\,x\,m$ first order discrete-time linear time-invariant systems. $\Omega_1$ is the system matrix and the elements of $\widehat{\Omega}_2$ are the inputs. Since $|\Omega_1| < 1$ and $\widehat{\Omega}_2$ is bounded, $\widehat{W}$ is bounded. Then, noting that ideal weights are bounded, we can conclude that $\widetilde{W}$ is bounded.

**Remark 13** Due to the typing or calculation mistake made in Corollary 2 in [5], the authors ended up with an incorrect expression for the exponential convergence rate to the ultimate bound. The corrected version is given in (121) and it is independent of $\tau$. One can still find out an expression dependent on $\tau$ using $m_2 = m_1\tau$ and $q_2 - q_1 = 1$. Then, convergence rate becomes independent of $\lambda_{min}(Q)$ and it increases with decrease in $\tau$. This inference is the exact opposite of the one in [5]. However, it should be noted

that the estimated ultimate bound and convergence rate to that bound depend on the inequality in (141) that we have doubt in the correctness of it.

**Remark 14** If $\tau$ is regarded as step size, $\kappa_2$ is set to $\tau\Gamma$, and $\Omega_1$ is set to 1, Euler discretization of (12) results in (107). However, $\Omega_1 = 1$ is not allowed and $\tau$ does not have to be equal to step size in DF-MRAC. (108) introduces forgetting property into the weight update law that is effective when ideal weights encounter sudden changes. On the other hand, selecting $\tau$ greater than step size provides short-term memory. Moreover, $\kappa_2$ acts as a learning rate $\Gamma$ in MRAC. To sum up, DF-MRAC has more tuning flexibility than MRAC because of the additional design parameters, $\Omega_1$ and $\tau$.

## 2.10 Conclusion

This chapter extends the field of application of CL-MRAC by relaxing the constant ideal parameters assumption. In order to apply this extended theorem to problems, existing data recording algorithms are modified. We test CL-MRAC with modified algorithms in simulation by using sample regulation and tracking problem. The simulation results show that the performance of CL-MRAC is highly dependent on problems and data recording algorithms. In addition to this extension, we repeat the proofs of the existing CL-MRAC and DF-MRAC theorems to fill or emphasize the observed missing parts.

# CHAPTER 3

# CONTROL OF WING ROCK MOTION

## 3.1 Introduction

Wing rock is a complicated aerodynamic phenomenon for slender delta wing aircraft. Its onset is observed in high angles of attacks below the occurrence of stall. If it is uncontrolled, then it causes limit cycle, even instability in body roll axis. Theoretical results which have performed to understand the dynamics of wing rock, predict the frequency & amplitude of limit-cycle, and roll divergence can be found in [30], [31]. Since it degrades the performance of aircraft at high angles of attack, the control of wing rock motion has been extensively studied in the literature. Approaches used in wing rock control can be divided into two groups. One approach is that controller is developed at fixed angle of attack and it is sometimes tested other angles to claim robustness. In [32], [33], this approach was used. Another approach is that angle of attack is allowed to vary with time and thus controller design can take account of time variation in angle of attack. The latter was applied to wing rock control in [34], [35]. In this study, we apply the second one because it is more general and it corresponds to parameter variation that fits our comparison purposes. The uncertainty in [35] and the random disturbance in [36] are also added to test the performance of controllers under high level of uncertainty and problematic disturbance.

## 3.2 Wing Rock Dynamics

Analytical nonlinear models that describe subsonic wing rock phenomenon for slender delta wings have been developed in [30], [31]. In [37], [34], the wing rock equation of motion presented in [31] has been used. In [34], an interpolation function has also been proposed to interpolate the aerodynamic coefficients smoothly with corresponding angles of attack. Thus, time-varying model of the wing rock has been built. In this chapter, we use the model presented in [34] and it is given by

$$\ddot{\phi} = -\omega^2\phi + \mu_1\dot{\phi} + b_1\phi^3 + \mu_2\phi^2\dot{\phi} + b_2\phi\dot{\phi}^2 + gu + \delta\left(t, \phi, \dot{\phi}\right) \tag{149}$$

where $\phi$ is the roll angle, $u$ is the aileron deflection, $g = 1.5$ is the input gain, and $\delta$ includes unmodeled function and disturbance input as follows:

$$\delta\left(t, \phi, \dot{\phi}\right) = d'\left(\phi, \dot{\phi}\right) + d(t) \tag{150}$$

The aerodynamic coefficients in (149) are functions of the angle of attack $\alpha$:

$$\begin{aligned} \omega^2 &= -c_1 a_1(\alpha) \\ \mu_1 &= c_1 a_2(\alpha) - c_2 \\ b_1 &= c_1 a_3(\alpha) \\ \mu_2 &= c_1 a_4(\alpha) \\ b_2 &= c_1 a_5(\alpha), \end{aligned} \tag{151}$$

where $c_1 = 0.354$ and $c_2 = 0.001$. Using Table 1 in [34], interpolated aerodynamic coefficients are reproduced here in Figure 25. In [31], uncontrolled wing rock model with $\delta = 0$ was analyzed and the authors showed that the origin of (149) is a stable focus for $\alpha < 19.5\, deg$ approximately. For higher angles, the origin is an unstable focus and it is enclosed by a limit cycle. This qualitative behavior is represented for $\alpha = 15\, deg$ and $\alpha = 25\, deg$ in Figure 26. In this study, we consider that the angle of attack varies between $15\, deg$ and $25\, deg$. Thus, the qualitative behavior presented in Figure 26 changes with angle of attack.

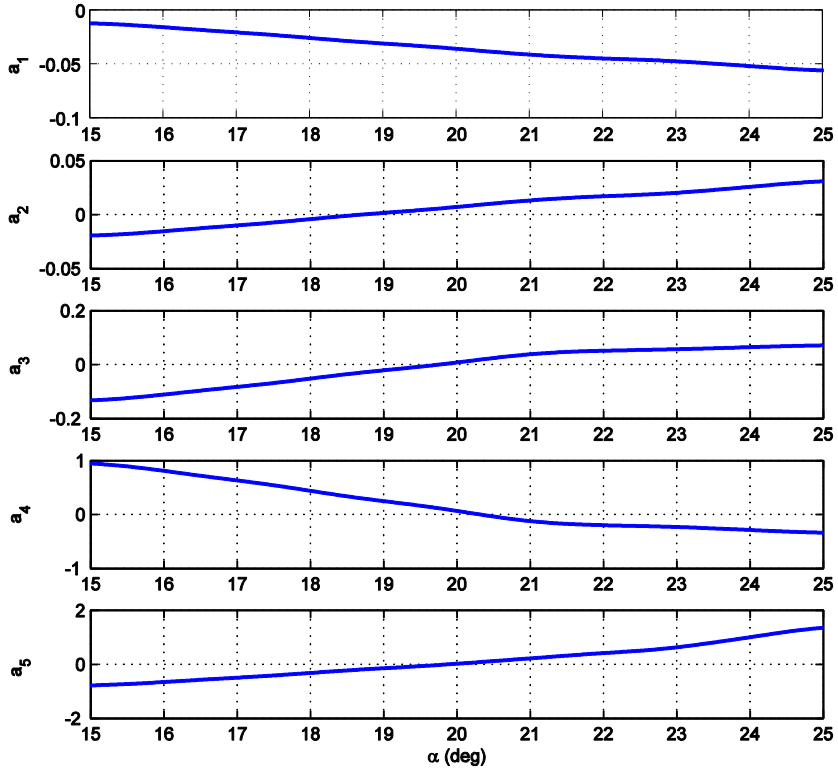


**Figure 25 Interpolated aerodynamic coefficients**

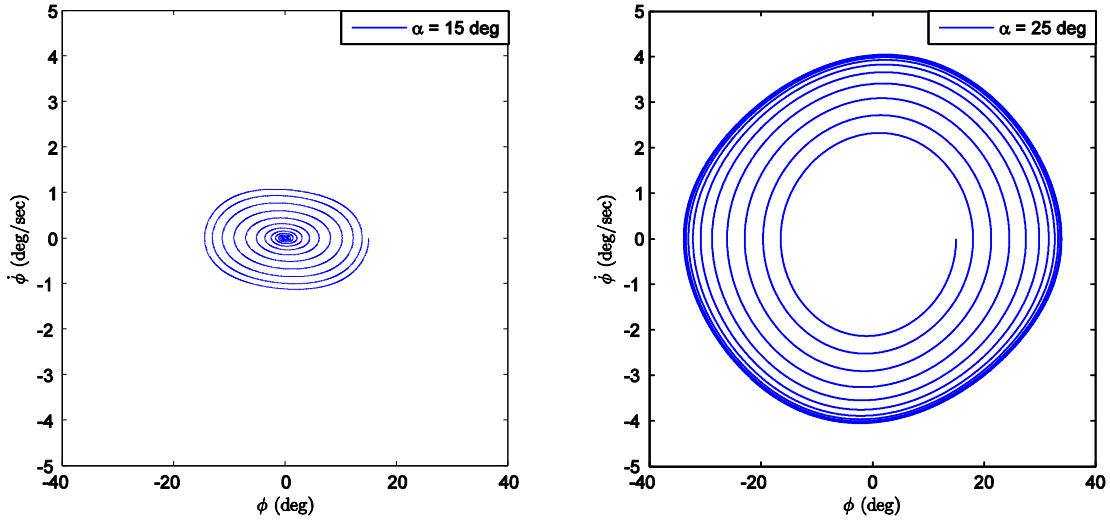


**Figure 26 Phase Plane Trajectories for $\alpha = 15\ deg$ and $\alpha = 25\ deg$ with initial conditions of $\phi(0) = 15\ deg$ and $\dot{\phi}(0) = 0\ deg/sec$**

Define the state vector $x = [x_1,\ x_2]^T \coloneqq \left[\phi,\ \dot{\phi}\right]^T$, then (149) can be written in the state space form given in (46) as

$$\begin{bmatrix}\dot{x}_1\\ \dot{x}_2\end{bmatrix} = \begin{bmatrix}0 & 1\\ 0 & 0\end{bmatrix}\begin{bmatrix}x_1\\ x_2\end{bmatrix} + \begin{bmatrix}0\\ g\end{bmatrix}[u + \Delta(t,x)], \tag{152}$$

where

$$\Delta(t,x) = \frac{-\omega^2 x_1 + \mu_1 x_2 + b_1 {x_1}^3 + \mu_2 {x_1}^2 x_2 + b_2 x_1 {x_2}^2 + \delta(t,x)}{g}. \tag{153}$$

Furthermore, $A \coloneqq \begin{bmatrix}0 & 1\\ 0 & 0\end{bmatrix}$ and $B \coloneqq \begin{bmatrix}0\\ g\end{bmatrix}$. Using (150) and (151), we can rewrite (153) as

$$\Delta(t,x) = W(t)^T \beta(x) + d'(x)/g, \tag{154}$$

where the basis function

$$\beta(x) = [1 \quad x_1 \quad x_2 \quad x_1^3 \quad x_1^2 x_2 \quad x_1 x_2^2]^T \tag{155}$$

and the ideal weights

$$W(t) = \begin{bmatrix}d(t)/g\\ w_1(\alpha)\\ w_2(\alpha)\\ w_3(\alpha)\\ w_4(\alpha)\\ w_5(\alpha)\end{bmatrix} = g^{-1}\begin{bmatrix}d(t)\\ c_1 a_1(\alpha)\\ c_1 a_2(\alpha) - c_2\\ c_1 a_3(\alpha)\\ c_1 a_4(\alpha)\\ c_1 a_5(\alpha)\end{bmatrix}. \tag{156}$$

Similar to the assumption in [34], we assume that the angle of attack varies according to the following exogenous function

$$\alpha(t) = 20 + 4.25\sin\left(\frac{\pi}{6}t\right) + \sin\left(\frac{2\pi}{3}t\right) + 0.1\sin(\pi t). \tag{157}$$

As it is seen in Figure 27, the angle of attack varies between $15\,deg$ and $25\,deg$ periodically. The variation in angle of attack could be due to the pilot inputs in longitudinal axis.

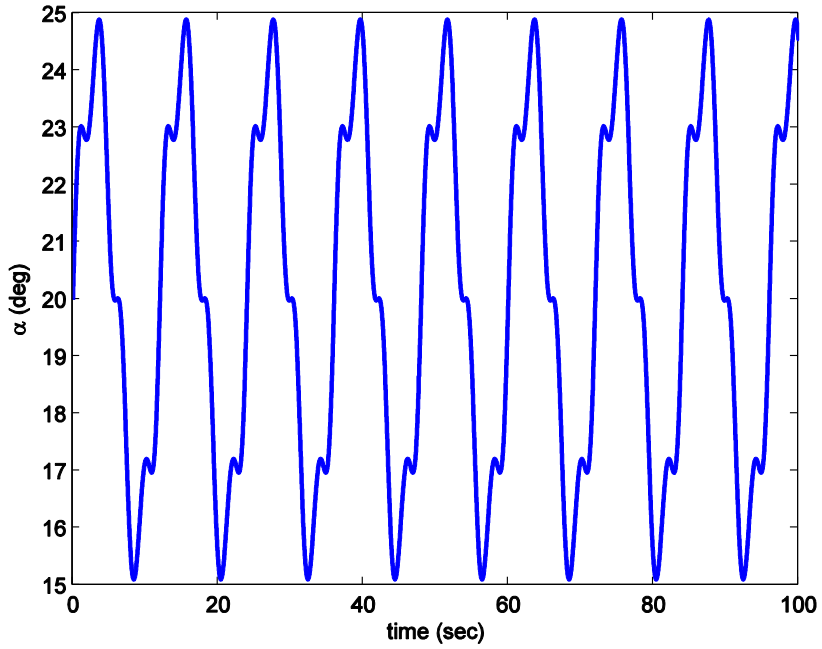


**Figure 27 Angle of attack**

## 3.3 Nominal Controller

System and input matrix of the reference model are selected as (44) with a pair of complex conjugate eigenvalues which have natural frequency $\omega_n = 1$ and damping ratio $\zeta = 0.5$. From the matching condition given in Assumption 2, nominal controller gains are $K_1 = [2/3,\ \ 2/3]$ and $K_2 = 2/3$. Performance of nominal controller is going to be presented prior to the adaptive augmentation.

### 3.3.1 Simulation Results with $d' = 0$ & $d = 0$

Figure 28 shows the reference model tracking performance of the nominal controller and Figure 29 shows the aileron deflection. It is obvious that the nominal controller performs well and adaptive augmentation is not required. This satisfactory performance can be explained by the low uncertainty level presented in Figure 29.

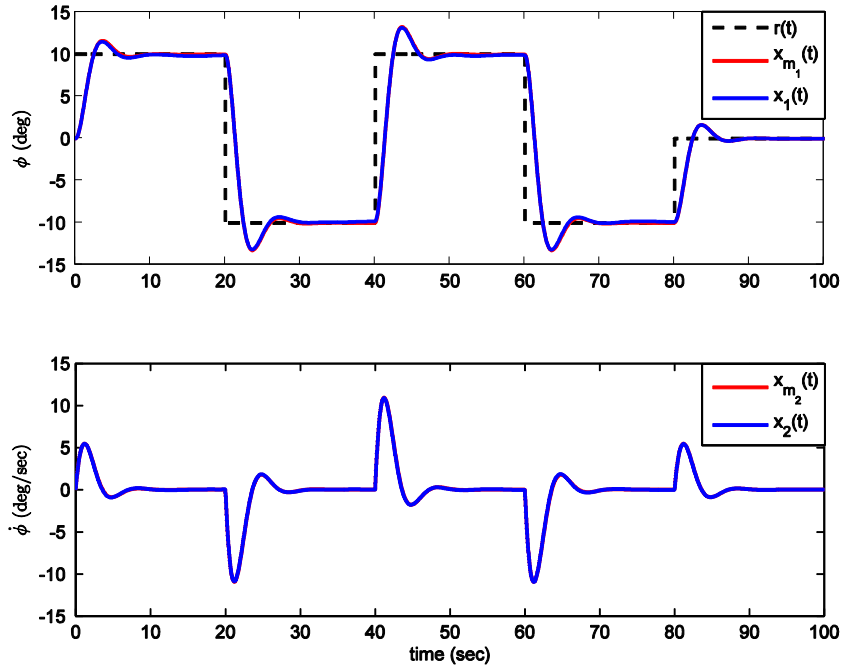


**Figure 28 Responses with nominal controller with $d' = 0$ & $d = 0$**

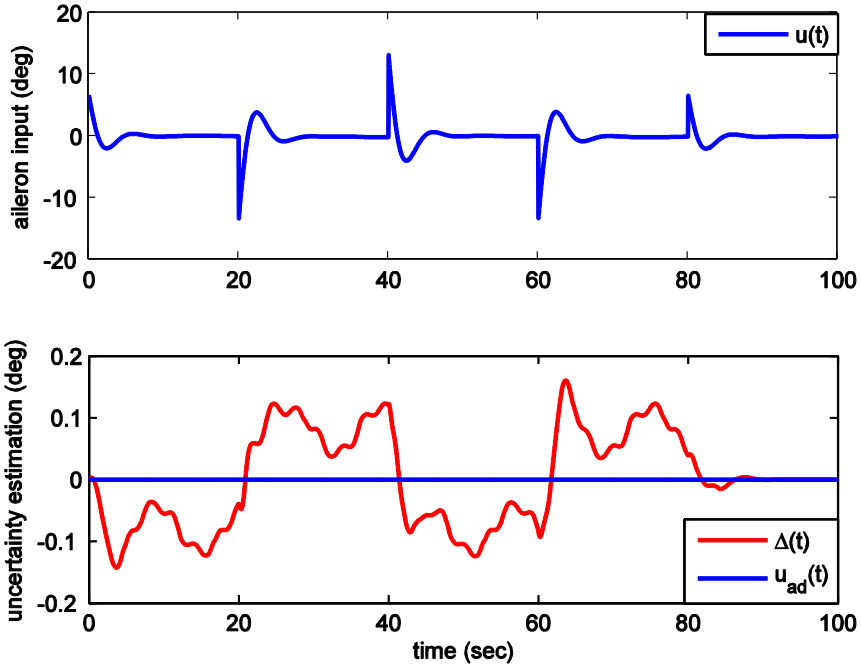


**Figure 29 Aileron deflection with nominal controller with $d' = 0$ & $d = 0$**

### 3.3.2 Simulation Results with $d' \neq 0$ & $d = 0$

In this section, we are going to check the performance of the nominal controller in the presence of unmodeled function $d'$. We consider the following function given in [35]

$$d' = 0.6141\phi + 1.2099\dot{\phi} + 0.0135\phi^3 - 0.0513\phi^2\dot{\phi} + 0.035\phi\dot{\phi}^2. \quad (158)$$

Note that this unmodeled function $d'$ is going to be used throughout the simulations. (158) can be rewritten as

$$d'(x) = [0 \quad 0.6141 \quad 1.2099 \quad 0.0135 \quad -0.0513 \quad 0.035]\beta(x). \quad (159)$$

Now, (154) becomes

$$\Delta(t,x) = W(t)^T\beta(x), \quad (160)$$

where

$$W(t) = \begin{bmatrix} d(t)/g \\ w_1(\alpha) \\ w_2(\alpha) \\ w_3(\alpha) \\ w_4(\alpha) \\ w_5(\alpha) \end{bmatrix} = g^{-1}\begin{bmatrix} d(t) \\ c_1a_1(\alpha) + 0.6141 \\ c_1a_2(\alpha) - c_2 + 1.2099 \\ c_1a_3(\alpha) + 0.0135 \\ c_1a_4(\alpha) - 0.0513 \\ c_1a_5(\alpha) + 0.035 \end{bmatrix}. \quad (161)$$

In Figure 30 and Figure 31, the first three seconds of the simulation is demonstrated because bounded reference input yields unbounded states. It is clear that nominal controller cannot survive the uncertainty shown in Figure 31. Therefore, adaptive augmentation is considered a solution to suppress or cancel the current uncertainty.

## 3.4 Adaptive Augmentation

In the simulations, three different adaptive controllers are used to augment the nominal controller. The first adaptive controller which are going to be tested is the baseline adaptive law (12) with *e* modification [12]:

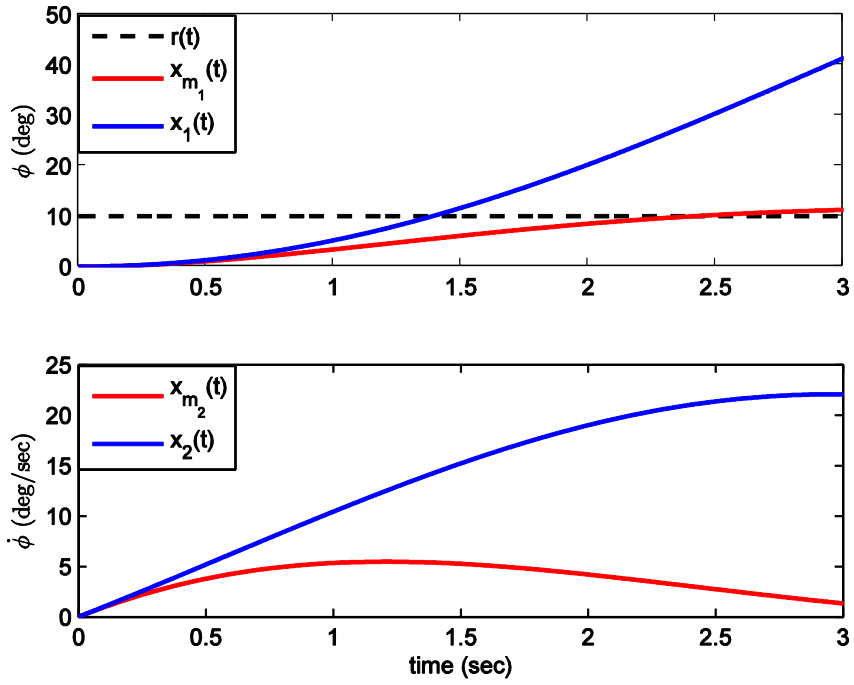


**Figure 30 Responses with nominal controller with $d' \neq 0$ & $d = 0$**

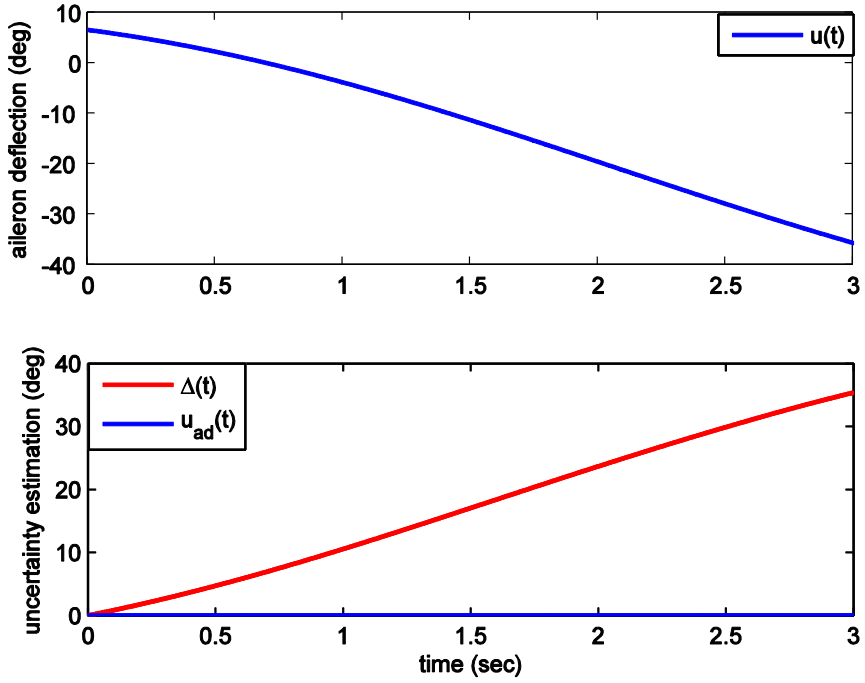


**Figure 31 Aileron deflection with nominal controller with $d' \neq 0$ & $d = 0$**

$$\dot{\hat{W}}(t) = \Gamma\big(\beta\big(x(t)\big)e^T(t)PB - \sigma\|e(t)\|\hat{W}\big), \tag{162}$$

where $\sigma$ is a positive modification gain. Instead of (12), we select (162) to test in the simulations because of its robustness to bounded perturbations. The second adaptive controller which is going to be tested is the concurrent learning adaptive law in (13). Derivative-free adaptive law in (107) is the third one. Since $\lambda_{min}(Q)/\lambda_{max}(P)$ is maximized with the choice $Q = diag[1,\ 1]$ (Example 9.1 in [9]) and convergence rate to the ultimate bound in (58) & (121) is proportional to this ratio, we choose $Q = diag[1,\ 1]$ for all adaptive controllers and this parameter is not going to be tuned.

Other constant parameters are as follows. Modification gain $\sigma$ in (162) is tried to be kept small because it increases high frequency oscillations in control inputs. It is set to $0.1$. In concurrent learning, maximum number of recorded data points $\bar{p}$ is $12$ and $\varepsilon$ used in data recording algorithms is $0.01$. It should be noted that as we increase $\bar{p}$, minimum singular value of the history stack may increase, see Remark 6, but it causes irrelevant memory which lags the system response to variation in dynamics. Therefore, we kept it small compared to constant ideal parameter problems. $\varepsilon$ is also kept small to make algorithms less selective about data recording. Simulations are started with pre-recorded history-stack satisfying Condition 1. These data points are obtained from the simulation when $d' = 0$ & $d = 0$. It has 6 linearly independent columns, i.e. $p = 6$ and $\|\eta(0)\|_F = 6.1$, $\lambda_{min}(\eta(0)) = 10^{-8}$, which are required to determine $\bar{\eta}$ and $\bar{\lambda}$. Considering these initial values, $\bar{\eta}$ and $\bar{\lambda}$ are set to 30 and $10^{-8}$ respectively. In order to allow new data inclusion or old data removal, we usually choose $\bar{\eta}$ three-six times higher than $\|\eta(0)\|_F$. Otherwise, $\eta$ saturates for a long time and variation in history-stack is hindered. In derivative-free, $\tau$ is set to $0.01$ seconds and $\Omega_1$ is set to $0.95$. To make adaptive law responsive to variation in dynamics, $\tau$ is kept small and thus it acts as a short-term memory. To get benefit from this memory, $\Omega_1$ is set to a value which is close to the upper bound given in (108).

### 3.4.1 Simulation Results with $d' \neq 0$ & $d = 0$

Figure 32 shows the tracking performance and aileron deflection of MRAC with *e* modification for $\Gamma = 2$ & $\Gamma = 20$. In Figure 33, the weight estimation performances of them are demonstrated. As learning rate is increased, transient response of roll angle and roll rate is improved. However, high learning rate causes high frequency oscillations in weight estimation & aileron input and thus in states. Moreover, weight estimation performance is not improved by increasing learning rate.

In Figure 34, the tracking performances and aileron deflection of the concurrent learning adaptive controllers are presented for $\Gamma = 2$. Figure 35 shows the weight estimation performances of them. There is no considerable difference in the performance and the weight estimation of the algorithms. Both roll angle and roll rate encounter overshoot in the first ten seconds. Their tracking performances are satisfactory except that overshoot.

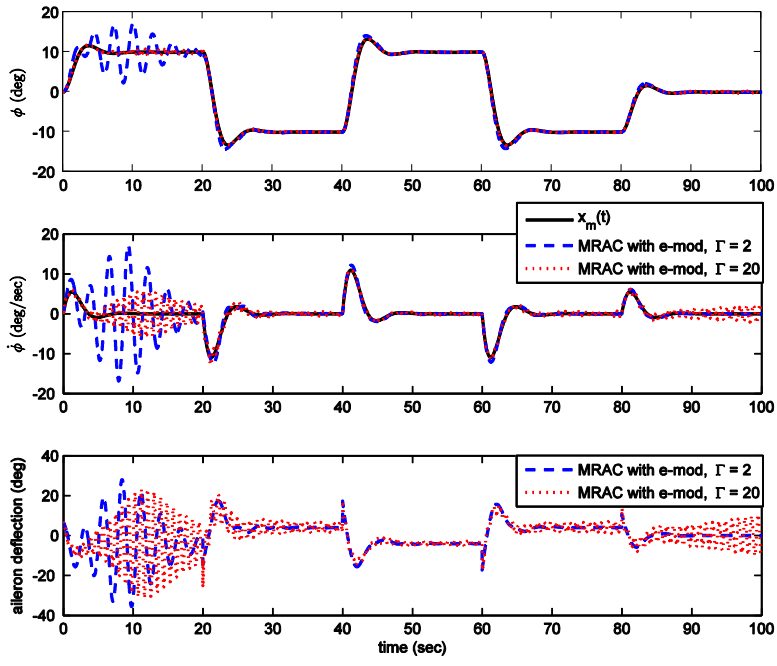


**Figure 32 Responses and aileron deflection with MRAC with *e* modification**

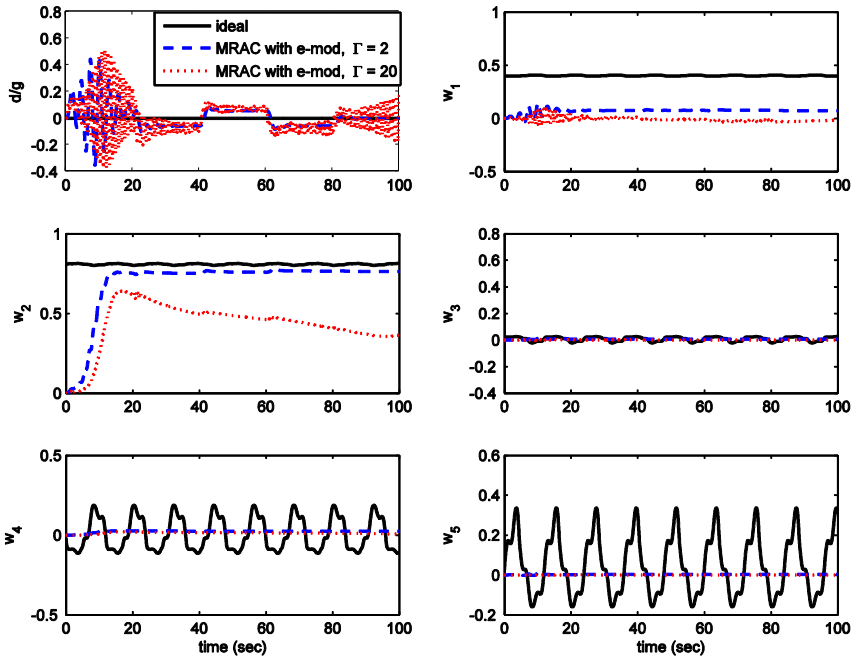


**Figure 33 Estimate of the ideal weights with MRAC with *e* modification**

It is also clearly seen from the weight evolution that the estimated weights are close to the ideal weights, especially $d, w_1$, and $w_2$. Recall from nominal controller part that the uncertainty level due to the angle of attack variation is low compared to unmodeled function $d'$ and $d'$ has constant weights. It may explain why the weight estimation performance is good though the ideal weights are time-varying and vary fast.

All algorithms properly work as it is desired. Algorithm 4 achieves the lowest condition number of the history-stack. Although Algorithm 5 uses the most recent data points, these data points can be considered irrelevant due to the fast variation in ideal weights. This may explain why the estimation of $w_3, w_4$, and $w_5$ is poor.

In order to see whether high learning rate improves transient response of roll angle and roll rate, causes high frequency oscillations in weight estimation & aileron input, we increase it from $\Gamma = 2$ to $\Gamma = 20$. In Figure 36, the tracking performances and aileron deflection of the concurrent learning adaptive controllers are presented for $\Gamma = 20$. Figure 37 shows the weight estimation performances of them. There is no considerable

difference in the performance and the weight estimation of the algorithms again. Transient response of roll angle and roll rate is improved. In contrast to MRAC with *e* modification, CL-MRAC does not encounter any high frequency oscillation in weight estimation & aileron input due to the increase in learning rate. Discussions we have had about the weight estimation performance and algorithms for $\Gamma = 2$ are still valid for $\Gamma = 20$. The only difference is that Algorithm 3 achieves the lowest condition number of the history-stack for $\Gamma = 20$.

Figure 38 shows the tracking performance and aileron deflection of DF-MRAC for $\kappa_2 = 0.25$ & $\kappa_2 = 2.5$. Tracking performance of DF-MRAC with $\kappa_2 = 2.5$ is the best one we obtain among the tested controllers. Furthermore, aileron deflection time history is acceptable. In Figure 39, the weight estimation performances of DF-MRAC are demonstrated. Estimated weights are not close to the ideal weights. However, it is highly responsive to the uncertainty and suppresses it very effectively. According to the simulation results, we can conclude that while CL-MRAC cares about long-term learning, DF-MRAC does not care about learning.

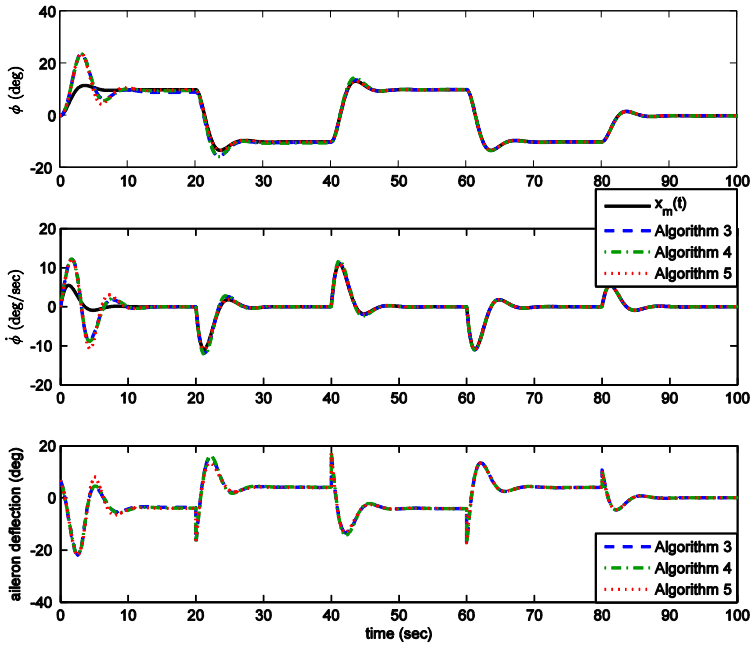


**Figure 34 Responses and aileron deflection with CL-MRAC, $\Gamma = 2$**

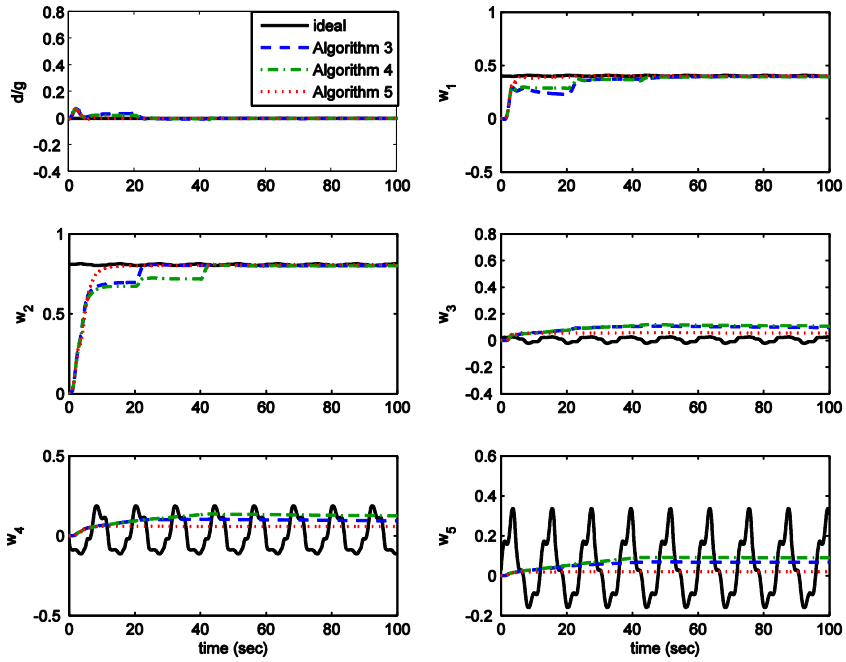


**Figure 35 Estimate of the ideal weights with CL-MRAC, $\Gamma = 2$**

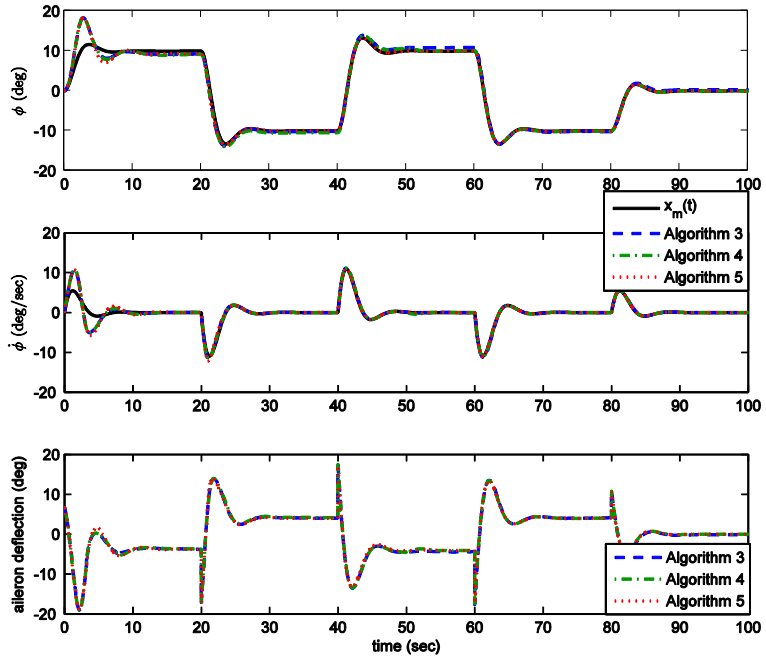


**Figure 36 Responses and aileron deflection with CL-MRAC, $\Gamma = 20$**

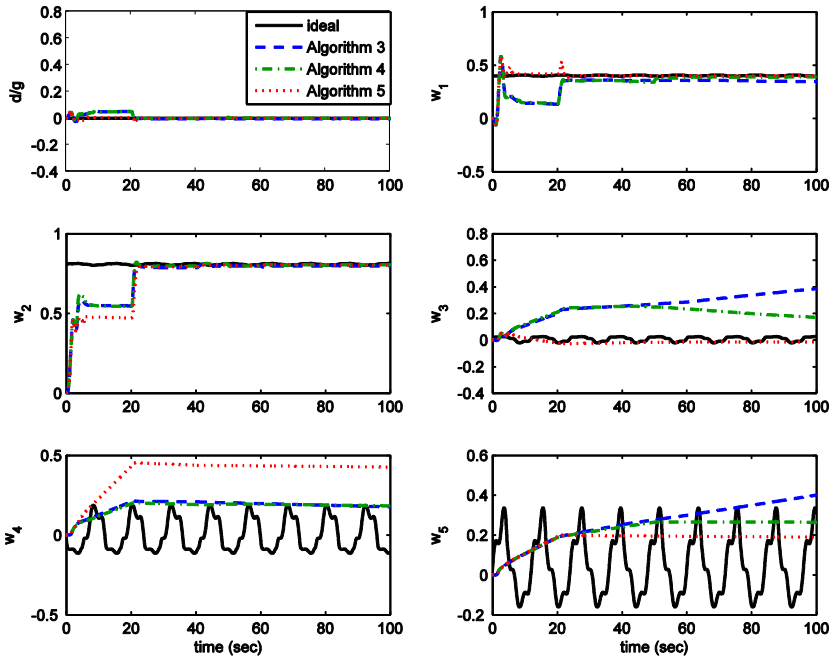


**Figure 37 Estimate of the ideal weights with CL-MRAC, $\Gamma = 20$**

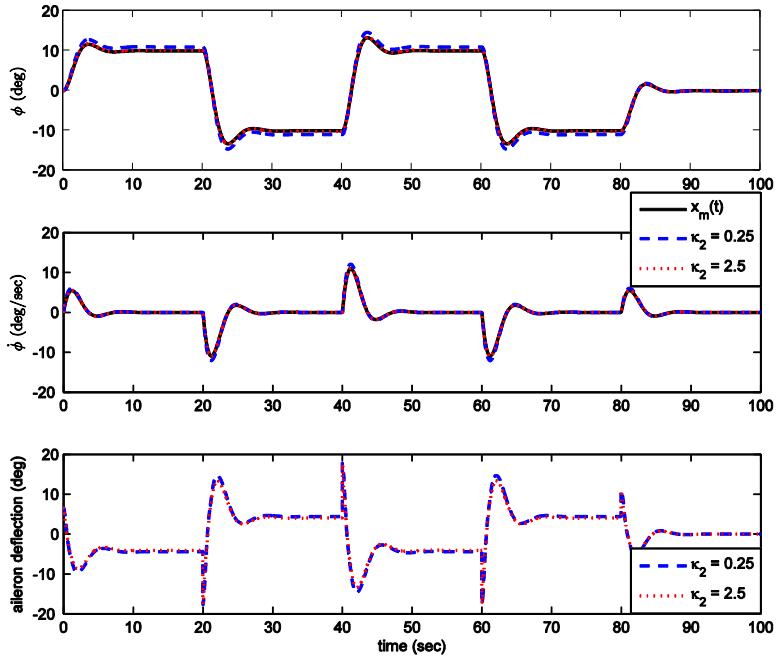


**Figure 38 Responses and aileron deflection with DF-MRAC**

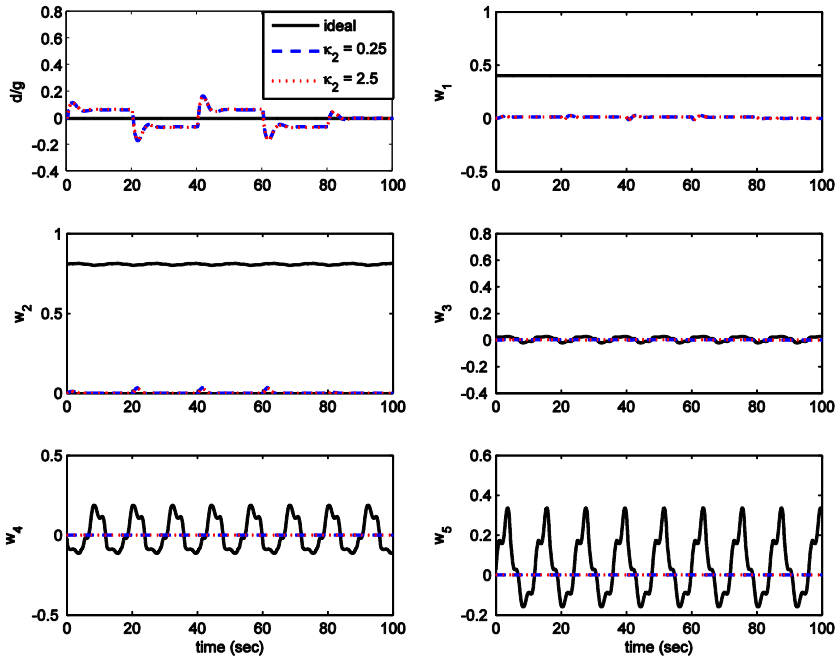


**Figure 39 Estimate of the ideal weights with DF-MRAC**

### 3.4.2 Simulation Results with $d' \neq 0$ & $d \neq 0$

In addition to $d'$, we consider random disturbance $d$ presented in [36]. It is introduced to represent the effects of the gust and wind on the rolling dynamics. In contrast to the uncertainty due to angle of attack variation and unmodeled function $d'$, random disturbance $d$ is nonvanishing perturbation. Therefore, it should be uniformly cancelled by control to stabilize the origin. Since uniform cancellation is not possible for unknown time-varying signal, we can only achieve practical stabilization in that case. This feature of the disturbance increases the difficulty of the problem. The disturbance we are going to use in the simulations is presented in Figure 40.

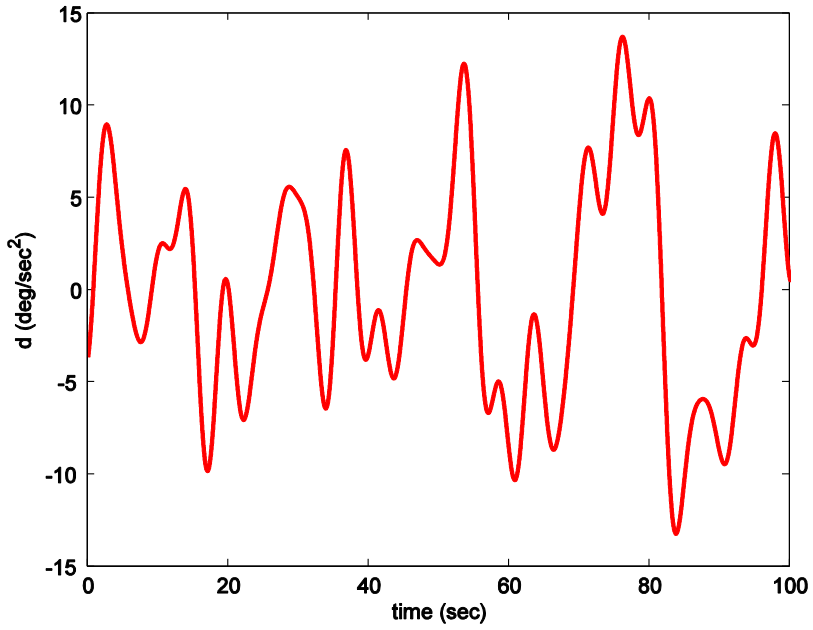


**Figure 40 Random disturbance**

Figure 41 shows the tracking performance and aileron deflection of MRAC with $e$ modification for $\Gamma = 2$ & $\Gamma = 20$. In Figure 42, the weight estimation performances of them are demonstrated. Similar to $d' \neq 0$ & $d = 0$ case, increase in learning rate improves tracking performance with unacceptable high frequency oscillations in aileron. Moreover, weight estimation performance is not improved by increasing learning rate.

Figure 43 and Figure 45 show the tracking performance and aileron deflection of the concurrent learning adaptive controllers for $\Gamma = 2$ and $\Gamma = 20$ respectively. Moreover, Figure 44 and Figure 46 present the weight estimation performance of the algorithms for $\Gamma = 2$ and $\Gamma = 20$ respectively. As it is seen in Figure 43 and Figure 45, none of the algorithms achieve satisfactory tracking performance regardless of learning rate. In contrast to $d' \neq 0$ & $d = 0$ case, the estimated weights are not close to the ideal weights, see Figure 44 and Figure 46 . It may be explained by the increase in the time-varying uncertainty level due to the random disturbance $d$ and fast variation in it.

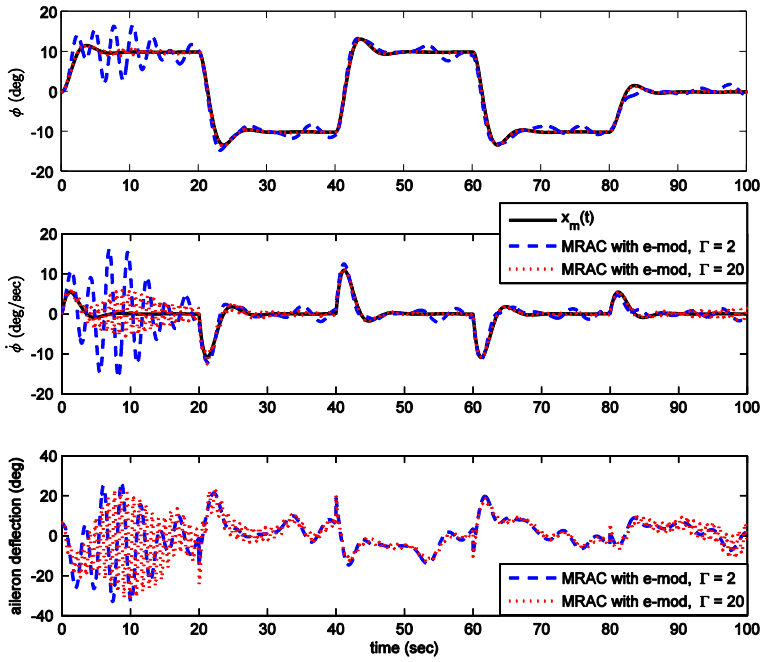


**Figure 41 Responses and aileron deflection with MRAC with *e* modification**

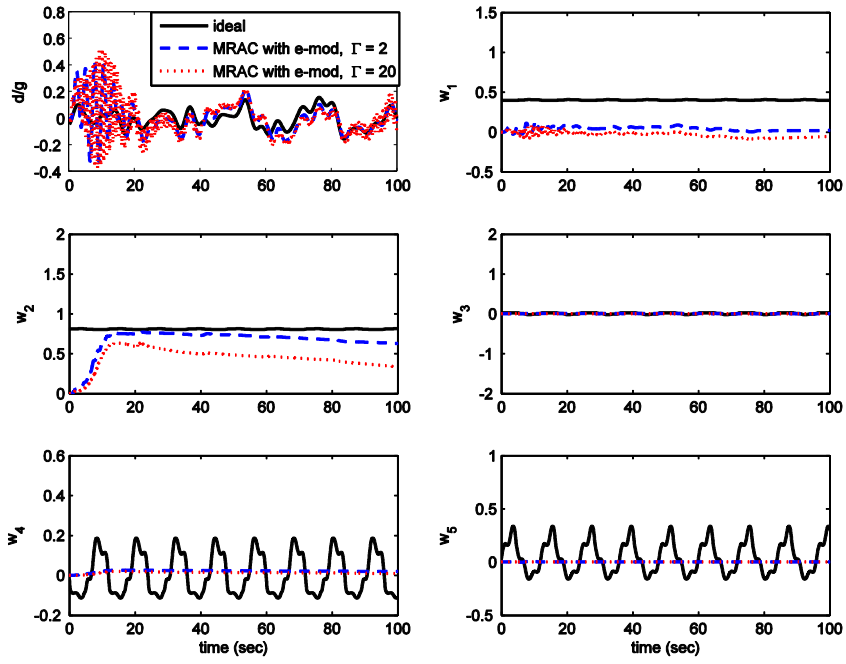


**Figure 42 Estimate of the ideal weights with MRAC with *e* modification**

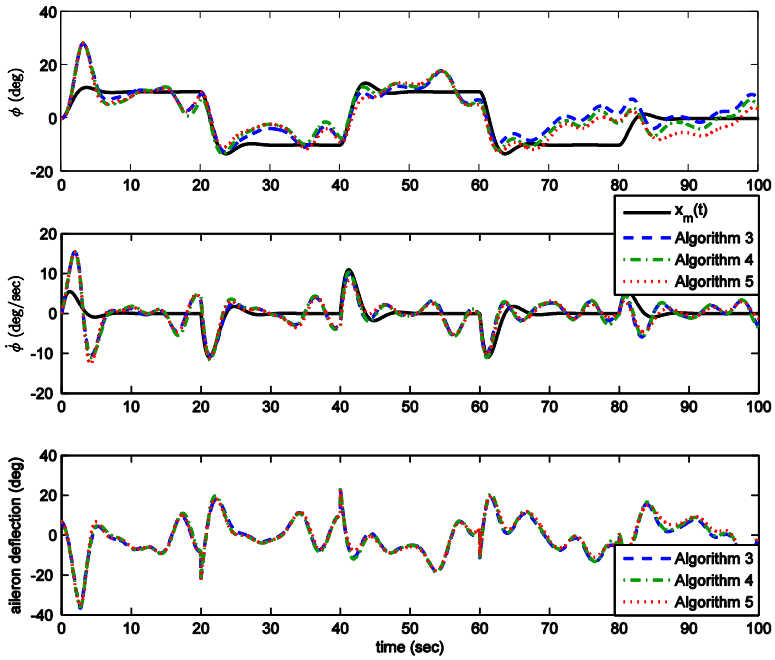


**Figure 43 Responses and aileron deflection with CL-MRAC, $\Gamma = 2$**

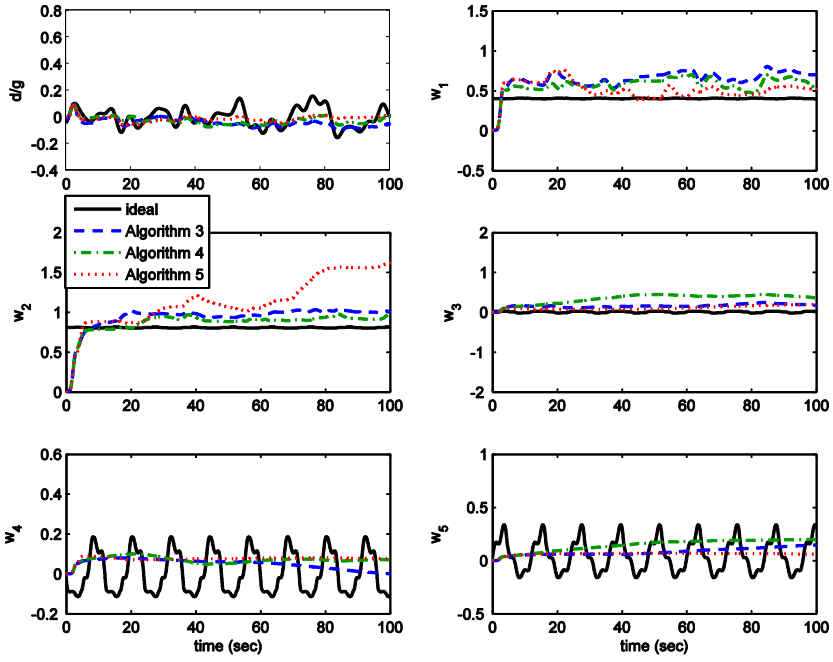


**Figure 44 Estimate of the ideal weights with CL-MRAC, $\Gamma = 2$**

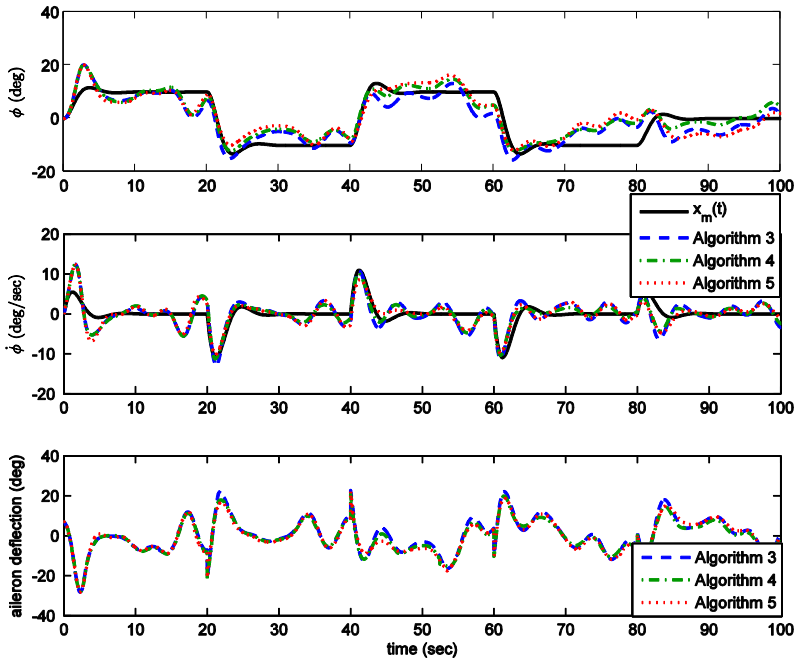


**Figure 45 Responses and aileron deflection with CL-MRAC, $\Gamma = 20$**

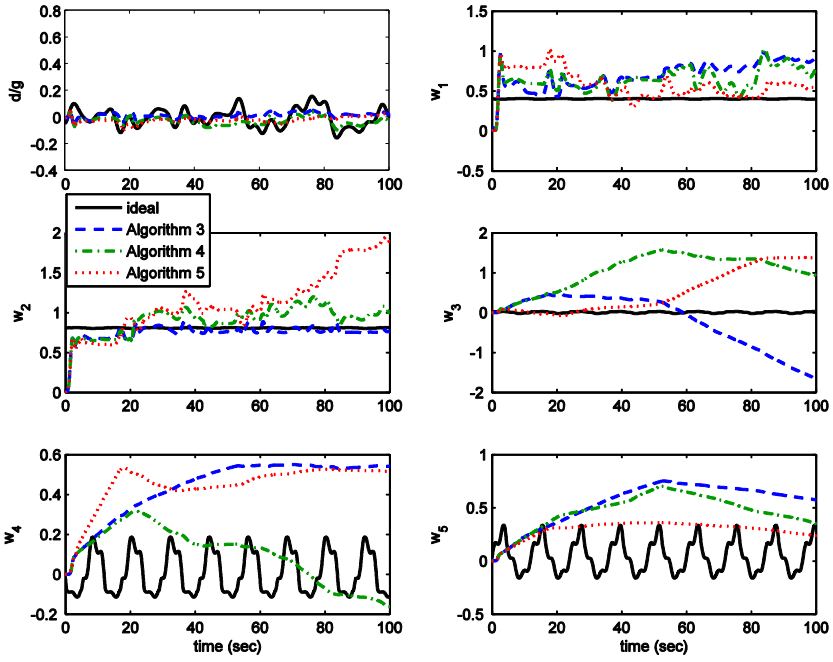


**Figure 46 Estimate of the ideal weights with CL-MRAC, $\Gamma = 20$**

Figure 47 demonstrates the tracking performance and aileron deflection of DF-MRAC for $\kappa_2 = 0.25$ & $\kappa_2 = 2.5$. In Figure 48, the weight estimation performances of DF-MRAC are shown. Similar to $d' \neq 0$ & $d = 0$ case, DF-MRAC with $\kappa_2 = 2.5$ outperforms other tested controllers in terms of tracking performance and it has reasonable aileron deflection history. The inference about the weight estimation we drew from $d' \neq 0$ & $d = 0$ case is still valid when we have random disturbance $d$. It is again observed that CL-MRAC tries to learn the uncertainty. On the other hand, DF-MRAC tries to suppress it. Actually, it is very powerful in uncertainty suppression.

Until now, we assume that uncertainty basis is exactly known since all theorems in Chapter 2 were proved by using this information. However, uncertainty basis is not exactly known in real applications. Since DF-MRAC tries to suppress the uncertainty without learning it, we are motivated to test the performance of DF-MRAC by approximating the uncertainty in (160) with functions different than (155). Three different functions are selected for this comparison. The first one is symmetric sigmoid functions used in [5]:

$$\beta(x) = [1 \quad \beta_1(x) \quad \beta_2(x)]^T, \tag{163}$$

where $\beta_i(x) = \frac{1-e^{-x_i}}{1+e^{-x_i}}$, $i = 1, 2$. The second one is Fourier series with a long enough period and sufficient series length used in [36]:

$$\beta(t) = [1 \quad \beta_1(t) \quad \beta_2(t) \ \dots \ \beta_{10}(t)\ ]^T, \tag{164}$$

where $\beta_i(t) = \cos\left(\frac{2\pi i}{T}t\right)$, $i = 1, 2, \dots, 5$ and $\beta_i(t) = \sin\left(\frac{2\pi(i-5)}{T}t\right)$, $i = 6, 7, \dots, 10$. In [36], the author proposes that period should be selected at least three times longer than the simulation or operation time. Therefore, $T$ is set to $500$ seconds. The third and the last one we are going to test is just bias. That is, $\beta = 1$.

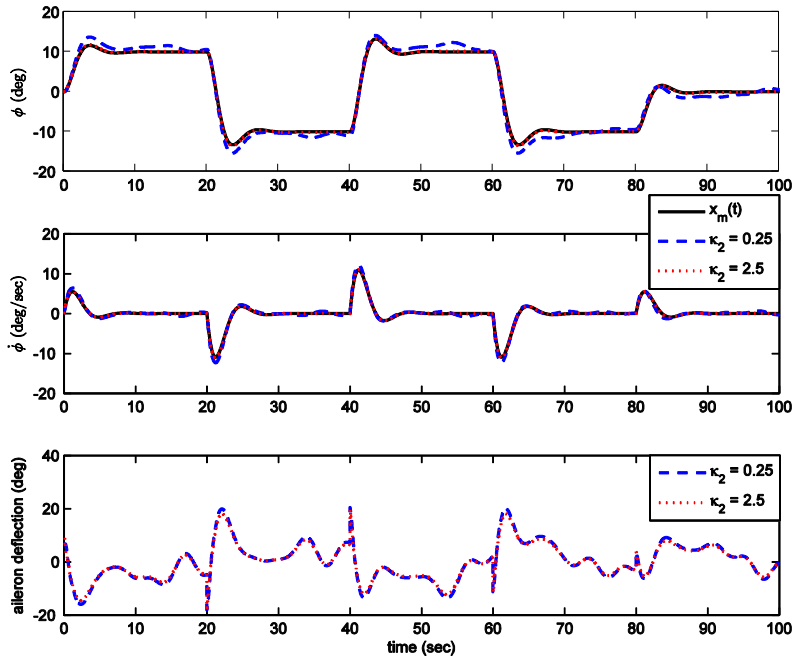


**Figure 47 Responses and aileron deflection with DF-MRAC**

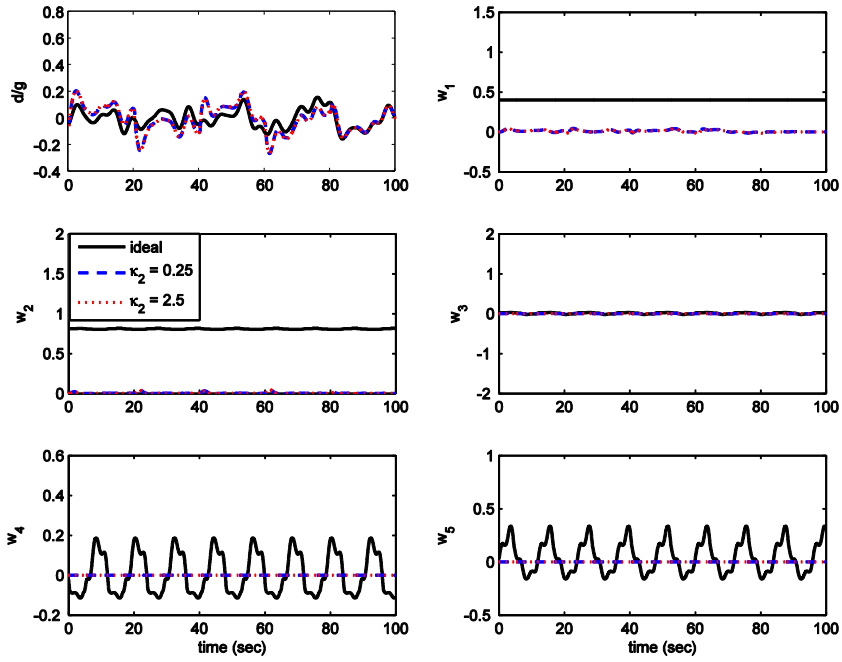


**Figure 48 Estimate of the ideal weights with DF-MRAC**

As it is seen in Figure 49, the responses of DF-MRAC with symmetric sigmoid functions, Fourier series, and bias are almost indistinguishable from the response with the known basis in (155). In this problem, DF-MRAC performs excellent even if the uncertainty is approximated by using only bias as a basis function.

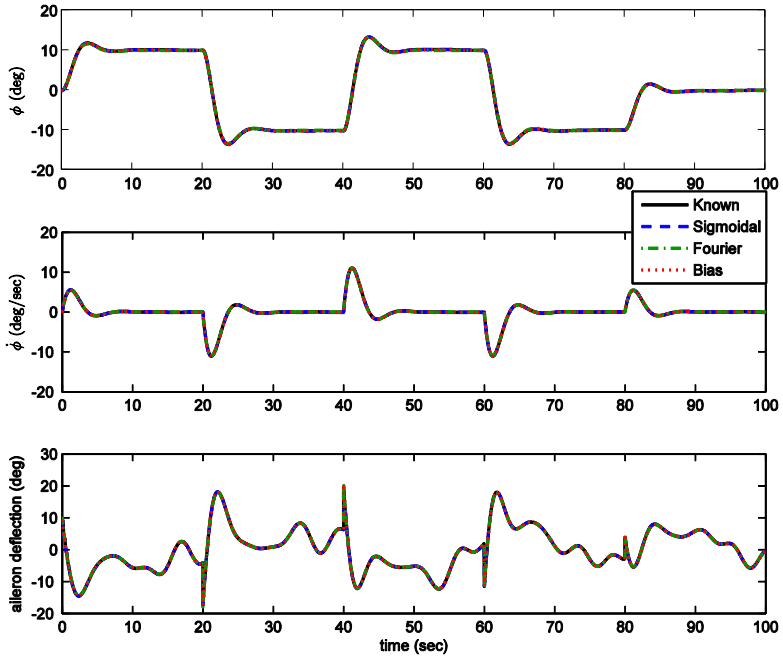


**Figure 49 Responses and aileron deflection with DF-MRAC, $\kappa_2 = 2.5$**

## 3.5 Conclusion

In this chapter, wing rock problem with time-varying angle of attack is studied for numerical illustration. Under high level uncertainty and problematic disturbance, controllers are tested and it is shown that DF-MRAC performs better than CL-MRAC. Due to the excellent performance of DF-MRAC and its efficient adaptation strategy, its performances with different basis functions are also tested. The simulation results still present the excellent performance of DF-MRAC.

# CHAPTER 4

# CONCLUDING REMARKS

## 4.1 Conclusions

The intent of this thesis has been to make a fair comparison of CL-MRAC and DF-MRAC against parameter variation. For this purpose, we extend the field of application of CL-MRAC by relaxing the constant ideal parameters assumption and prove that the solution of the closed-loop system is UUB. In order to apply this extended theorem to problems, we also modify the existing data recording algorithms. We then test CL-MRAC with modified algorithms in simulation by using sample regulation and tracking problem. The simulation results show that the performance of CL-MRAC is highly dependent on problems and data recording algorithms. It should be noted that CL-MRAC is not as promising as it is expected in [4]. We believe that CL-MRAC cannot pave the way for flight certification of adaptive controllers. In addition to this extension, we repeat the proofs of the existing CL-MRAC and DF-MRAC theorems because we have observed one misuse, one unnecessary use of stability theorems and one claim without reasoning in the standard exponential stability theorem of CL-MRAC developed in [4], [7] and one missing part and one incorrect expression in the uniform ultimate boundedness theorem of DF-MRAC developed in [5], [21].

Using wing rock problem with time-varying angle of attack, we have compared the performances of two controllers. Under high level uncertainty and random disturbance, controllers are tested and DF-MRAC performs better than CL-MRAC. Perfect performance of DF-MRAC and its efficient adaptation strategy motivate us to test its

performances when different basis functions are used. The simulation results still present the excellent performance of DF-MRAC. Although we have similar theoretical results for CL-MRAC and DF-MRAC, their adaptation strategies are completely different and the effect of this difference in the performance is obviously seen in the simulations.

Even though CL-MRAC is more complicated than DF-MRAC in terms of implementation, DF-MRAC outperforms CL-MRAC in the simulations. It sounds interesting but this is what we have observed. CL-MRAC requires an efficient data recording algorithm, a memory and first derivative of the state for a recorded data point. These requirements make it an expensive controller. On the other hand, DF-MRAC requires neither data recording algorithm nor derivative of the state. Thus, it is obviously cheaper than CL-MRAC and its implementation is quite easy. Besides, the lack of performance in CL-MRAC may be due to the data usage. In other words, data usage lags the system response to fast variation in dynamics. However, it should be kept in mind that it guarantees the boundedness of the closed-loop system solution.

## 4.2 Recommended Future Research

In this work, we present the simulation results which reveal that CL-MRAC is not promising in terms of performance under fast time-varying ideal parameters or disturbance. However, it is still effective in time-invariant systems or time-varying systems with slow variation in dynamics because of its parameter convergence capability. This capability can be useful in closed-loop system identification of nonlinear time-invariant systems. Moreover, identified model can be used to improve the nominal controller synthesis. For example, we can decide whether identified nonlinear term is stabilizing or destabilizing and if it is stabilizing, we should not try to cancel it in stabilization problem. Thus, it may reduce the control effort.

To improve the performance of CL-MRAC under time-varying ideal parameters, one can still look for alternative data recording algorithms. Besides, different learning rates

for instantaneous update and update on recorded data can be considered. This will add a new dimension to the controller design.

In the simulation results presented in this thesis, the performance of DF-MRAC is outstanding. This superiority of derivative-free weight update law should be transferred to general class of nonlinear plants. Furthermore, DF-MRAC performs excellent even if the uncertainty is approximated by using only bias as a basis function in wing rock problem. However, selecting bias as a basis is an intuitive approach. Thus, it requires rigorous analysis. Another research direction of interest is to compare derivative-free weight update law with disturbance estimators. For example, derivative-free disturbance estimator may require less strict assumptions than extended high-gain observer as disturbance estimator in [38]. It may also be combined with high-gain observers in output feedback control.

# REFERENCES


[1] K. S. Narendra and A. M. Annaswamy, *Stable Adaptive Systems*. New Jersey: Prentice Hall, 1989.

[2] K. J. Astrom and B. Wittenmark, *Adaptive Control*. Massachusetts: Addison Wesley, 1995.

[3] P. A. Ioannou and J. Sun, *Robust Adaptive Control*. New Jersey: Prentice Hall, 1996.

[4] G. Chowdhary, "Concurrent Learning for Convergence in Adaptive Control without Persistency of Excitation," PhD thesis, Georgia Institute of Technology, Atlanta, Georgia, 2010.

[5] T. Yucelen and A. J. Calise, "Derivative-free model reference adaptive control," *Journal of Guidance, Control, and Dynamics*, vol. 34, no. 4, pp. 933-950, 2011.

[6] T. Yucelen and W. M. Haddad, "Low-frequency learning and fast adaptation in model reference adaptive control," *IEEE Transactions on Automatic Control*, vol. 58, no. 4, pp. 1080-1085, 2013.

[7] G. Chowdhary, M. Mühlegg, and E. Johnson, "Exponential parameter and tracking error convergence guarantees for adaptive controllers without persistency of excitation," *International Journal of Control*, vol. 87, no. 8, pp. 1583-1603, 2014.

[8] A. Maity, L. Hocht, and F. Holzapfel, "Higher order direct model reference adaptive control with generic uniform ultimate boundedness," *International Journal of Control*, vol. 88, no. 10, pp. 2126-2142, 2015.

[9] H. K. Khalil, *Nonlinear Systems*. New Jersey: Prentice Hall, 2002.

[10] S. Boyd and S. S. Sastry, "Necessary and sufficient conditions for parameter convergence in adaptive control," *Automatica*, vol. 22, no. 6, pp. 629-639, 1986.

[11] I. Ioannou and P. V. Kokotovic, "Instability analysis and improvement of robustness of adaptive control," *Automatica*, vol. 20, no. 5, pp. 583-594, 1984.

[12] K. S. Narendra and A. M. Annaswamy, "A new adaptive law for robust adaptation without persistent excitation," *IEEE Transactions on Automatic Control*, vol. 32,

no. 2, pp. 134-145, 1987.

[13] J. B. Pomet and L. Praly, "Adaptive nonlinear regulation: estimation from the Lyapunov equation," *IEEE Transactions on Automatic Control*, vol. 37, no. 6, pp. 729-740, 1992.

[14] K. Y. Volyanskyy, W. M. Haddad, and A. J. Calise, "A new neuroadaptive control architecture for nonlinear uncertain dynamical systems: beyond σ and e modifications," *IEEE Transactions on Neural Networks*, vol. 20, no. 11, pp. 1707-1723, 2009.

[15] A. J. Calise and T. Yucelen, "Adaptive loop tranfer recovery," *Journal of Guidance, Control, and Dynamics*, vol. 35, no. 3, pp. 807-815, 2012.

[16] N. T. Nguyen, "Optimal control modification for robust adaptive control with large adaptive gain," *Systems & Control Letters*, vol. 61, pp. 485-494, 2012.

[17] G. Chowdhary and E. Johnson, "Lyapunov-based integration of a data recording algorithm in adaptive control," in *AIAA Guidance, Navigation, and Control Conference*, Portland, Oregon, 2011.

[18] M. Muhlegg, G. Chowdhary, and F. Holzapfel, "Optimizing reference commands for concurrent learning adaptive-optimal control of uncertain dynamical systems," in *AIAA Guidance, Navigation, and Control*, Boston, Massachusetts, 2013.

[19] G. Chowdhary, T. Yucelen, M. Muhlegg, and E. Johnson, "Concurrent learning adaptive control of linear systems with exponentially convergent bounds," *International Journal of Adaptive Control and Signal Processing*, vol. 27, no. 4, pp. 280-301, 2013.

[20] G. Chowdhary and E. Johnson, "A singular value maximizing data recording algorithm for concurrent learning," in *American Control Conference*, San Francisco, California, 2011.

[21] T. Yucelen, "Advances in Adaptive Control Theory: Gradient- and Derivative-Free Approaches," PhD thesis, Georgia Institute of Technology, Atlanta, Georgia, 2012.

[22] W. M. Haddad and V. Chellaboina, *Nonlinear Dynamical Systems and Control*. New Jersey: Princeton University Press, 2008.

[23] D. Liberzon, "Switched Systems," in *Handbook of Networked and Embedded Control Systems*. Massachusetts: Birkhauser, 2005, pp. 559-574.

[24] D. Liberzon, *Switching in Systems and Control*. Massachusetts: Birkhauser, 2003.

[25] B. N. Parlett, *The Symmetric Eigenvalue Problem*. New Jersey: Prentice Hall, 1980.

[26] H. Neudecker, "Some theorems on matrix differentiation with special reference to Kronecker matrix products," *Journal of the American Statistical Association*, vol. 64, no. 327, pp. 953-963, 1969.

[27] G. De La Torre, G. Chowdhary, and E. Johnson, "Concurrent Learning Adaptive Control for Linear Switched Systems," in *American Control Conference*, Washington, DC, 2013.

[28] J. P. Hespanha, *Linear Systems Theory*. New Jersey: Princeton University Press, 2009.

[29] H. K. Khalil, *Nonlinear Control*. Massachusetts: Pearson, 2015.

[30] C. Hsu and C. E. Lan, "Theory of wing rock," *Journal of Aircraft*, vol. 22, no. 10, pp. 920-924, 1985.

[31] A. H. Nayfeh, J. M. Elzebda, and D. T. Mook, "Analytical study of the subsonic wing-rock phenomenon for slender delta wings," *Journal of Aircraft*, vol. 26, no. 9, pp. 805-809, 1989.

[32] S. N. Singh , W. Yim, and W. R. Wells, "Direct adaptive and neural control of wing-rock motion of slender delta wings," *Journal of Guidance, Control, and Dynamics*, vol. 18, no. 1, pp. 25-30, 1995.

[33] M. M. Monahemi and M. Krstic, "Control of wing rock motion using adaptive feedback linearization," *Journal of Guidance, Control, and Dynamics*, vol. 19, no. 4, pp. 905-912, 1996.

[34] R. Ordonez and K. M. Passino, "Wing Rock Regulation with a Time-varying Angle of Attack," in *Proceedings of the 15th IEEE International Symposium on Intelligent Control*, Rio, Patras, Greece, 2000.

[35] D. K. Kori, J. P. Kolhe, and S. E. Talole, "Extended state observer based robust control of wing rock motion," *Aerospace Science and Technology*, vol. 33, pp. 107-117, 2014.

[36] R. B. Gezer, "Fourier Series Based Model Reference Adaptive Control," Middle East Technical University, Ankara, Turkey, MS thesis 2014.

[37] A. D. Araujo and S. N. Singh, "Variable structure adaptive control of wing-rock motion of slender delta wings," *Journal of Guidance, Control, and Dynamics*, vol. 21, no. 2, pp. 251-256, 1998.

[38] L. B. Freidovich and H. K. Khalil, "Performance recovery of feedback-linearization-based designs," *IEEE Transactions on Automatic Control*, vol. 53, no. 10, pp. 2324-2334, 2008.